DISS. ETH NO. 23148

The role of the novel muscle-specific microRNA-501 in myogenic progenitor cells during skeletal muscle regeneration

A thesis submitted to attain the degree of DOCTOR

OF SCIENCES of ETH ZURICH

(Dr. sc. ETH Zurich)

Presented by

Amir Mizbani

M.Sc. in Biotechnology, University of Tehran

born on 14.04.1985

citizen of Iran

accepted on the recommendation of

Prof. Dr. Christian Wolfrum, examiner
Prof. Dr. med. Jan Krützfeldt, co-examiner
Prof. Dr. Wilhelm Krek, co-examiner

2015

Acknowledgements

First I would like to thank my supervisor, Prof. Jan Krützfeldt, for his guidance, ideas, support, and encouragement during my Ph.D. He was always eager to discuss new ideas and strategies, and I learnt from him many things, such as perseverance, logical thinking, and problem solving. I found his dedication to science endless.

I am thankful to my Ph.D. committee members, Prof. Christian Wolfrum and Prof. Wilhelm Krek, for their advice and constructive discussions and ideas, making each of the meetings a good opportunity for me to think outside the box.

I am also grateful to my colleagues in the lab, Tatiane Gorski, Angelika Hartung, Edlira Luca, Katarina Turcekova, and Artur Galimov. We always had a nice and friendly atmosphere in the lab, and I enjoyed working with them. I learned from Tatiane how to be organized, from Angelika hard working and always keeping a smile, from Edlira how to be a good researcher and a good parent at the same time, from Katarina alertness, and from Artur focusing the most on one's own work.

My deepest and sincere gratitude goes to my family. No words can describe my parents' love, support, encouragement, and sacrifices for me, without which I would have never made it this far. Last but not least, I would like to heartily thank my wife, Pegah. Thanks for being, among so many other things, my best friend, and never leaving me alone amid all the difficulties I would have never been able to withstand. With you I learned that love knows no end.

<div dir="rtl">سپاسگزارم!</div>

Table of Contents

Summary

Skeletal muscle has an outstanding regenerative capacity. This ability is mainly due to the presence of muscle-resident adult stem cells, named satellite cells or myogenic progenitors. It is well established that proper function of satellite cells is essential for development and maintenance of skeletal muscle. microRNAs are a class of small noncoding RNAs involved in the regulation of gene expression, and they have been reported to play major roles in fine-tuning of many cellular pathways to maintain tissue homeostasis, with their function being more prominent under conditions of stress or injury. There is a growing body of evidence that microRNAs are important regulators of skeletal muscle function, homeostasis, and regeneration. In the present study, we have identified a novel muscle-specific microRNA, miR-501, and investigated its role in myoblasts during skeletal muscle regeneration. We observed that miR-501 is significantly upregulated in activated satellite cells and the whole regenerating muscle, and this is accompanied by upregulation of its host gene, Clcn5. Among the two different splice variants of Clcn5, we observed a much stronger upregulation of isoform 2 transcript, which encompasses the intron containing miR-501. However, post-transcriptional regulation plays a major role in processing miR-501 from this intron. Expression profile of miR-501 in different tissues indicated its remarkably high expression levels in satellite cells and primary myoblasts. While not changing the proliferation rate of myoblasts, pharmacological inhibition of miR-501 in regenerating skeletal muscle resulted in drastic reduction of embryonic myosin heavy chain protein (eMHC) levels. We identified and validated several miR-501 target genes using a loss-of-function screening approach in primary myoblasts. Overexpression of individual target genes in myoblasts identified gigaxonin as the potential mediator of miR-501 function that mimicked the effect of in vivo miR-501 inhibition on eMHC in primary myoblasts. Considering the reported role of gigaxonin in degrading intermediate filaments, we hypothesize that upregulation of miR-501 during skeletal muscle regeneration protects embryonic myosin heavy chain proteins against gigaxonin-mediated ubiquitination and degradation. Finally, we observed significantly elevated miR-501 levels in the skeletal muscle and serum of *mdx* mice compared to those of wild-type animals. In addition, serum miR-501 levels change during aging of *mdx* mice in a similar trend with the well-known myomiRs, such as miR-1, miR-133, and miR-206; this highlighting its potential application as a biomarker for Duchenne muscular dystrophy.

The presented findings introduce miR-501 as a novel muscle-specific miRNA that regulates the muscle regeneration process by repressing a gene, with no previously known function in muscle,

and controls the turnover of a developmental myosin. This opens up a new regulatory pathway, leads to a better understanding of regulatory mechanisms in skeletal muscle regeneration, and might contribute to therapeutic approaches for muscle degenerative disorders.

Zusammenfassung

Das Skelettmuskel verfügt über eine bemerkenswerte Regenerationsfähigkeit. Diese Fähigkeit ist vor allem durch das Vorhandensein von muskelansässigen adulten Stammzellen, den so genannten Satelliten-Zellen oder myogenen Vorläuferzellen, gegeben. Eine ordnungsgemäße Funktion der Satelliten-Zellen ist essentiell für die Entwicklung und Aufrechterhaltung der Skelettmuskulatur. MicroRNAs sind eine Klasse von kleinen, nicht-kodierenden RNAs, die bei der Regulation der Genexpression beteiligt sind. Sie spielen eine wichtige Rolle bei der Feinabstimmung vieler zellulärer Signalwege und tragen so zur Gewebe-Homöostase bei, wobei ihre Funktion unter Stressbedingungen oder Verletzungen vermehrt zum Tragen kommen. Hinweise häufen sich, dass microRNAs wichtige Regulatoren der Skelettmuskelfunktion, Homöostase und Regeneration sind. In der vorliegenden Studie haben wir eine neuartige muskelspezifische microRNA, miR-501 identifiziert und ihre Rolle in Myoblasten im Rahmen der Skelettmuskelregeneration untersucht. Wir beobachteten, dass miR-501 gemeinsam mit dem Wirtsgen Clcn5 in aktivierten Satellitenzellen und in den regenerativen Muskeln deutlich hochreguliert wird. Im Vergleich der zwei verschiedenen Spleißvarianten Clcn5 fanden wir eine deutlich stärkere Hochregulierung der Isoform 2-Transkripte, welche miR-501 im Intron beherbergen. Allerdings spielt die post-transkriptionelle Genregulation eine wichtige Rolle bei der Verarbeitung von miR-501 aus diesem Intron. Expressionsprofile von miR-501 in verschiedenen Geweben zeigten ihre außerordentlich hohen Expressionsniveaus in Satellitenzellen und primären Myoblasten. Die pharmakologische Hemmung von miR-501 bei der Regeneration der Skelettmuskulatur führte zur drastischen Reduzierung von embryonalen Myosin Heavy Chain Proteinen (eMHC), während die Proliferationsrate von Myoblasten unverändert blieb. Wir identifizierten und validierten mehrere miR-501 Zielgene durch Loss-of-Function Screenings in primären Myoblasten. Durch Überexpression einzelner Zielgene in Myoblasten, fanden wir Gigaxonin als potentiellen Mediator der miR-501-Funktion, welche die Wirkung einer miR-501 induzierten Hemmung von eMHC in primären Myoblasten nachahmte. Da Gigaxonin bekannt ist für den Abbau von Intermediärfilamenten, stellen wir die Hypothese auf, dass eine Hochregulation von miR-501 während der Skelettmuskelregeneration die eMHC Proteine gegen eine Gigaxonin vermittelte Ubiquitinierung und Degradation schützt. Schließlich

beobachteten wir deutlich erhöhte miR-501 Werte in der Skelettmuskulatur und im Serum von *mdx*-Mäusen. Ähnlich zu den bekannten myomiRs miR-1, miR-133 und miR-206, ändern sich die miR-501 Blut-Werte während der Alterung von *mdx*-Mäusen, was ihre mögliche Anwendung als Biomarker für Duchenne-Muskeldystrophie hervorhebt. Die vorgestellten Ergebnisse zeigen miR-501 als neuartige, muskelspezifische microRNA, die den Muskel-Regenerationsprozess reguliert, indem sie ein Gen unterdrückt, dessen Funktion im Muskel bislang unbekannt war, und somit den Umsatz eines Entwicklungs-Myosins steuert. Dies führt zu einem besseren Verständnis der Regulationsmechanismen in der Skelettmuskelregeneration und könnte zu therapeutischen Ansätzen für degenerative Muskelerkrankungen beitragen.

Abbreviations

7-AAD	7-aminoactinomycin D
Ago	Argonaute
ATP	Adenosine triphosphate
bp	Base pair
cAMP	Cyclic adenosine monophosphate
cDNA	Complementary DNA
CK	Creatine kinase
CTR	Calcitonin receptor
CTX	Cardiotoxin
Cx43	Connexin 43
DAPC	Dystrophin-associated protein complex
DAPI	4',6-diamidino-2-phenylindole
DGC	Dystrophin-glycoprotein complex
DGCR8	DiGeorge syndrome critical region gene 8
DMD	Duchenne muscular dystrophy
DMEM	Dulbecco's modified Eagle's medium
DNA	Desoxyribonucleic acid
DNase	Deoxyribonuclease
dNTP	Desoxynucleoside triphosphate
dsRNA	Double-stranded RNA
ECM	Extracellular matrix
EDTA	Ethylenediaminetetraacetic acid
EdU	5-ethynyl-2′-deoxyuridine
EGF	Epidermal growth factor
eGFP	enhanced green fluorescent protein

eMHC	Embryonic myosin heavy chain
ERK	Extracellular signal-regulated kinase
FAP	Fibro-adipogenic precursors
FGF	Fibroblast growth factors
FPKM	Fragments Per Kilobase of transcript per Million mapped reads
Fstl1	Follistatin-like 1
GAPDH	Glycerinaldehyd-3-phosphat-Dehydrogenase
GW182	Glycine-tryptophan repeat-containing protein of 182 kDa
HDAC	Histone deacetylase
HGF/SF	Hepatocyte growth factor/scatter factor
HSPG	Heparan sulfate proteoglycan
JNK	c-Jun N-terminal kinases
LIF	Leukemia inhibitory factor
MAPK	Mitogen-activated protein kinases
Mef2	Myogenic regulatory factors 2
miRNA	MicroRNA
MMP	Matrix metalloproteinases
mRNA	Messenger RNA
Myf5	Myogenic Factor 5
MyoD	Myogenic differentiation 1
NMJ	Neuromuscular junction
NO	Nitric oxide
nPTB	Neuronal polypyrimidine tract-binding protein
NTX	Notexon
PAGE	Polyacrylamide gel electrophoresis
Pax3	Paired box 3

Pax7	Paired box 7
PBS	Phosphate buffered saline
PCP	Planar cell polarity
PCR	polymerase chain reaction
PDGF-BB	Platelet-derived growth factor-BB
Pdgfra	Platelet-derived growth factor receptor alpha
qPCR	Quantitative PCR
qRT-PCR	Quantitative reverse transcription polymerase chain reaction
RAC	Ras-Related C3 Botulinum Toxin Substrate
RISC	RNA-induced silencing complex
RNA	Ribonucleic acid
ROCK	Rho-associated protein kinase
S1P	Sphingosine-1-phosphate
SDF1	Stromal cell-derived factor 1
SDS	Sodium dodecyl sulfate
Six1	Sine oculis homeobox 1
SMA	Smooth muscle actin
SRF	Serum response factor
ssRNA	Single-stranded RNA
TA	Tibialis anterior
Tie2	TEK tyrosine kinase, endothelial 2
TRBP	TAR-RNA binding protein
Vangl2	VANGL Planar Cell Polarity Protein 2
WNT	Wingless-related integration site
WT	Wild type
YY1	Ying Yang 1

Chapter 1 - Introduction

1.1 Skeletal muscle structure

Skeletal muscle is the most abundant tissue in the human body, composing 40-50% of the total body mass (1). Major functions of skeletal muscles include skeletal movement and maintaining posture and body position (2). In addition, there is growing body of evidence introducing skeletal muscle as an endocrine organ, as it secretes a variety of molecules referred to as myokines (3).

Skeletal muscles are mainly consisted of myofibers, interlaced by a network of nerves and blood vessels, and held together by connective tissue and ECM. In the first level, fibers are surrounded by the basal lamina (composed of Laminin, collagen IV, fibronectin, and proteoglycans) and then again by reticular lamina, which is made of collagen fibrils. These two layers are collectively named basal membrane. The most exterior layer is endomysium, which is mostly consisted of collagen fibers and is in direct contact with blood vessels and nerves (4-6).

Each muscle fiber is formed by fusion of several mononucleated myoblasts during development (7). As a result, myofibers are very long cells, measuring up to 30 cm in human, and multinucleated. Having several nuclei is necessary to meet the high demand for protein synthesis in these cells. However, these nuclei are postmitotic and cannot enter the cell cycle and divide anymore (4). In their interior, myofibers are mainly constituted of myofibrils. Myofibrils are composed of tandem arrays of sarcomeres, which are the basic functional units of the skeletal muscle (8). Within the sarcomeres are thick and thin filaments, mainly composed of myosin and actin filaments, respectively. Triggered by release of calcium into cytoplasm and powered by ATP hydrolysis, sliding the filaments leads to shortening of the sarcomeres and generation of contractile force (8, 9). A schematic representation of skeletal muscle structure is shown in Fig 1.1.
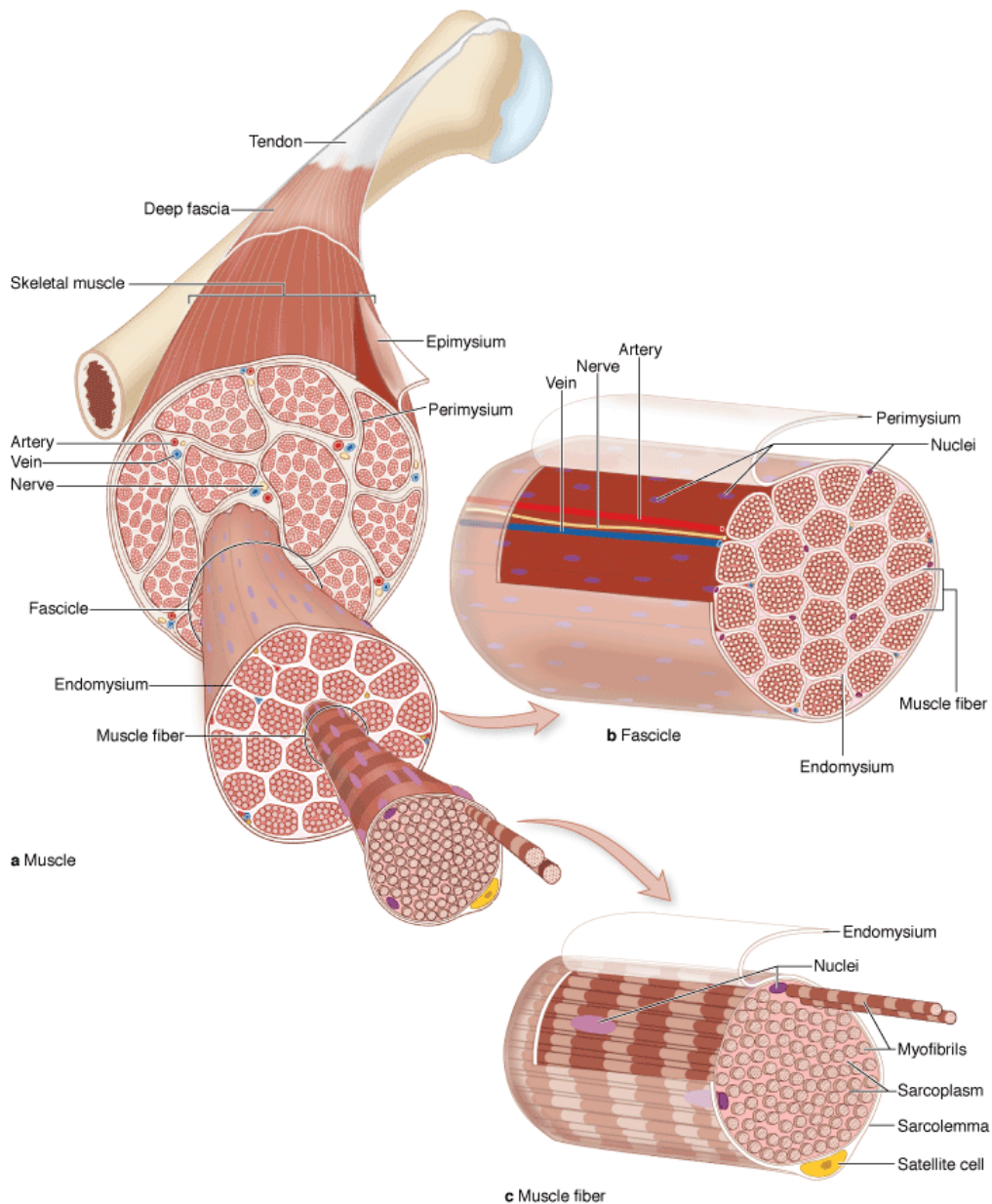
Figure 1.1. Structural organization of skeletal muscle. A) The entire skeletal muscle is enclosed within a dense connective tissue layer called the epimysium continuous with the tendon binding it to bone. **B)** Each fascicle of muscle fibers is wrapped in another connective tissue layer called the perimysium. **C)** Individual muscle fibers (elongated multinuclear cells) are surrounded by a very delicate layer called the endomysium, which includes an external lamina produced by the muscle fiber (and enclosing the satellite cells) and ECM produced by fibroblasts. Figure adapted from (10).

1.2 Skeletal muscle regeneration

1.2.1 Discovery of Satellite cells

Skeletal muscle has an enormous capacity to regenerate. This has been known since the 19th century (11). Although some basic characterizations of muscle regeneration were performed, there was no clear idea about the origin of the new myofibers (4, 12). Among several hypotheses was existence of special cells in the muscle, apart from myofibers, possessing myogenic potential. The first evidence for presence of such cells was reported in 1917; it was observed that when put in culture media, small chick embryonic muscles gave rise to "myoblasts" and finally multinucleated myotubes (13). In 1961, two independent observations were reported using electron microscopy on frog and rat muscles, by Alexander Mauro and Bernard Katz, respectively (14, 15). Mauro described some small mono-nucleated cells "wedged between the plasma membrane of the muscle fiber and the basement membrane", "the surface of the fiber is not distorted outward, but instead the satellite cell protrudes inward pushing the myofibrils of the muscle cell aside", he reported (16). It was already speculated by Mauro that those are the dormant cells able to proliferate and generate new myofibers during regeneration. As these cells were engulfed by the basement membrane yet outside of the sarcolemma, he named them "satellite cells". They have been observed in virtually all vertebrate species. Satellite cells contribution to the total myonuclei in mammalian muscles ranges from 30% in newborns to 1-5% in adults (17, 18).

1.2.2 Satellite cells in hypertrophy and regeneration

Myofiber nuclei are post-mitotic, but there is a low turnover of the myonuclei in the muscle (19). Using satellite cells labeled with [^{3}H]TdR, it was demonstrated that satellite cells can fuse to myofibers or make new fibers, in an ex vivo experiment (20). Several other studies have provided more evidence for the hypothesis that satellite cells are the source of new myonuclei, and play essential roles in skeletal muscle regeneration (21). Though this notion has been widely accepted, the definite proof for indispensability of satellite cells for muscle regeneration came in a study by Sambasivan et al. (22). Using transgenic mice expressing diphtheria toxin receptor under control of Pax7 promoter, they ablated all Pax7^{+} satellite cells by injection diphtheria toxin. After induction of muscle injury by CTX injection or by strenuous resistance exercise and monitoring the regenerating muscles, there was virtually no myofiber with centrally-located nuclei observed

in Pax7$^{DTR/+}$ mice. This phenotype was rescued by transplantation of adult Pax7$^+$ satellite cells. Although there have been some other cell populations in skeletal muscle suggested to participate in regeneration, this study showed that none of them can compensate for the depletion of Pax7$^+$ satellite cells.

It has been a matter of debate whether satellite cells are true "stem cells" (23). A rather stringent criterion for stemness is that a stem cell must maintain the long-term capability to make at least one differentiated cell type and to self renew (24). Nevertheless, there are several lines of evidence proving satellite cells to be stem cells. For example, engraftment of a single myofiber along with its few associated satellite cells into radiation-ablated TA muscle of *mdx* mice gave rise to generation of more than a hundred myofibers and a pool of new satellite cells, all originated from the engraft (25). In another study, a single transplanted Pax7$^+$ satellite cell could significantly contribute to generation of new fibers after repeated rounds of NTX-induced injury, and donor-derived cells were observed in the satellite cell niche and could be re-isolated based on Pax7 expression (26). The most striking evidence for stemness of satellite cells is provided by a more recent study (27). A pool of satellite cells isolated from Pax7-nGFP mice were transplanted to injured muscle, and GFP$^+$ satellite cells were isolated three weeks later from the regenerating muscle and transplanted again. The injury-isolation-transplantation circle was repeated for six times successfully. Altogether, participation of satellite cells in skeletal muscle regeneration can be elucidated briefly as in Fig. 1.2.
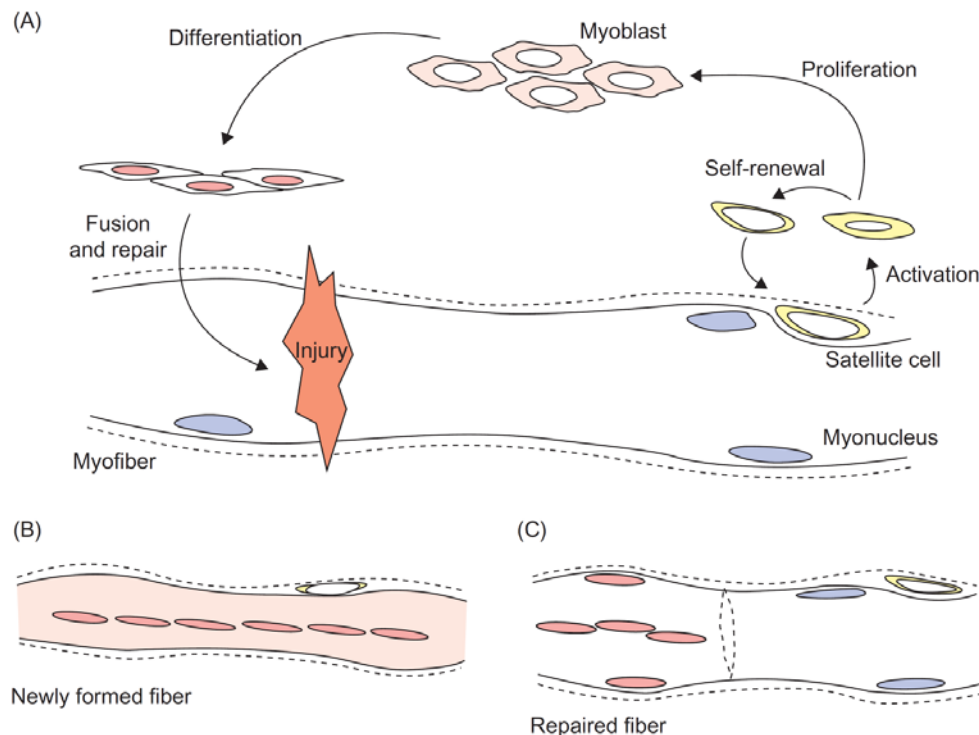
Figure 1.2. Satellite cells in skeletal muscle regeneration. A) Injury or exercise activates the muscle-resident satellite cells. They proliferate and generate committed myoblasts or self-renew. Myoblasts fuse together to make new myofibers **(B)** or fuse into partially damages fibers **(C)**. Figure adapted from (28).

1.2.3 Myogenic regulatory factors involved in skeletal muscle regeneration

The regeneration process includes activation of satellite cells, their proliferation and differentiating to committed myoblasts, which finally fuse to make or repair myofibers. The entire procedure is elaborately regulated by various transcription factors, Pax7 and the four myogenic regulatory factors (MRFs): MyoD, Myf5, Myogenin, and MRF4. Accordingly, muscle regeneration can be split into several steps (4). All quiescent satellite cells express Pax7 (29-32), and most of them (~90%) express Myf5 as well (33). Muscle injury leads to releasing of several factors which activate the satellite cells, their movement toward the site of injury, and re-entering the cell cycle. Some cells do not express Myf5, and go back to quiescence to replenish the stem cell pool (4). Proliferating Myf5$^+$ myoblasts, however, still express Pax7 as well as MyoD. At the end of proliferation phase Myf5 expression increases and Pax7 is downregulated as the myoblasts approach the differentiation. MyoD upregulates myogenin and MRF4, which are required for functional development of muscle by inducing the expression of structural proteins of the muscle contractile machinery (16). At this step, expression of Pax7 and Myf5 is inhibited while the cells, now called myocytes, are positive for MyoD, myogenin, and MRF4. Progression of satellite cells toward myotubes is indicated in Fig. 1.3.
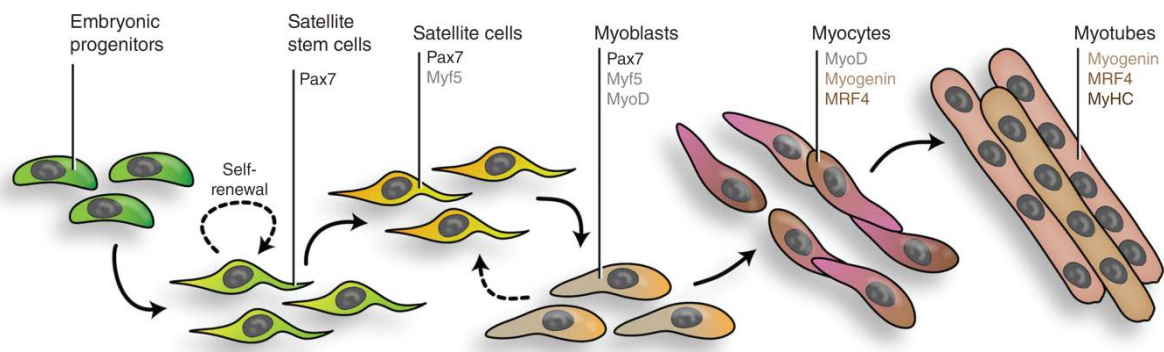
Figure 1.3. Myogenic regulatory factors regulate maintenance, proliferation, and differentiation of satellite cells. Adapted from (4).

1.2.4 Activation of satellite cells

Muscle injury, induced by either toxin injection or exercise, triggers the activation of satellite cells via both intrinsic and extrinsic signals. For instance, expression of Calcitonin receptor (CTR) is downregulated quickly when the satellite cells are activated. Via cAMP signaling CTR inhibits activation of satellite cells, and muscle regeneration was shown to be dramatically compromised when CTR was inhibited (7, 32, 34). Muscle injury induces metabolization of sphingomyelin, which is in the inner side of only quiescent satellite cell plasma membranes, to Sphingosine-1-phosphate (S1P). S1P promotes the proliferation of satellite cells ex vivo, and enhances muscle regeneration (35, 36). Moreover, inhibition of S1P biogenesis from sphingomyelin disturbs muscle regeneration (37). There is evidence that S1P acts in both autocrine and paracrine modes by binding its receptors, S1PRs, on satellite cells (38, 39).

Activation signals can originate also from the myofiber niche, e.g. necrotic and degenerating myofibers. Compromising the integrity of sarcolemma or basal lamina leads to increased extracellular calcium levels (40). This activates the calpain enzymes, a group of calcium-activated cysteine proteinases (41-43), which initiate the disintegration of the myofibers by proteolysis of structural proteins, such as actin, myosin, titin, and components of Z-disk (44). In addition to providing a protective niche, basal lamina has a critical role in transmitting the activation signals to satellite cells. Growth factors bound to proteoglycans in ECM are released upon degeneration of myofibers and remodeling of ECM (45-47). Growth factors are also released by proliferating myoblasts, acting in an autocrine or paracrine fashion. Infiltrating cells such as neutrophils, macrophages, T-cells, and platelets are another source of growth factors. Part of the newly synthesized growth factors will be deposited in ECM again, ready to be releases in

case of an injury. The best characterized growth factors controlling satellite cell proliferation are IGF-1, IGF-2, FGF-2, EGF, PDGF-BB, HGF/SF, SDF-1, and LIF (8, 44, 48-54). However, HGF/SF is the only one which besides acting as a growth factor is able to force the satellite cells exit the quiescent state and enter the cell cycle, making it indispensable for efficient skeletal muscle regeneration (55, 56).

The first step in search for growth factors in muscle which can activate the satellite cells was an experiment by Bischoff in 1986 (55). He reported that crushed muscle extract, by factors he could not identify, is able to specifically activate the satellite cells attached to isolated myofibers from rat. A similar experiment on murine satellite cells was performed in 1993 (57). Five years later, HGF/SF was identified by Tatsumi and colleagues as the underlying growth factor (56). They observed increased cell proliferation in rat TA muscle injected with HGF/SF, while neutralizing HGF/SF by antibody injection decreased cell proliferation. The same effect of HGF inhibition was observed on rat myoblasts cultured ex vivo (58). Interestingly, HGF/SF expression in injured muscle is proportional to the extent of injury and the number of satellite cells (59). Myofiber damage leads to release of nitric oxide synthase from basal lamina. Production of NO activates MMPs, which release the HGF entrapped in local HSPGs (34, 60-62). HGF acts by binding to c-Met receptor, expressed in quiescent satellite cells. The signal is transduced by autophosphorylation of tyrosine kinase residues of c-Met intracellular domains (63, 64). Subsequently, ERK1 and ERK2 become activated by phosphorylation and translocate into the nucleus and induce transcription of Cyclin D1, which is required for progression through G1 phase of cell cycle (65).

1.2.5 Asymmetric division and self-renewal of satellite cells

A hallmark of satellite cells, as of other stem cells, is their ability to self-renew. This can be done in two modes of cell division: asymmetric, and symmetric. Asymmetric cell division gives rise to two different daughter cells, one keeps the stem cell characteristics and the other is committed toward differentiation. In contrast, in symmetric cell division two similar daughter stem cells are generated. Either of the fashions will maintain the pool of stem cells. Neuronal stem cells and mammalian spermatogonial stem cells are well-studied examples for self-renewal by asymmetric and symmetric divisions, respectively (66-68).

$Pax7^+/Myf5^-$ satellite stem cells are shown to be able to divide in both symmetric and asymmetric modes (33). The major decisive factor seems to be the orientation of mitotic spindle relative to the myofiber. Asymmetric divisions predominantly happen in basal-apical divisions, i.e. when the mitotic spindle is perpendicular to the length of the flanking myofiber. The division generates a satellite "stem" cell ($Pax7^+/Myf5^-$), adjacent to the basal lamina, and a satellite "myogenic" cell ($Pax7^+/Myf5^+$), touching the sarcolemma. In contrary, in most of the symmetric (planar) divisions the mitotic spindle is parallel to the myofiber, and both daughter cells will consequently be in touch with both basal lamina and myofiber membrane. Both $Pax7^+/Myf5^-$ and $Pax7^+/Myf5^+$ satellite cells can undergo symmetric division (66) (Fig. 1.4).
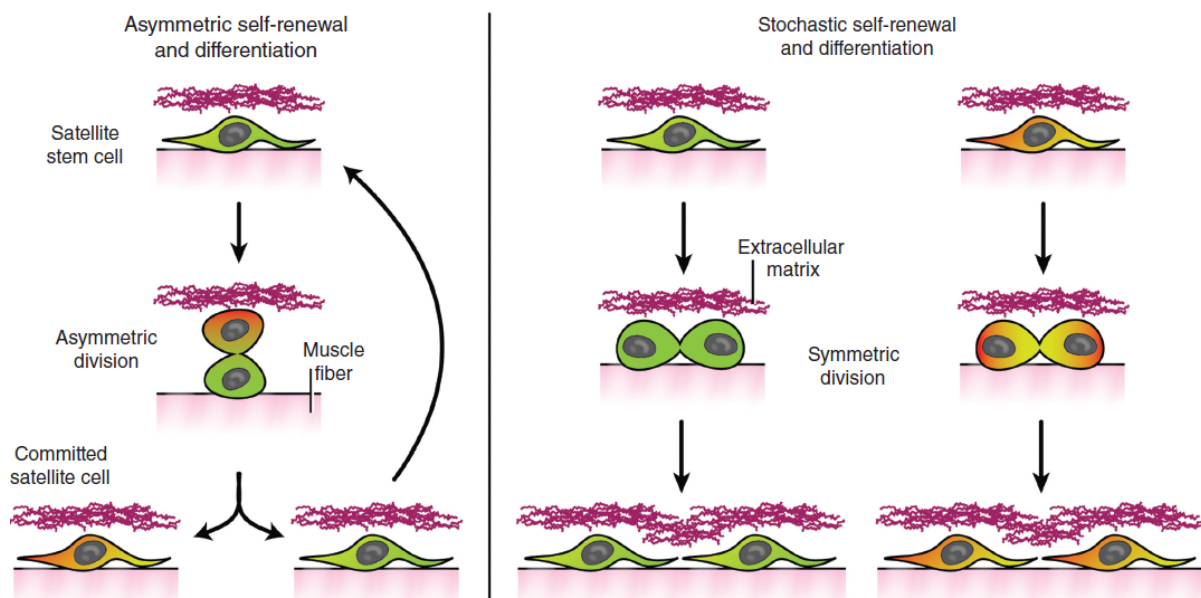
Figure 1.4. Asymmetric and symmetric division of satellite cells. The type of division is mainly dictated by the orientation of mitotic spindle. Adapted from (4).

While both asymmetric and symmetric divisions are possible for satellite stem cells under physiological conditions, the former is preferred during acute injuries or chronic muscle diseases (69). For instance, the percentage of $Myf5^-$ satellite cells increases from ~10% in normal muscle to ~30% three weeks after injury (33).

The critical role of Notch signaling in asymmetric division and self-renewal of satellite cells was shown by Kuang and colleagues (33). Despite $Myf5^-$ cells, $Myf5^+$ cells express high levels of Notch ligand Delta-1 and also Notch3. On freshly isolated myofibers, blocking of Notch signaling in proliferating satellite cells by treating with DAPT reduced the total cell number in

culture after three days. This is while the relative frequency of Pax7$^+$/MyoD$^-$ satellite cells was increased significantly (33). Consistently, the Notch antagonist Numb was observed to be localized asymmetrically in proliferating satellite cells, segregating together with desmin and M-cadherin towards the myogenic daughter cell (70).

On the other hand, non-canonical Wnt planar cell polarity (PCP) pathway regulates the symmetric division of satellite cells (71). Frizzled7, the receptor for Wnt7a, is highly expressed in Myf5$^-$ cells, and Wnt7a is upregulated during regeneration. Binding of Wnt7a to Frizzled7 activates the Rac/JNK and Rho/ROCK pathways through the cytoplasmic phosphoprotein Disheveled (72). When isolated myofibers and their associated satellite cells were treated with recombinant Wnt7a in the culture media, the rate of symmetric cell divisions increased more than two folds. In contrary, knocking down Vangl2, a core component of PCP pathway, significantly increased the rate apical-basal cell divisions (71). The Wnt7a/Frizzled7-mediated symmetric cell division is enhanced by binding of fibronectin, an ECM protein, to Frizzled7. This exemplifies the important role of physical interaction with the microenvironment in supporting self-renewal of satellite cells (4, 33).

Self-renewal of the satellite cells also relies on their ability to exit the cell cycle and return to quiescent state. BrdU$^+$ quiescent satellite cells were detected after muscle regeneration in the presence of BrdU (73). Transcriptome analysis on quiescent and proliferating satellite cells has indicated a general decrease in mRNA and miRNA amount, which can be attributed to the observed increase in the activity of RNAseL enzyme, when satellite cells shift to quiescence (4, 74). ERK1/2 pathway plays an important role in regulating the return to quiescence. Tie-2 receptor is expressed preferentially by quiescent satellite cells is targeted by Angiopoietin-1 secreted from smooth muscle cells and fibroblasts in the micro-environment during regeneration. This interaction was shown to decrease both proliferation and differentiation of myogenic precursor cells, promote cell cycle exit and the expression of quiescence markers such as Pax7 and M-cadherin (75). Furthermore, the homeodomain transcription factor Six1 in proliferating satellite cells has been shown to directly control the transcription of Dusp6, which inhibits phosphorylation of MAPK (76).

1.2.6 Contribution of FAPs in skeletal muscle regeneration

A new population of progenitor cells resident in skeletal muscle was characterized independently by two groups in 2010 (77, 78). Joe and colleagues isolated $CD45^-CD31^-\alpha7$-integrin$^-$ScaI$^+$CD34$^+$ cells by FACS from digested preparation of mouse muscle, and termed these cells as FAPs (fibro/adipogenic progenitros) (77). Using slightly different cell surface markers, Uezumi and colleagues isolated the same population based on $CD45^-CD31^-$SM/C2.6$^-$PDGFRα^+ selection strategy, and named them mesenchymal progenitors (78). FAPs were indicated to undergo spontaneous differentiation to adipocytes and fibroblasts in culture, characterized by expression of perilipin/peroxisome and α-SMA, respectively. In vivo experiments by both groups showed that FAPs differentiate to adipocytes when transplanted to skeletal muscle injected with glycerol. Fibrogenic potential of FAPs in vivo was documented later on by transplantation into CTX-injected γ-irradiated skeletal muscle (79). FAPs are located predominantly close to the blood vessels associated with myofibers, as revealed by immunohistochemistry (77-81). However, being negative for neuroglial 2 proteoglycan distinguishes them from pericytes (81).

Interestingly, similar to satellite cells, FAPs are activated and proliferate massively after muscle injury (77, 78). Nevertheless, cell tracking experiments show that these cells do not contribute to the myonuclei pool (77). This was corroborated by in vitro experiments, showing that FAPs never give rise to myotubes expressing myosin heavy chain, in any of the culturing conditions tested (77, 78). However, they are reported to secrete pro-differentiation factors to facilitate myotubes formation, as suggested by co-culture experiment results (77). They can also boost myogenesis by releasing IGF-1 and increasing removal of degeneration debris by phagocytes (77, 82). Reciprocally, cell fate of the FAPs seems to be mainly determined by non-cell autonomous mechanisms; FAPs in CTX-injected muscle do not differentiate to adipocytes, while they show prominent adipogenic capability when muscle damage is induced by glycerol injection. Remarkably, FAPs isolated from both injury models showed the same cellular characteristics (78). Co-culturing isolated GFP$^+$ FAPs with myogenic progenitors dramatically inhibited their adipogenic potential (78).

Altogether, the current model for the function of FAPs during regeneration suggests mutual regulatory mechanisms between proliferating myoblasts and FAPs (83). While FAPs provide necessary signals for differentiation of myoblasts, the fate of FAPs is dependent mainly on the efficiency of regeneration. Efficient regeneration leads to ablation of FAPs and their return to the original number before injury, while a failed regeneration promotes differentiation of FAPs to

adipocytes (78, 83) (Fig. 1.5). Increased population of FAPs and fatty degeneration due to their aberrant differentiation to fibroblasts and adipoocytes is reported in several chronic muscular pathologies, including Duchene muscular dystrophy (84).
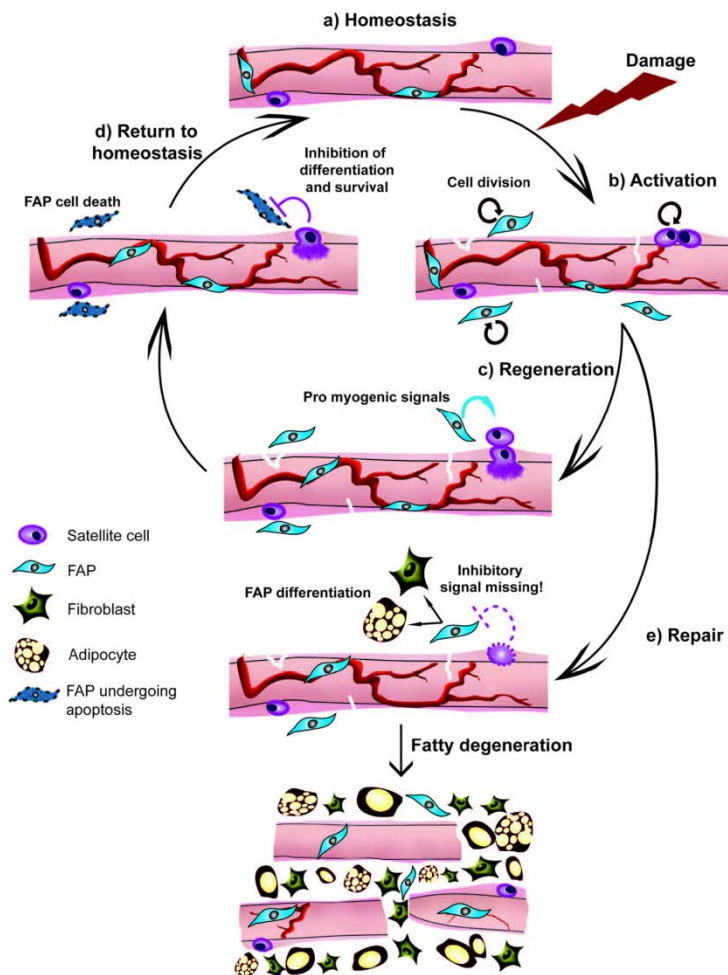

Figure 1.5. Function of FAPs during muscle regeneration. Muscle injury activates both MPs and FAPs (b); FAPs enhance the regeneration process by releasing trophic factors (c), and undergo apoptosis after successful regeneration (d). FAPs differentiate when regeneration fails (e).Adapted from (83).

1.2.7 Myosin heavy chain isoforms in skeletal muscle development

The contractile force in skeletal muscle is generated by ATPase activity of a class of muscle-specific myosin molecules, known as Myosin II or conventional myosins. They exhibit a hexameric protein structure, composed of two myosin heavy chains (MHCs), two essential myosin light chains (MLCs), and two regulatory MLCs (85, 86). Importantly, there are several MHC isoforms encoded by different genes, which show a high degree of regulation within different muscle types and also during development (87-90). Indeed, myofibers are categorized based on their expression pattern of MHCs; myofibers expressing MHC I, encoded by Myh7 gene, are slow-twitch or type-1 fibers. Fast-twitch myofibers are divided to type IIa, IIb, and IIx, as they express MHCs encoded by Myh2 (IIa), Myh4 (IIb), or Myh1 (IIx) genes (91). Accordingly, MHC composition explains the contractile, metabolic, and morphological heterogeneity among different muscles. This is mainly due to difference in ATPase activity among MHC isoforms (92).

Apart from the above-mentioned MHCs expressed in adult mammalian skeletal muscles, in 1981 two so-called "developmental MHCs" were found to be expressed in developing rat skeletal muscle, preceding the expression of adult fast MHCs (93). They were referred to as embryonic and perinatal/neonatal MHCs (eMHC and neo-MHC, respectively), and their corresponding genes were reported as Myh3 and Myh7 (94, 95). In situ hybridization on mouse embryo detected eMHC and neo-MHC transcripts as early as E9.5 and E10.5, respectively (96). Based on the presence of E-boxes responsive to Myf5 and MyoD in proximal promoters of eMHC and neo-MHC, it is suggested that the expression of developmental myosins is controlled by these transcription factors (97, 98).

During the early postnatal development, in most skeletal muscles the adult myosins are upregulated in parallel with quick downregulation of the developmental myosins. For instance, in a comprehensive study on postnatal changes in different types of mouse skeletal muscles, it was observed that while in new-born mice eMHC and neo-MHC constituted about 30% and 65% of MHC protein content respectively, at three weeks of age no eMHC was detected and neo-MHC was undetectable as well or was present at strongly reduced levels (99). While all the examined muscles showed the same pattern of transition from developmental to adult MHC, the timing is greatly varied between different muscles, in both mRNA and protein levels (99, 100).

Mechanisms responsible for controlling the switch from developmental to adult MHCs are not very well understood; however, it is known that hormonal and neural factors can modulate this process (101). Thyroid hormone signaling is known to be essential for this transition, as hyperthyroidism propels the expression of adult fast MHCs, and the switch is delayed or incomplete in the absence of the thyroid hormone (102-104). Thyroid hormone-regulated transcription of an antisense RNA from Myh8-Myh4 intergenic region is recently indicated to mediate repression of neo-MHC expression (105). While the expression of fast adult MHCs seems to be independent of the nerve activity, slow MHC expression and replacement of eMHC is absolutely dependent on the stimulation by neural activity (103, 106, 107).

1.2.8 Developmental myosins in regenerating muscle

Skeletal muscle regeneration resembles the myogenesis during development in many aspects, such as the expression of developmental myosins (100, 108). At 2-3 days after injury, eMHC and neo-MHC start to express, and for about two weeks stay detectable by immunostaining of tissue sections (101). This renders the developmental myosins a useful marker for skeletal muscle regeneration in both animal models and human myopathies (109, 110). For instance, application of eMHC as a diagnostic marker is suggested for rhabdomyosarcoma (111, 112).

Neuronal regulation of developmental-to-adult MHC transition applies also to the muscle regeneration. Again, switch to fast adult MHCs is nerve-independent, while switch to type I MHCs depends not only on the nerve activity, but also on the pattern of the signals, as they need to resemble those of the slow-twitch motor neurons (113-116). In a study on regeneration of rat soleus muscle, which is consisted mainly of slow-twitch myofibers, it was observed that denervation prevents the expression of type I MHCs, leading to accumulation of fast MHCs replacing developmental myosins (117).

1.2.9 Function of developmental myosins

Decades after their identification, the role of developmental myosin heavy chains is still not completely understood (101). From a structural point of view, there is no support for the hypothesis that developmental myosins facilitate the correct assembly of the myofibrils, though class II non-muscle myosins are known to contribute to this process (118). It should also be noted that generation of myofibrils in cardiac muscle, which are almost identical to those in skeletal

muscle, happens without eMHC being expressed (119). Another hypothesis could be that developmental myosins have properties which make them more suitable for the prenatal period. It is known that the ATPase activity of neo-MHC is higher than eMHC and lower than any of the adult MHCs (120). This means that developmental myosins enable contractions with the lowest energy expenditure (101). Concordant with this idea, it is speculated that mechanical stimuli derived from slight muscle contractions are required for proper development of fetal joints, tendons, and bones, but the contraction must not be too strong (101). Considering the fact that extraocular muscles need to generate much lower contractile force compared to other striated muscles, this can also help explain why they keep on expressing the developmental myosins (121).

1.2.10 Hereditary myopathies associated with Myh3 mutations

Mutations in the Myh3 gene, encoding eMHC, are associated with three forms of distal arthrogryposis (DA): DA1, Freeman-Sheldon syndrome (FSS, or DA2A), and Sheldon-Hall syndrome (SHS, or DA2B) (122-124). DA syndromes are characterized by contractures of the distal regions of the hands and feet (125). Facial involvement and scoliosis are also observed in types 2A and 2B (126). Myh3 mutations account for almost all cases of FSS and about one third of SHS cases (124). SHS can also be caused by mutations in Tnni2 (encoding fast troponin I), or Tnnt3 (encoding fast troponin T) genes, with no difference in the phenotype (124).

FSS is the most severe form of DA, and is easily characterized by striking contractures of the orofacial muscles (127). Typical symptoms are prominent nasolabial folds, 'H-shaped' dimpling of the chin, down-slanting palpebral fissures. Pinched lips and a very small mouth are also prevalent, making FSS known also as "whistling face syndrome" (124, 128). Analysis of the detected mutations indicated that virtually all of them compromise the catalytic activity of eMHC, which supports the idea that the congenital contractures are caused by defects in myofiber contractile activity during prenatal development; however, the mechanisms underlying the phenotypes caused by Myh3 mutations are not clear yet (124). It is worth mentioning that mutations in Myh3 do not cause weakness, progressive contractures or noticeable histological abnormalities of skeletal muscle (123, 124).

1.3 Duchenne muscular dystrophy

Duchenne muscular dystrophy (DMD) is an X-linked recessive disease affecting about 1 in 3,500 boys, making it the most common sex-linked lethal disease and the most frequent and severe type of muscular dystrophy in humans (129, 130).

1.3.1 Clinical considerations

DMD patients show no sign of the disease at birth, though the level of muscle-isoform Creatine kinase (CKM) is elevated in their serum. Affected boys achieve motor milestones later than normal; only 44% of them are able to walk before the age of 18 months (131). The first clinical manifestations appear between 3 and 5 years of age, often by excessive clumsiness, abnormal gait, difficulty in walking and running, and inability to jump (132). Progressive muscle weakness and joint contractures makes the virtually all patients wheelchair-dependent by the age of 12 (133). Finally, most of the clinical mortality is reported in the third decade of life, due to involvement of diaphragm and cardiac failure. In addition, one third of the patients suffer various degrees of cognitive inefficiency (129, 130).

1.3.2 Genetics of DMD

According to Haldane's hypothesis for a X-linked recessive disorder, the mutation rate equals 1/3(I)(1+f), where I denoted the disease incidence and f is the reproductive fitness. Since DMD is a lethal disorder, f = 0, and mutation rate is predicted to be one third of disease incidence; in other word, one third of the DMD cases are due to new mutations and not inherited. This has been shown to be close to reality according to direct mutation detection methods (134-136). The mutation rate for dystrophin gene is about 10^{-4} genes per generation, which makes it one of the highest rates of mutation reported. This can be attributed to the huge size of the DMD locus (131).

DMD gene allocates to itself the third largest locus in human genome, spanning 2.22Mbps on Xp21 band of X chromosome (137). The protein coding sequence is composed of 79 exons, which in conjugation with the 7 promoters and alternative splicing are transcribed to three full-length isoforms- M (in Muscle), B (in Brain), and P (in Cerebral Purkinje neurons)- and four truncated isoforms (Dp 260, Dp 140, Dp 116, and Dp 71). The muscle (M) isoforms encodes a

427-kDa protein, hence nameed Dp 427 (138). About two-third of the cases of DMD are due to deletion of part of coding sequence, and about 5% are caused by duplications (139). The rest of mutations are point mutations which lead to a truncated protein, e.g. nonsense mutations and small insertion/deletions which cause a frame shift. Mutations in the exon-intron boundaries or even in the introns can also cause DMD by affecting the splicing of the nascent mRNA (140, 141). Finally, inversions and rearrangements in the DMD locus are also reported, though they seem to be rare (142, 143).

1.3.3 Structure and function of dystrophin

Dystrophin protein folds into four major structural domains (Fig. 1.6). The N-terminal contains an actin-binding domain, encoded by exons 1-8 and composed of a pair of calponin homology (CH) modules. The majority of the protein, encoded by exons 9-63, forms 24 triple helical spectrin-like repeats interrupted by four hinge or spacer domains. This part of the molecules gives it a long rod-like flexible shape (144, 145). The third domain, encoded by exons 64-67, is a custeine-rich domain composed of two EF hand-like modules. The C-terminal domain is encoded by exons 68-79 and is responsible for binding to the dystrophin-associated protein complex (DAPC) in the sarcolemma and making a functional dystrophin-glycoprotein complex (131, 144, 146).
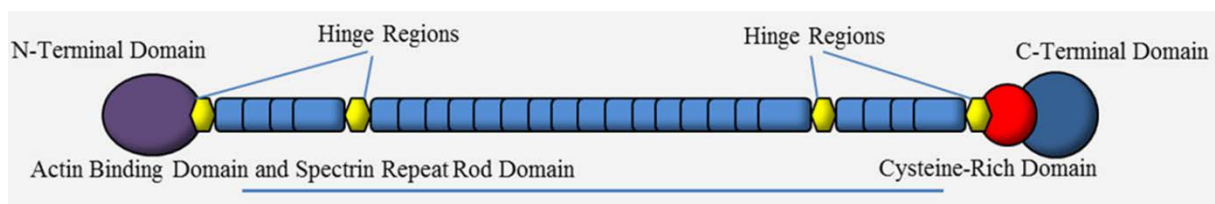
Figure 1.6. Structure of full-length dystrophin (Dp 427). Adapted from (147).

Dystrophin-glycoprotein complex (DGC) is a complex of several membrane-associated proteins which help maintain the sarcolemma integrity. In myofibers this complex is composed of dystrophin, the six sarcoglycans (α, β, δ, ε, γ, ζ), two dystroglycans (α and β), sarcospan, syntrophins (α1, β1, β2), dystrobrevins (α and β), caveolin-3, and nNOS (148, 149). Dystrophin binds to cytoplasmic actin and the β subunit of sarcoglycan, via its N- and C- terminal domains, respectively. On the extracellular side, α subunit of sarcoglycan connects the transmembrane β

subunit to the laminin-2 in basal lamina (146, 150, 151) (Fig. 1.7). Moreover, α-dystroglycan also binds the chondroitin sulfate proteoglycan biglycan to the two heparane sulfate proteoglycans present in the basement membrane, agrin and perlecan (149, 152-155). Therefore, DGC is considered to have a critical function by protecting the sarcolemma against contraction-induced shear force and rupture, by linking the ECM to the myofiber cytoskeleton (156, 157). Consistent with this supposition, loss or malfunctioning of components of this complex leads to a range of muscular dystrophies, as the loss of dystrophin causes DMD (149).
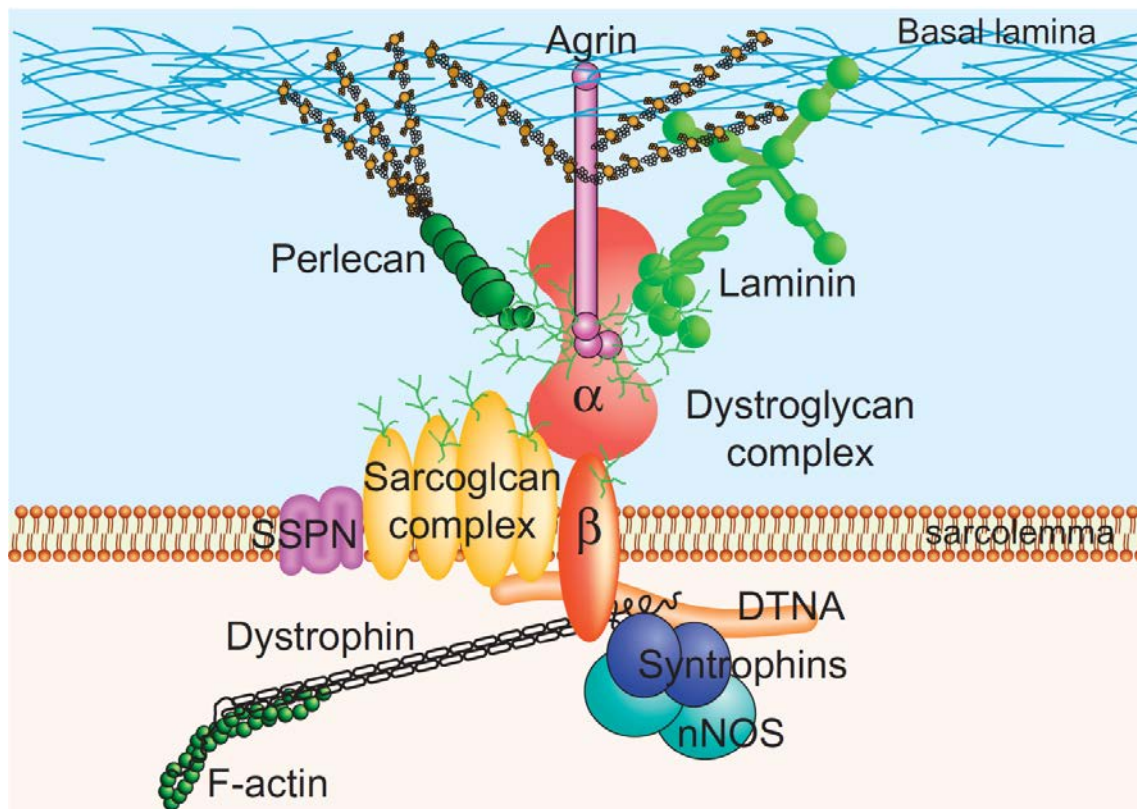
Figure 1.7. Components of the dystrophin-glycoprotein complex in skeletal muscle. DTNA: dystrobrevin; SSPN: sarcospan. Adapted from (158).

1.3.4 Mechanisms of pathogenesis in DMD

Two scientific breakthroughs on Duchenne muscular dystrophy were achieved in 1987: cloning of the DMD gene (159) and characterization of the encoded protein, dystrophin (160). Despite the anticipation that the disease would be soon conquered, there is no effective therapy for DMD available yet (161). Although the disease is certainly initiated by the lack of functional dystrophin, the pathology is most likely driven by several pathways, adding to the complexity of the disease (131).

Skeletal muscle biopsies from DMD patients are characterized by clusters of necrotic fibers, surrounded by macrophages and CD4$^+$ lymphocytes, with small immature myofibers (161-163). Thus, the symptoms of DMD are thought to arise from an imbalance between myofiber necrosis and regeneration (164). Dystrophin is a key component of DGC, the main function of which is to stabilize the myofiber plasma membrane during eccentric contractions. This has been the basis of the exercise-induced damage hypothesis (165, 166). Complete loss of DAPC has been shown as a consequence of dystrophin deficiency, and this is thought to cause membrane fragility (167, 168). Indeed, there is ample evidence for permeability of myofiber membrane in DMD. For instance, sarcoplasmic accumulation of albumin and immunoglobulins, along with absorption of Evans Blue and Procion orange dyes into the immersed muscles, have been reported (165, 169-172).

The mechanical hypothesis together with the loss of calcium homeostasis are the currently the main consensus hypotheses on the pathophysiology of DMD (161). The crucial role of calcium ion homeostasis in proper muscle function is well established (173). Remarkably, intracellular calcium accumulation and hypercontracted fibers are observed in muscle biopsies from DMD patients (161, 174-176). Increased flow of calcium, which is most likely via mechanosensitive voltage-independent channels, is also observed through membrane deficient in dystrophin (177-181). Therefore, it can be inferred that in a dystrophic muscle with permeabilized membrane the cytosolic calcium concentration in myofibers will be higher than normal; this will inhibit mitochondrial activity, cause myofiber hypoercontraction, and activate the cytosolic proteases, especially calpains, which in turn causes more membrane disintegration. Extremely high calcium level will finally cause cell death (138, 182-184). Consistently, normal control of calcium homeostasis is lost in *mdx* mice, and inhibition of calpains in *mdx* mouse muscle via overexpression of calpastatin is shown to reduce necrosis (161, 185-188).

1.3.5 The murine model for DMD: *mdx* mice

The *mdx* mice were first noticed during a screening concerning biochemical abnormalities in red blood cells (189). High levels of serum creatine kinase (CK) accompanied by extensive necrosis in myofibers were observed in some animals in an inbred C57BL/10 colony, and the phenotype was inherited in an X-linked manner. After identification of DMD locus in human, it turned out that the *mdx* mice are actually a naturally-occurring genetic homologue for this disease (190, 191). The molecular basis was revealed to be a point mutation making a premature stop codon in exon 23 of the dystrophin gene (192).

The *mdx* mouse has been the most extensively-used animal model to better understand the pathophysiological mechanisms of DMD and to test different therapeutic approaches (147). Histological analysis of *mdx* muscle shows well-defined pathological stages as in humans. The first disease manifestations appear as necrotic/apoptotic myofibers along with inflammation in muscle tissue at about 3 weeks of age (189). This provokes regeneration of the muscle, which is in its highest rate during the age of 6-12 weeks (109, 193-195). Within this time interval more than 50% of the myofibers have centrally-located nuclei, indicative of being regenerative fibers. This ratio approaches 100% at about 3 months of age (196). The regeneration in this phase is quite successful, and a balanced state is gradually reached, making it difficult to distinguish the *mdx* muscle from that of wild-type mice when the mice are older than 6 months (197). Nevertheless, the pathological process goes on during the whole life of the mice, even though in a low rate. The regeneration capacity is finally compromised due to decline in satellite cell number and proliferation capacity, and necrosis becomes prominent from 20 months of age on (198, 199). Similar to human DMD phenotype, accumulation of collagen is observed in the muscles of old *mdx* mice, they show progressive weakness muscle deterioration as they age, and have a 50% reduction in lifespan (198, 200, 201).

Although the *mdx* mice and DMD patients have the same genetic defect, a notably milder phenotype is observed in the *mdx* mice. There are at least two factors considered to contribute to such a difference, helping the mice better overcome the disease.

The first factor is functional compensation of dystrophin by utrophin. Despite dystrophin, utrophin is expressed in a wide range of tissues. It shows 85% similarity in amino acid sequence within N- and C-terminal regions with dystrophin (202, 203). They share their binding partners to some extent, as utrophin binds to cytoplasmic F-actin and dystroglycans in DAPC via its N- and C- terminal domains, respectively (138, 204). In human fetus utrophin is detected all over the sarcolemma, but upon appearance of dystrophin it becomes confined to neuromuscular junctions (NMJs) and myotendinous junctions (205-207). Remarkably elevated levels of utrophin are detected in muscles of *mdx* mice, and it is observed that utrophin becomes spread along the sarcolemma. Though a similar phenomenon is observed in DMD patients, it occurs at a lower extent (208, 209). Consistent with this hypothesis, it is found that mice lacking both dystrophin and utrophin show a much severe pathology compared to *mdx* mice, and die between 4-14 weeks of age (210).

Another possibility is the much higher proliferative ability of satellite cells in mice compared to human. While human satellite cells are exhausted relatively early, mice satellite cells can keep on proliferating and generating new fibers efficiently (211). This ability is believed to be, at least in part, due to the much-longer telomeres in murine cells compared to human satellite cells. Consistent with this idea, shortening the telomeres in muscle cells by knocking out the telomerase RNA component Terc (mTR) in *mdx* mice resulted in more severe muscular dystrophy phenotype and a decline in regenerative capacity, which could be ameliorated by transplanting wild-type satellite cells (212).

1.4 microRNAs and their role in skeletal muscle

1.4.1 Biology of microRNAs

microRNAs (miRNAs) are a class of small endogenous RNAs, 18-24 nucleotides in length, which regulate gene expression post-transcriptionally by binding to complementary sequences in their target mRNAs (213). MiRNAs are found in the genome of green algae, plants, animals, and some DNA viruses (214, 215). MiRNAs regulate many cellular pathways, including but not limited to proliferation, apoptosis, and differentiation (213, 216-219). Aberrant regulation of miRNAs is associated with many diseases, such as neurodegeneration and cancer (219-224). It is shown that more than 60% of human protein-coding genes have conserved binding sites for miRNAs (225), and to date there are more than 1,900 and 2,500 miRNAs identified in mouse and human genomes, respectively (miRBase release 21).

The first miRNA was discovered in 1993 during a study on *lin-4* gene. It was known that this gene regulates the timing of *C. elegans* development, but when isolated it was revealed that it does not encode a protein, rather two small RNAs, ~ 22 and 61 nucleotides in length (226). Sequence analysis showed that the *lin-4* small RNAs have complementarity to parts in the 3′ UTR of *lin-14* gene which were known to mediate its repression by *lin-4* (226, 227). Although a repression mechanism via binding of a small RNA to 3′ UTR of a protein-coding gene was defined, it was considered as a special case in *C. elegans*, until *let-7*, another 21-nt regulatory RNA, was discovered in the same species in 2000 (228, 229). *Let-7* or its homologs were shortly identified in 13 species, including human (230). Hence, the term microRNA was coined to refer to similar short RNAs, and a number-based nomenclature is used to name the miRNAs as they are discovered (231-235).

1.4.2 Biogenesis of microRNAs

miRNAs are located all over the genome. Their loci in the genome is used to categorize them as intergenic, intronic, or exonic (236, 237). Intergenic miRNAs are those which are transcribed as a separate transcription unit, independent from their flanking genes. In other words, the locus has its own regulatory elements and promoter, and the miRNA is the only transcription product of that locus (237, 238). The locus may also code several miRNAs which give rise to a polycistronic transcript. Intronic miRNAs are located in an intron of a gene, which might be protein-coding (such as miR-25 in MCM7) or a long noncoding RNA (such as miR-15a in DLEU2) (239, 240). Therefore, these microRNAs share the same promoter with their host gene, and they are certainly transcribed by RNA pol. II and need to be processed by the spliceosomal machinery (241). It is worth mentioning that if the miRNA is coded on the opposite strand relative to the host gene it cannot be categorized as an intronic miRNA, since its transcription is not driven by the host gene promoter and they are not released from the nascent transcript of the gene (242, 243). Mirtrons are a sub-category of intronic miRNAs which are directly generated from a short intron independent of the microprocessor (239, 244-246). Exonic microRNAs are relatively rare, and can be located on an exon in a protein-coding gene, such as miR-985 in CACNG8 gene, or a gene coding for a long noncoding RNA, such as miR-155 in BIC gene (Fig. 1.8) (239, 247).
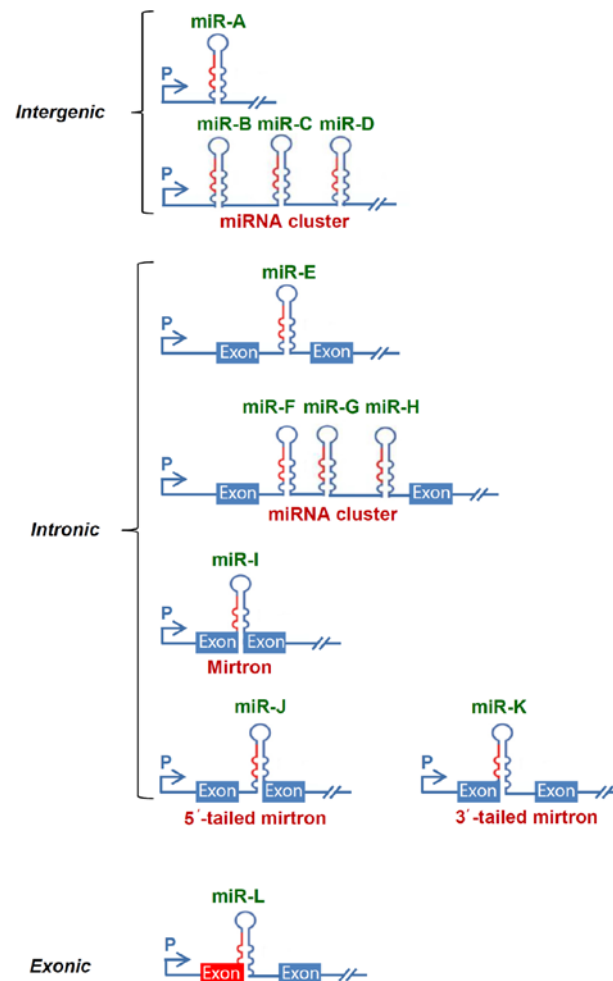
Figure 1.8. Genomic localization of miRNAs. Adapted from (248).

Transcription

There are several lines of evidence that most of the miRNAs are transcribed by RNA pol. II (249, 250). For example, miRNA primary transcripts (pri-miRNAs) can be longer than 1kb, and they often have consecutive uridine residues, both of which make RNA pol. III-mediated transcription unlikely. In addition, differential expression pattern of many miRNAs suggests their transcription by RNA pol. II. Finally, fusion of an ORF downstream of a miRNA has led to protein expression, which necessitates transcription by RNA pol. II (234, 251, 252). However, RNA pol. III-mediated transcription of miRNAs interspersed with Alu repeats in human genome is reported (253). In either case, the pri-miRNA needs to undergo the maturation process to release the mature miRNA (Fig. 1.9).

Nuclear processing and export

The first step of miRNA maturation is nuclear processing of the pri-miRNA transcript, which can be up to several kilobases long, is performed by the RNase III protein Drosha and its co-factor protein DGCR8 (known as Pasha in *D. melanogaster* and *C. elegans*) in the Microprocessor complex (254, 255). The miRNAs in the pri-miRNA transcript fold into stem-loop secondary structures about 70 nucleotides in length, flanked by the rest of transcript which stays single-stranded. This structure is recognized and bound by DGCR8, which interacts via its C-terminal with Drosha and guides it to make cleavages at about 11 nucleotides inside the stem part (256-259). This will release the ~65-nucleotide pre-miRNA hairpin, containing the miRNA imperfectly base-matched in a short stem having a 2-nucleotide 3′ overhang (256, 260, 261). Knocking out DGCR8 in embryonic stem cells leads to a global loss of miRNA in these cells, indicating the essential role of DGCR8 in miRNA biogenesis (262).

Several lines of evidence suggest a model in which processing of pri-miRNA transcript is performed co-transcriptionally (263-265). In the case of intronic miRNAs, it is hypothesized that cleaving the pri-miRNA by Drosha happens after the transcript is bound to the early spliceosome complex and before cutting out the introns, in a highly-coordinated manner (239). Drosha processing of intronic pri-miRNAs does not interfere with splicing, but in case of exonic miRNAs it destabilizes the transcript causing a reduction in protein synthesis (263, 266). In fact, Drosha is shown to downregulate its co-factor by cleavage of an exonic hairpin in DGCR8 transcript, and this mechanism might not be limited to DGCR8 only (239, 266).

Mirtrons are found in *C. elegans* (244), mammals (246, 267), avians (268) and Drosophila (245), and they are processed in the nucleus in a so-called "non-canonical" pathway. After splicing of the flanking exons, the lariat-shaped intermediate is debranched and a hairpin resembling the pre-miRNA is generated, bypassing the microprocessor via exploiting the spliceosome. However, the debranched intron may have single-strand extension at 3′ or 5′ side of the stem-loop, which will be trimmed by exonucleases in the nucleus (269) (Fig. 1.9C).

Finally, all the pre-miRNAs are exported to the cytoplasm in an energy-dependent manner by exportin 5 (EXP5), which belongs to the nuclear transport receptor family (270-273). EXP5 distinguishes the structural pattern composed of a dsRNA stem (longer than 14 bps) ending with a short (1-8-nt) 3′ overhang. The pre-miRNA is released in the cytoplasm following hydrolysis of GTP by Ran-GTPase bound to EXP5 (271, 274-276).

Cytoplasmic processing by Dicer

The second step of processing happens in the cytoplasm. Endonuclease Dicer makes cleavages at both sides of the loop region in pre-miRNA, producing a duplex RNA about 21 nucleotides in length (277-280). Binding of Dicer to pre-miRNA is facilitated by TRBP (281, 282). The exact sequence of the two ~21-nt RNA molecules is determined by the nucleotide locations where Drosha and Dicer cleavages are made. However, sequence analysis of the mature miRNAs indicates that this position can change 1-2 nucleotides, leading to mature miRNAs with different 5′ and/or 3′ ends, called isomiRs (283, 284). Change in isomiR frequency preference leads to differential target repression and altered biological activity of the miRNA, especially if the change is in the 5′ end. IsomiR preference can depend on the cell type, and aberrant changes in isomiR frequencies are observed in some diseases (285-287). However, the related molecular mechanisms are not well understood (238). Additional untemplated nucleotides, often uracil and adenine, are sometimes observed at the 3′ end of mature miRNA, but the responsible terminal uridyl/adenyl transferases are not known (239).

RISC loading and target regulation

The miRNA duplex generated by Dicer is loaded into Ago protein in RISC (288, 289). Of this duplex one strand, which will be the mature miRNA, is retained in the Ago and the other strand, called the passenger strand or miRNA[*], is degraded. There are four Ago proteins in human (288, 289). The duplexes which do not have mismatches in the middle are rather loaded on Ago2, and the passenger strand is degraded by slicer activity of Ago2, which is the only Ago with this ability. However, most of duplexes do have mismatches, and the unwinding and degradation of the passenger strand is performed by some helicases instead (290-294). The mechanism of strand selection is not very well understood; it is indicated that the strand with less thermodynamic stability in its 5′ end is more likely to be selected as mature miRNA (295, 296). The stringency of this selection depends on the miRNA, and it is indicated that for virtually all miRNAs the passenger strand is also loaded into Ago, albeit with low frequencies (297). In addition, the strand preference in some miRNAs changes between cell types or may depend on the biological state (285).

MiRNAs exert their regulatory function by incorporating in the Ago and guiding the miRISC to bind the target mRNAs in 3′ UTR based on sequence complementarity to the mature miRNA. The nucleotides in the positions 2-7 from 5′ end of miRNA, called the "seed" region, are indicated to have a critical role in target specificity (298, 299). In general, miRNAs repress their target genes by destabilizing and degrading the mRNA or by inhibiting the translation process (300-304). The target mRNA will be cleaved by endonuclease activity of Ago2 if in addition to seed, nucleotides in positions 9-11 are also fully complementary to the bound mRNA (305, 306). This is very rare in animals, however, and in most cases where this central complementarity is lacking, translation is repressed by joining of Ago to a complex including GW182 in cytoplasmic P bodies (238). This is followed by facilitating target mRNA degradation when CCR4-NOT deadenylase complex joins the miRISC and removes the poly(A) tail (238, 307-309). In animal cells, miRNAs may inhibit protein biosynthesis directly at initiation step (310-313), or inhibit ribosome assembly (314), post-initiation steps (315), or elongation and termination (316, 317). However, it is indicated that mammalian miRNAs exert their inhibitory effect mainly via destabilizing the target mRNA (318).
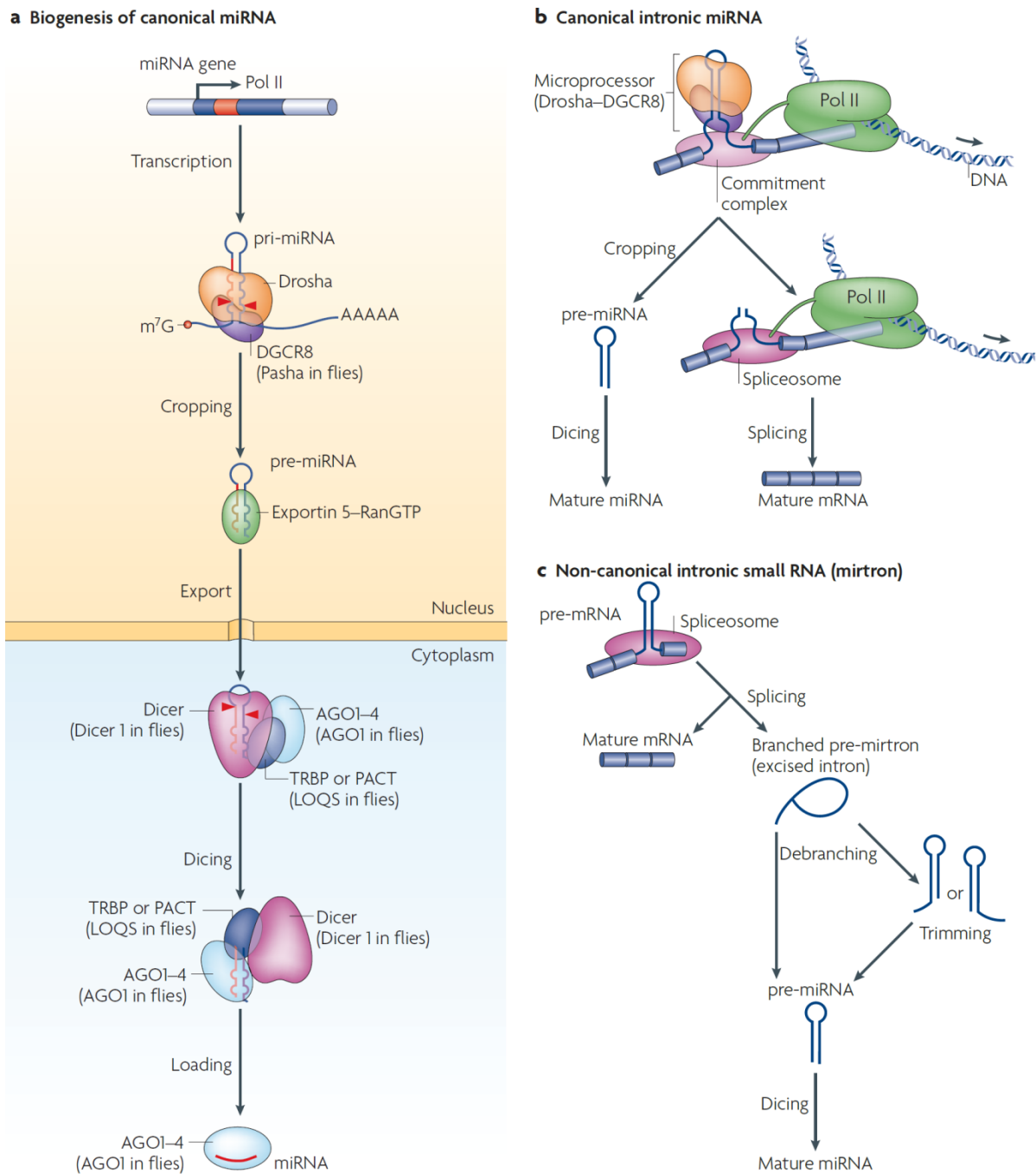
Figure 1.9. Biogenesis miRNAs. A,B) In canonical pathway a m^7G-capped poly-adenylated transcript is generated by Pol II. Processing by the Microprocessor releases the pri-miRNA hairpin. **C)** mirtron hairpins are generated during splicing of the host gene without needing Drosha. Pri-miRNAs are exported by EXP5, and the mature miRNA is loaded on Ago in miRISC. Adapted from (239).

1.4.3 miRNAs in muscle development and function

Characterization of several Dicer-deficient mouse strains has revealed the enormous significance of miRNAs as regulators of gene expression during cell differentiation and tissue development. In the first study, it was observed that knocking out Dicer globally in mice results in lethality early in development, before configuring the body plan during gastrulation (319). Several tissue-specific Dicer knockout strains have been generated thereafter, and importance of miRNAs for proper tissue development has been documented for vertebrate lung, skin, limb, cardiac and skeletal muscle (320-326). Notably, knocking out Dicer using Cre-lox system in mice, Cre recombinase being expressed under control of MyoD promoter, caused major defects in skeletal muscle development during embryogenesis, such as muscle hypoplasia, dramatically reduced muscle mass, and irregularly-shaped myofibers, leading to perinatal death (325).

While the above-mentioned studies provide solid proofs for essentiality of miRNA pathways in skeletal muscle, they are unable to specify the underlying miRNAs. Although many miRNAs are expressed ubiquitously, tissue-specific miRNAs have been identified since the beginning of miRNA discovery (327). The first report on striated-muscle specific miRNAs, by Sempere and colleagues, introduced miR-1, miR-133a, and miR-206, subsequently named myomiRs (328, 329). Later studies have added miR-208, miR-208b, miR-499, and miR-486 to the myomiR family (330-333). Most myomiRs are expressed in both cardiac and skeletal muscle, though miR-208a and miR-206 are expressed only in cardiac and skeletal muscles, respectively (332, 334).

The miR-1/miR-206 and miR-133a/miR-133b are the most studied myomiRs, and they are closely related in their function and expression (335). As indicated in Figure 1.10, they are located in three distinct genomic loci, transcribed into three bicistronic transcripts, and processed to the four mature miRNAs (336). Being under control of SRF, MyoD, and Mef2 transcription factors, they have a major role in regulating myogenesis in both myoblast proliferation and differentiation phases (234, 337-340). They are also regulated at pri-miRNA processing level via KSRP, which is a RNA-binding protein present in the microprocessor complex (341, 342). One week after a functional overload transcript levels of pri-miRNAs and mature miRNAs were up- and down-regulated about two folds, respectively, for miR-1 and miR-133 (343). Consistent with their critical regulatory role, all the three miRNAs are upregulated during muscle regeneration; however, miR-1 and miR-206 levels decline immediately after muscle injury, which is ascribed to their inhibitory role on proliferation of satellite cells (344-347). These two miRNAs have identical seed sequences and belong to the same miRNA family, hence have the same or similar target mRNAs (348).

miR-1-1 UGGAAUGUAAAGAAGUAUGUAU   miR-133a-1 UUUGGUCCCCUUCAACCAGCUG   miR-208a AUAAGACGAGCAAAAAGCUUGU

miR-1-2 UGGAAUGUAAAGAAGUAUGUAU   miR-133a-2 UUUGGUCCCCUUCAACCAGCUG   miR-208b AUAAGACGAACAAAAGGUUUGU

miR-206 UGGAAUGUAAGGAAGUGUGUGG   miR-133b UUUGGUCCCCUUCAACCAGCUA   miR-499 UUAAGACUUGCAGUGAUGUUU
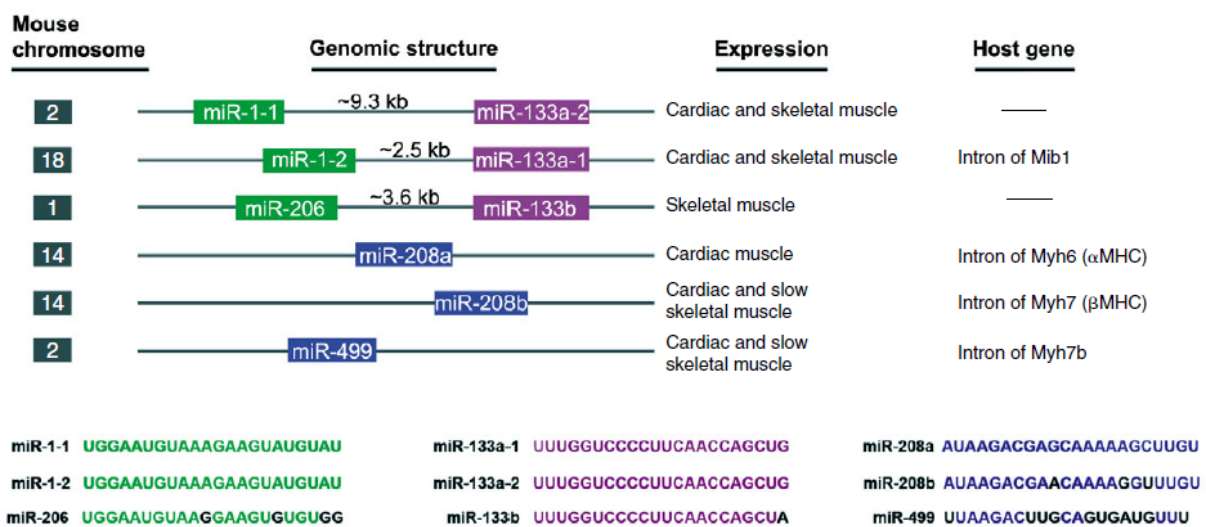
Figure 1.10. Genomic organization of myomiRs and their sequence. Adapted from (348).

Both miR-1 and miR-206 are upregulated during differentiation of myoblasts and promote it. miR-1 targets HDAC4, which is a repressor of muscle differentiation. This upregulates Mef2, and consequently induces the transcription of genes involved in myogenesis program (349). Mef2 also upregulates miR-1, making a feedback-positive loop between miR-1 and Mef2 (340, 349). YY1 transcription factor, an epigenetic repressor of myogenesis, is also targeted by miR-1 (350). Downregulation of Pax7 is critical for the initiation of differentiation in proliferating myoblasts, and it is indicated that miR-1 and miR-206 play a major role in repressing Pax7 by targeting binding sites in its 3′ UTR (347).

MiR-206 is indicated to facilitates the terminal differentiation of myoblasts in part by targeting gap-junction protein Cx43 to decrease he electrical coupling between myofibers through gap junctions (351). Translation of the p180 subunit of DNA polymerase-α (polA1) is also repressed by miR-206, which inhibits DNA synthesis and consequently cell proliferation (348, 352). Furthermore, being induced by MyoD, miR-206 acts as the mediator of MyoD-dependent repression of Fstl1 and utrophin genes in myoblasts (338). Despite the absence of an overt skeletal muscle phenotype in miR-206 knockout mice, they indicate a remarkably delayed regenerative response to cardiotoxin-induced muscle injury (334, 353). When crossed to *mdx* mice, it was observed that lack of miR-206 aggravates the dystrophic phenotype (353).

In contrast to miR-1 and miR-206, miR-133 inhibits the differentiation of myoblasts and promotes their proliferation. This is done, at least in part, via inhibition of SRF, which is a critical transcription factor controlling myoblast differentiation (349, 354). MiR-133 also modulates the differential splicing of transcripts during skeletal muscle development by repressing the splicing factor nPTB (355). While transcribed together in a bicistronic transcript and upregulated during myoblast differentiation, miR-1 and miR-133 oppose each other on their regulatory effect on skeletal muscle development. This is suggestive of an intricate balance between proliferation and differentiation in myoblasts maintained by these myomiRs (348).

The miR-208 family, including miR-208a, miR-208b, and miR-499 are all intronic miRNAs. MiR-208a is located in and co-transcribed with the Myh6 gene, encoding α-myosin heavy chain, and expressed in cardiac muscle only (332). MiR-208b and miR-499 are processed from introns in Myh7 (β-myosin heavy chain) and Myh7b (myosin heavy chain 7b) genes, respectively, and are co-expressed with their host genes as well. Functioning in a redundant manner due to identical seeds, these two miRNAs control the fiber type switch in skeletal muscle by targeting Sox6, Sp3, Purβ, and HP-1β (356). Mice lacking both miR-208b and miR-499 have remarkably less abundance of type I fibers in soleus muscle, while overexpression of miR-499 in soleus leads to switching fast myofibers to type I slow myofibers (356, 357).

Chapter 2- Results

2.1 miR-501-3p is upregulated in activated satellite cells and regenerating skeletal muscle

In order to identify the microRNAs upregulated during activation of myogenic progenitors in skeletal muscle, muscle injury and regeneration was induced by intramuscular injection of CTX into TA muscles of C57BL/6 mice. A gating strategy based on expression of ScaI and α7-integrin surface proteins was used to distinguish between MPs and FAPs (Fig. 2.1A). Activation and proliferation of both myogenic and fibro/adipogenic progenitors was confirmed by EdU incorporation assay, comparing non-injected muscle with regenerating muscle three days after injury (Fig. 2.1B). RNA isolated from activated MPs and FAPs, sorted from TA muscle three days after CTX injection, was subjected to small RNA deep sequencing after checking for RNA integrity (Fig. 2.1C).

Based on the results of RNA sequencing, we selected the top five miRNAs meeting the criteria of high expression levels in MPs ($>10^4$ RPM) and differential enrichment in MPs compared with FAPs (Fig. 2.1D, E). The expression level of each miRNA was then measured by qRT-PCR in sorted MPs and FAPs, in both activated and quiescent states (Fig. 2.2A). We observed that among all the miRNAs, only miR-501-3p is significantly upregulated in MPs upon their activation. Consistent with this, we also observed the upregulation of this miRNA in the whole regenerating muscle. This is while miR-501 level is not regulated in FAPs, and its expression level is always less than in MPs or whole muscle, either in normal or regenerating conditions. This suggests a specific role for miR-501 in myogenic lineage, and highlights MPs as the major source of miR-501 in skeletal muscle.

Time course analysis of miR-501 expression during regeneration indicates a steady upregulation up to six days after injury (Fig. 2.2B). This is the time period in which the satellite cells are activated, proliferate, and start differentiating into committed myoblasts and nascent myofibers (358). This is while miR-206 upregulation starts with emergence of new fibers, and miR-1 levels are recovered later, since miR-1 is expressed only in mature myofibers. Comparison of miR-501 to two other well-known myomiRs introduces it as an early maker of muscle regeneration.

Expression of miR-501 in different tissues, including normal and regenerating skeletal muscle, was measured by qRT-PCR (Fig. 2.2C). Results showed relatively low expression levels in all the tissues, with prominently high expression in regenerating skeletal muscle. This was corroborated also by northern blot analysis; while being expressed in regenerating skeletal muscle, cultured myoblasts and myotubes, miR-501 was virtually undetectable in normal muscle, brain and kidney (Fig. 2.2D). Altogether, the results confirm the specific expression of miR-501 in myoblasts and newly-built myofibers.

2.2 The host gene of miR-501, Clcn5, is upregulated in regenerating skeletal muscle and highly expressed in primary myoblasts

Looking up miR-501 in a genome browser reveals that this miRNA, in both mouse and human, is located in an intron of the chloride channel 5 gene (Clcn5) in a cluster with other miRNAs. A schematic representation of the locus is shown in Fig. 2.3A, B. In mouse, according to data from NCBI RefSeq, an alternative splicing upstream of exon 5 leads to generation of two splice variants. Splice variant 1 (NM_016691) encodes a 746-amino acid protein, while splice variant 2 (NM_001243762) includes exons 1, 2, and 3 as well in its 5′ end, hence encoding a protein with 70 additional amino acids in its N-terminal. Interestingly, the intron harboring the miRNA cluster is located between exons 2 and 3, which are present only in isoform 2 of Clcn5. Organization of the locus in human is very similar, with an additional exon present in the 5′ UTR of isoform 1. Alignment of mouse and human miR-501-3p sequences indicate a high degree of conservation, including the seed region (Fig. 2.3C).

Since clustering of miRNAs can lead to similar expression patterns, we checked expression levels of other miRNAs in our RNA deep sequencing data, described in section 2.1, to examine this possibility. As indicated in Fig. 2.3D, we observed that other miRNAs in the cluster are several orders of magnitude less expressed than miR-501-3p, making it the only miRNA expressed higher than an assumed threshold for functionality (10^4 RPM). Therefore, we conclude that posttranscriptional mechanisms, such as miRNA maturation, play a major role in regulating the expression of miR-501.

There are several reports about intronic miRNAs co-expressed with their host gene. To check this for miR-501, we measured the expression level of Clcn5 during a 9-day time course after CTX injection. We observed that Clcn5 is upregulated by more than 8 folds on day 3, and then declines gradually (Fig. 2.4A). This pattern shows a positive correlation with miR-501 expression during

the same conditions (Fig. 2.2B). Since miR-501 is located in a region involved only in the maturation of splice variant 2, we decided to measure each isoform separately. Using specific primers indicated in Fig. 2.3A, we observed a much stronger upregulation of isoform 2 compared to isoform 1 (Fig. 2.4A). Besides showing a strong preference specifically towards isoform 2, this indicates that upregulation of isoform 2 contributes, at least partly, to upregulation of miR-501.

Clcn5 is known for its specific expression and function in kidney, and literature on the function of this gene is solely on isoform 1 (359). On the other hand, the closer resemblance (i.e. extent of upregulation) of whole Clcn5 (dashed line) to isoform 2 rather than isoform 1 in Fig. 2.4A suggests that isoform 2 contributes more to the Clcn5 transcripts compared to isoform 1. Therefore, we measured the expression level of Clcn5 and its isoforms across different tissues, and also included cultured myoblasts and myotubes (Fig. 2.4B). We observed that though Clcn5 is most expressed in kidney compared to other tissues, the expression is even higher in myoblasts. Comparing the expression of individual isoforms in the same panel showed that while isoform 1 is very highly expressed in kidney, myoblasts express isoform 2 in much higher levels relative to kidney (Fig. 2.4C, D). Using two particular DNA standards in qRT-PCR we could measure relative copy number of isoforms, as explained with details in section 3.7.3. Each of the DNA standards consisted of its cognate isoform-specific sequence followed by a sequence common between both isoforms. We observed that while less than 20% of Clcn5 transcripts in kidney belong to isoform 2, it constitutes the great majority of transcripts in TA muscle and myoblasts (Fig. 2.4E).

High expression of Clcn5 with a strong preference towards isoform 2 in myoblasts raises the question of whether myogenic progenitors show the same pattern *in vivo*. We sorted MPs and FAPs from normal TA muscles as well as CTX-injected TA muscles three days after injury. Measurement of Clcn5 expression in the sorted cells revealed that MPs express Clcn5 in higher levels compared to FAPs, either in quiescent or activated state (Fig. 2.5A). This is similar to the expression pattern of miR-501, though we do not see significant upregulation of Clcn5 in activated MPs. Interestingly, we again observed much higher expression of isoform 2 compared to isoform 1 in either condition, resembling the myoblasts cultured *ex vivo* (Fig. 2.5B). Isoform 1 was relatively very lowly expressed, and it was not detectable in quiescent MPs. Purity of the cDNA samples from sorted cells was confirmed by detection of Pax7 and Pdgfrα exclusively in MPs and FAPs, respectively. As expected, Pax7 is downregulated and Pdgfrα is upregulated by activation of the progenitors (Fig. 2.5C,D). Altogether, the results indicate relatively high

expression of Clcn5 in myoblasts and myogenic progenitors, with a tightly regulated mechanism of alternative splicing for isoform 2. In addition, regulation of miR-501 in activated MPs seems to be mainly at posttranscriptional level.

2.3 Inhibition of miR-501 in primary myoblasts has no effect on proliferation, apoptosis, or differentiation

miR-501 is upregulated in the early phase of skeletal muscle regeneration, characterized by extensive proliferation of myogenic progenitors to produce enough myoblasts required for repairing the damaged muscle. Therefore, we postulated that miR-501 could regulate the proliferation of myoblasts, and examined this by inhibiting miR-501 in primary myoblasts cultured *ex vivo*.

Due to unavailability of a validated target for miR-501, we checked the efficiency of transfection using a miR-501 sensor plasmid, made by cloning two 22-nt consecutive miR-501 binding sites with perfect complementarity in 3′ UTR of Firefly luciferase in pmirGLO. We observed increased and decreased firefly luciferase activity after transfection with miR-501 antagomir and mimic, respectively (Fig. 2.6A). This confirms the functionality of the miRNA, efficiency of transfection, and responsiveness of the sensor to miR-501 levels.

However, in EdU incorporation assay and flow cytometry analysis, we did not observe any change in proliferation rate of myoblasts, two or three days after inhibition of miR-501 (Fig. 2.6B). Next, we checked the rate of apoptosis in primary myoblasts after inhibition of miR-501. Flow cytometry of the cells after staining with Annexin V and PI did not show any difference in frequency of apoptotic cells (Fig. 2.6C).

Finally, we checked if miR-501 is involved in regulating the differentiation of myoblasts to myotubes. Differentiation of myoblasts for two days after inhibition of miR-501 was not altered, as measured by western blot analysis for embryonic myosin heavy chain (Fig. 2.6D).

2.4 Inhibition of miR-501 in regenerating skeletal muscle does not change the proliferation rate of progenitors

We next investigated if miR-501 regulates proliferation of myogenic or fibro/adipogenic progenitors *in vivo*. TA muscles were injected with CTX and antagomirs, and proliferation of MPs and FAPs was measured based on EdU incorporation and flow cytometry analysis. We

observed that inhibition of miR-501 does not influence proliferation of the progenitors, as measured 4 days after injury (Fig. 2.7).

2.5 Inhibition of miR-501 in regenerating skeletal muscle downregulates embryonic and adult myosin heavy chain isoforms

Next, we investigated if miR-501 plays a role in regulating the differentiation process in vivo, during which myoblasts stop proliferating, fuse together and make new myofibers. Antagomirs were injected to regenerating TA muscle as described in Fig. 2.8A. miR-501 levels were efficiently reduced by antagomir injection, as measured by qRT-PCR on the harvested muscles in all time points (Fig. 2.8B). Western blot analysis for eMHC on day 6, as the first type of myosin heavy chain expressed in new fibers, revealed a dramatic decrease in the muscles when miR-501 was inhibited (Fig. 2.8C). Interestingly, we noticed a remarkable and specific decrease in dye intensity in the associated protein band after running the muscle protein lysates on PAGE and staining with Coomassie Blue (Fig. 2.8D).

As the muscle regeneration process proceeds, the embryonic isoform of myosin heavy chain is replaced by adult isoforms. Therefore, we checked if reduced levels of eMHC are reflected also in the expression level of adult isoforms. Western blot analysis of regenerating muscles on days 9 showed significantly lower abundance of adult MHC when miR-501 was inhibited (Fig. 2.8E). We also observed a similar trend on a later time point (day 15), though it was not significantly different when compared to the control antagomir (Fig. 2.8F).

Finally, using qRT-PCR we measured the gene expression levels of two differentiation markers, myoglobin and myostatin, along with eMHC in the regenerating muscles on day 4 and 6 after injury. In the muscles injected with antagomir-501, we observed a significant downregulation of eMHC in transcript level on day 4 (Fig. 2.8G). However, this decrease cannot fully explain the absence of eMHC protein on day 6. On the other hand, we observe an upregulation of myoglobin and myostatin, which suggests that downregulation of eMHC is not due to a general inhibition of differentiation. Therefore, we conclude that post-transcriptional or post-translational mechanisms play a major role in regulating eMHC protein biosynthesis and turnover. The decrease in myosin heavy chain levels was not associated with altered muscle mass as measured 15 days after CTX injection (Fig. 2.8H).

2.6 Inhibition of miR-501 in regenerating skeletal muscle leads to smaller regenerating myofibers

A potential reason for the reduced levels of eMHC as observed by western blot analysis could be the reduced size or number of eMHC$^+$ fibers. In addition, the diameter of newly generated myofibers is used as an indicator for the efficiency of muscle regeneration. Thus, we measured fiber diameters in regenerating skeletal muscle, injected with either antagomir-501 or control antagomir, by immunofluorescence staining of muscle transverse sections. As indicated in Fig. 2.9, inhibition of miR-501 leads to a significant shift in myofiber size distribution towards an increase in relative frequency of small-sized fibers. This indicates that inhibition of miR-501 impairs the development of nascent myofibers and hence the regeneration of skeletal muscle. However, the magnitude of the observed difference is rather mild and cannot fully explain the western blot analysis results (Fig. 2.8C). The fact that also in the antagomir-501-treated muscle samples regenerating areas stained positive for eMHC indicates a remarkably higher sensitivity of immunofluorescence compared to western blotting.

2.7 Identification of miR-501 target genes by miRNA inhibition and transcriptome analysis

In order to find the relevant targets of miR-501, we performed quantitative analysis of the transcriptome in myoblasts with and without inhibition of miR-501. mRNA sequencing was performed on RNA isolated from myoblasts transfected with either control antagomir or antagomir-501. Mapping of sequence reads to the latest mouse genome showed a very good coverage of the transcripts, in a way that in average for 70% of transcripts at least 70% of the sequence was detected (Fig 2.10A). This was accompanied by a high degree of certainty in alignment, as at least for 90% of the reads only one hit was returned (Fig 2.10B). After differential gene expression analysis, visualization of the fold-changes against fdr values in a volcano plot shows a symmetric distribution of genes by fold change over a wide range of fdr values (Fig 2.10C). Importantly, derepression of the putative target genes, as predicted by Targetscan, correlated with the binding site efficacy quantified by context+ scores (Fig 2.10D). Context+ scores are calculated by considering the contribution of several known targeting features in order to rank the predicted targets of a miRNA; lower scores indicate higher degree of certainty in prediction of a miRNA target site (360). Altogether, these data confirm the high quality of the RNA-seq high throughput data, functionality of miR-501 in regulating target genes, and efficiency of miRNA inhibition by antagomir transfection.

Next, we aligned the list of all detected transcripts separately with the list of predicted miR-501 targets in mouse and human, generated by TargetScan v6.2. Among the overlapping genes, those which were significantly upregulated ($p < 0.05$) and are highly conserved miR-501 targets among mammals were considered for further analysis (Fig. 2.11A). Expression level of the selected genes in the same RNA samples used for RNA-seq was measured by qRT-PCR, and we observed a high degree of consistency between these two methods (Fig. 2.11B, C). We repeated the antagomir transfection on independent primary myoblast cultures, and also performed transfection with miRNA mimics in order to check the regulation of these genes when miR-501 is overexpressed. For a gene to be considered as a putative target, it is expected to be up- and down-regulated by inhibition and overexpression of the miRNA, respectively. Analyzing the qRT-PCR results showed that 6 of the tested genes met these criteria (Fig. 2.11D).

In order to validate the miRNA target genes, it is essential to show that the regulation of gene expression is mediated by direct interaction between the miRNA and its binding site in the 3′ UTR of the target transcript. To this end, we cloned parts of the 3′UTR of the selected genes

including the predicted miR-501 binding site in pmirGLO dual-luciferase miRNA target expression vector downstream of Firefly luciferase protein coding sequence. For genes containing several predicted miR-501 binding sites, parts flanking each site were cloned separately. Measuring the luciferase activity in transfected HEK293 cells indicated that all the examined genes have at least one responsive miR-501 binding site (Fig. 2.11E).

2.8 Overexpression in primary myoblasts identifies gigaxonin as potential mediator of miR-501 action in vivo

To identify the target genes underlying the miR-501 role in regulating eMHC turnover, we cloned the protein coding sequence of the above-mentioned validated targets in pcDNA3.1 expression vector. Before cloning, we inserted in the multiple cloning site of the vector a Kozak consensus sequence followed by a short open reading frame encoding a FLAG epitope. This was to increase the protein expression and to facilitate the detection of the proteins. A control expression construct was made by cloning eGFP (from pEGFP-N3) into the same modified pcDNA vector. Primary myoblast cultures were transfected with the expression constructs, and overexpression was confirmed at the mRNA level by several orders of magnitude (Fig. 2.12A). However, we could not detect the expressed proteins, including eGFP, by western blotting using a commercial anti-FLAG antibody. This is while we observed strong fluorescence signal when the same cells were transfected with pcDNA-eGFP (Fig. 2.12B). Nevertheless, we could detect all the proteins, except Sertad2, expressed in HEK293 cells transfected with the same constructs (Fig. 2.12C). As observed, different proteins show different expression levels. In case of Sertad2, we speculate that the expression level has been lower than detection limit by anti-FLAG antibody, which is also the most likely explanation for not detecting the overexpression of proteins in the primary myoblasts.

Next, for each overexpression construct we checked eMHC protein levels in transfected primary myoblasts by western blotting two days after induction of differentiation. Repeating the experiment several times revealed that gigaxonin, encoded by Gan gene, is the only protein that could reproducibly reduce eMHC protein levels when overexpressed in primary myoblasts (Fig. 2.12D). This mimics the effect of miR-501 inhibition in regenerating muscle, and could explain the function of miR-501 in vivo. Finally, using an antibody specific for gigaxonin we could detect its overexpression in the transfected myoblasts by western blotting (Fig. 2.12D).

2.9 miR-501 as a potential biomarker for Duchene muscular dystrophy

In our screening to identify miRNAs upregulated during activation of skeletal muscle satellite cells, we used cardiotoxin-induced acute injury to trigger the regeneration process. However, there are a range of chronic muscular dystrophies, in which the skeletal muscle is undergoing recurring rounds of degeneration and regeneration. This continuously keeps the satellite cells activated and proliferating. Therefore, we hypothesized that miR-501 is upregulated in such a milieu as well.

The most widely used animal model for muscular dystrophy is the *mdx* mouse. We first compared the expression level of miR-501 in skeletal muscle from *mdx* mice with age-matched wild-type C57BL/6 mice. Interestingly, we observed that miR-501 expression is more than 5 times higher in TA muscles from *mdx* mice (Fig. 2.13A). This was accompanied by higher miR-206 levels as well, as previously reported (361).

It has been shown that in addition to serum creatine kinase (CK), the level of circulating muscle-specific miRNAs is significantly increased in both *mdx* mice and DMD patients compared to wild-type animals and healthy individuals, respectively (361, 362). Hence, we checked if this is also the case for miR-501. Indeed, comparison of miR-501 levels in sera from age-matched *mdx* and C57BL/6 mice showed significantly higher abundance of this miRNA in *mdx* sera (Fig. 2.13B). We also detected remarkably higher CK activity in the sera from *mdx* mice, as expected (Fig. 2.13C).

It is known that the disease severity changes with age in *mdx* mice; the disease onset is in about three weeks of age, and muscle regeneration is most prominent between sixth and twelfth weeks of life, reaching its maximum at eighth week. Afterwards, the rate of both degeneration and regeneration decreases and a stabilized condition is reached (363). We measured levels of miR-501 and three other myomiRs (miR-1, miR-133, miR-206) along with creatine kinase activity in the sera from *mdx* mice at different ages between 3 and 42 weeks. We observed that miR-501 levels correlate with disease severity as well as other markers, e.g. creatine kinase and myomiRs (Fig. 2.14). This highlights the potential of serum miR-501 as a non-invasive biomarker for muscular dystrophy.
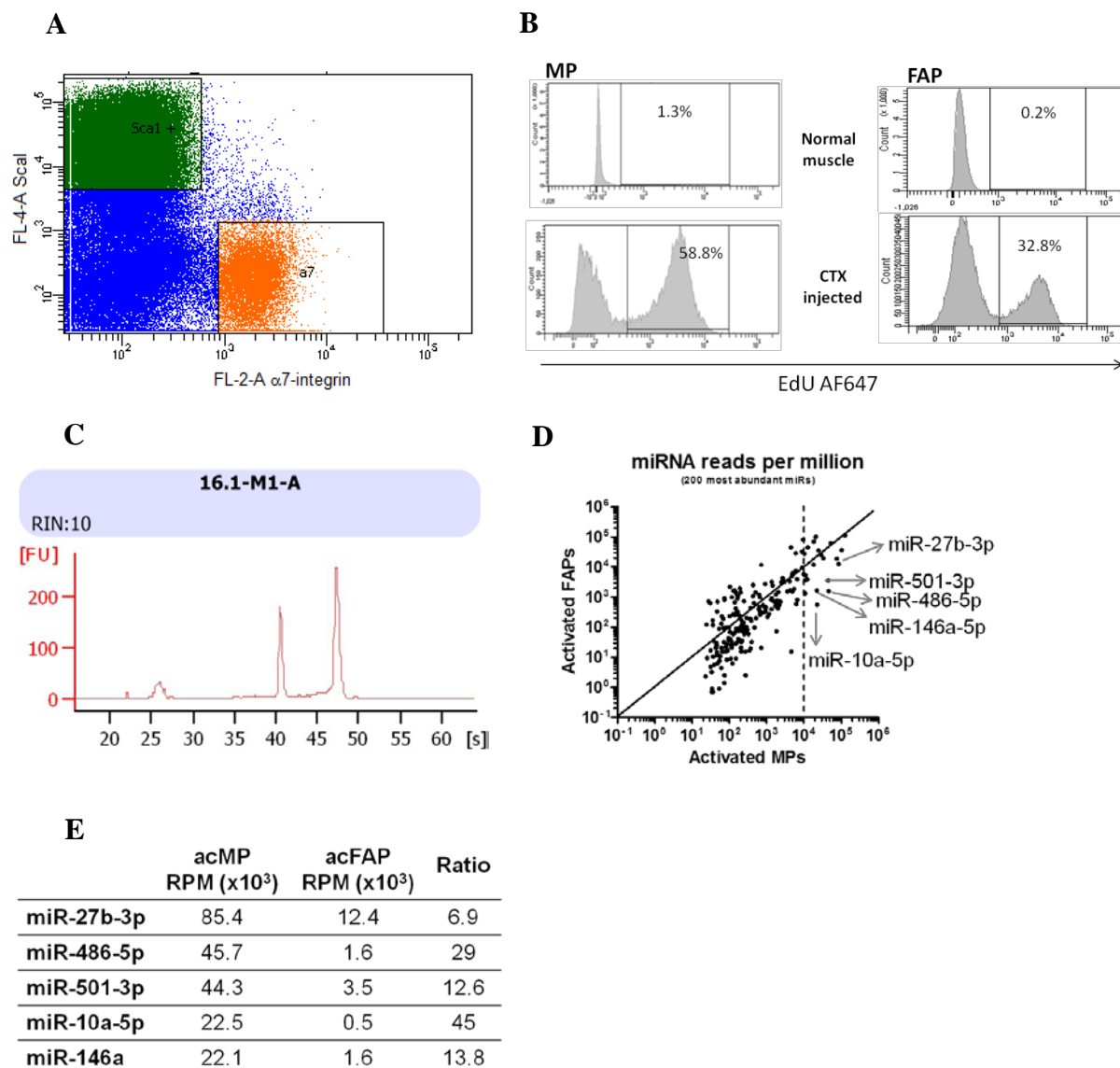
Figure 2.1. miR-501-3p is upregulated in activated satellite cells. TA muscles were injected with CTX and analyzed three days later. **A)** MPs and FAPs were identified based on their distinct expression pattern of ScaI and α7-integrin. **B)** Mice were injected i.p. with 10ug EdU per gram body weight 12 hours before harvesting. Proliferation was measured by EdU incorporation assay. **C)** Quality control of RNA samples isolated from the sorted progenitors using Agilent Pico RNA chips on a 2100 Bioanalyzer. **D)** Results of small RNA deep sequencing, comparing activated MPs and FAPs. N=2, each sample was from a pool of cells sorted from 7-9 mice for MPs and 2 mice for FAPs. **E)** Relative abundance of the five miRNAs selected based on high absolute expression level and enrichment in activated MPs (acMP) compared with activated FAPs (acFAP). RPM: Reads per million.

A

B

C
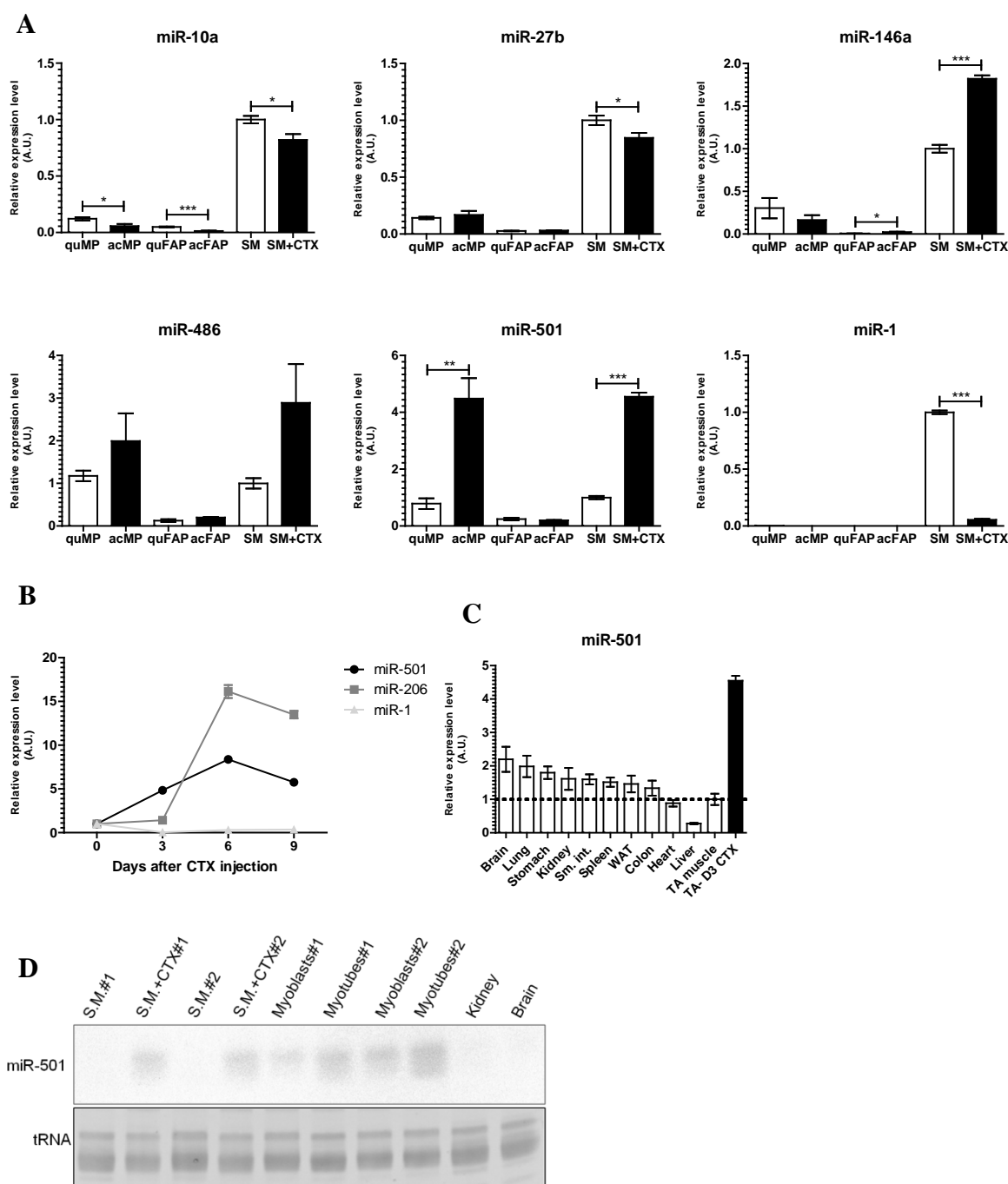
Figure 2.2. miR-501-3p is upregulated in regenerating skeletal muscle.
A) Expression of the selected miRNAs in MPs and FAPs sorted from normal (SM) or CTX-injected (SM+CTX) TA muscle, measured by qRT-pCR. Data were normalized to sno234. miR-1 was measured as an adult-muscle-specific miRNA. N=4-6.
B) Expression of miR-501, miR-206, and miR-1 up to 9 days after CTX injection in TA muscle, measured as in A. N=3 for each time point. **C)** Expression of miR-501 in different mouse tissues compared with CTX-injected TA muscle, measured as in A. N=5 for TA-CTX, n=3 for the rest.
D) Confirming the expression of miR-501 in CTX-injected TA, primary myoblasts, and myotubes by northern botting. Ethidium bromide staining of tRNA is shown as loading control. Data in A, B, and C are normalized to 18S rRNA and presented as the mean ± SEM relative to normal TA muscle. *, p<0.05, **, p<0.01, ***, p<0.001, student's t-test. SM: Skeletal muscle; CTX: cardiotoxin.
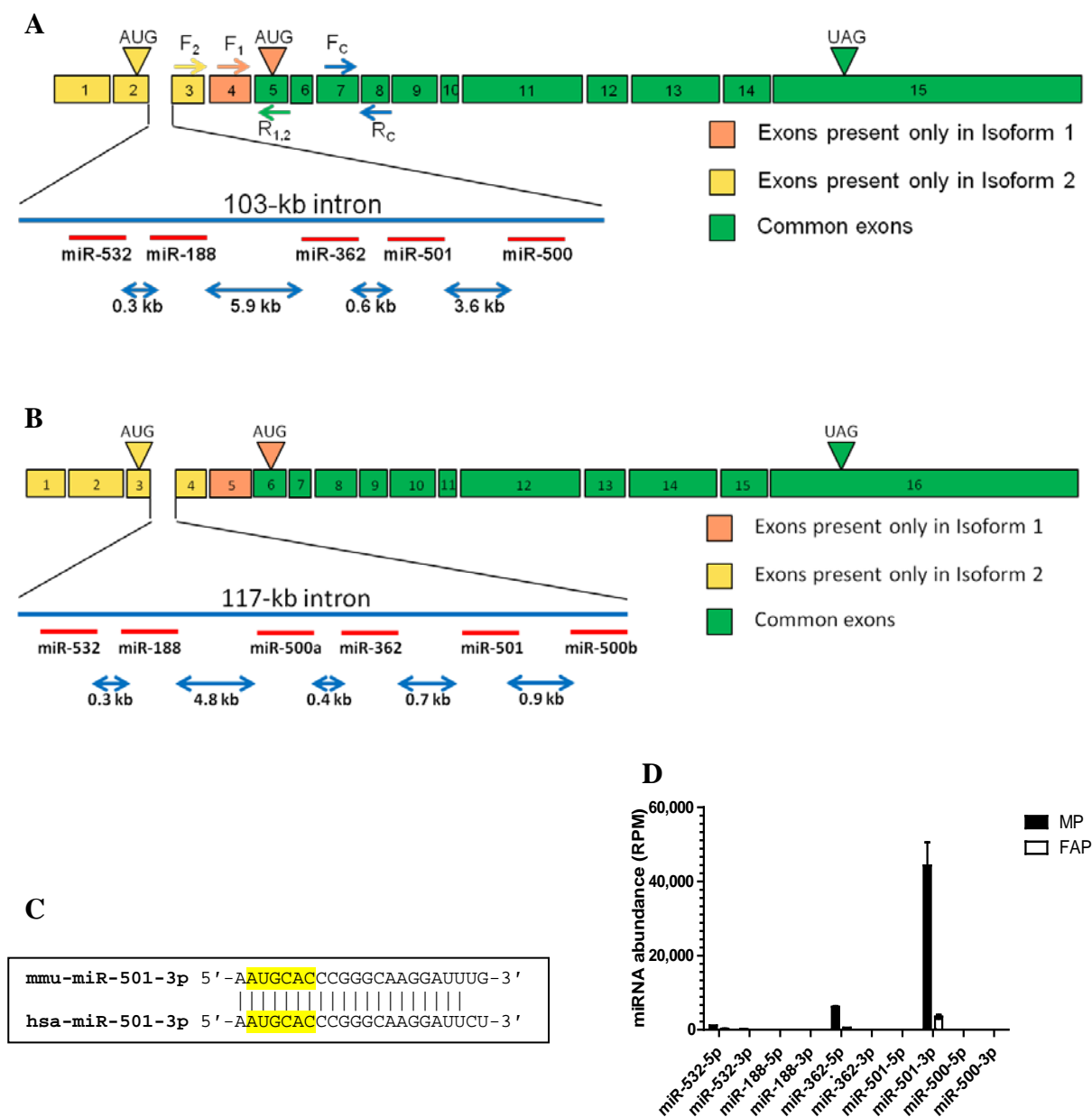
Figure 2.3. miR-501-3p resides in an intron in Clcn5 gene.
A, B) Schematic representation of mouse (A) and human (B) miR-501 locus and its host gene, Clcn5. The intron located between two isoform 2-specific exons harbors a cluster of miRNAs. Binding sites for isoform-specific (F1, F2, R1,2) and common primers (Fc, Rc) used for mouse transcripts are indicated. **C)** Alignment of mouse and human miR-501-3p sequences. The seed region is highlighted. **D)** Relative expression of the miRNAs clustered in intron 2 of Clcn5 in MPs and FAPs sorted from CTX-injected TA muscle, as in Fig. 1. Data are shown as the mean ± SEM. RPM: reads per million.
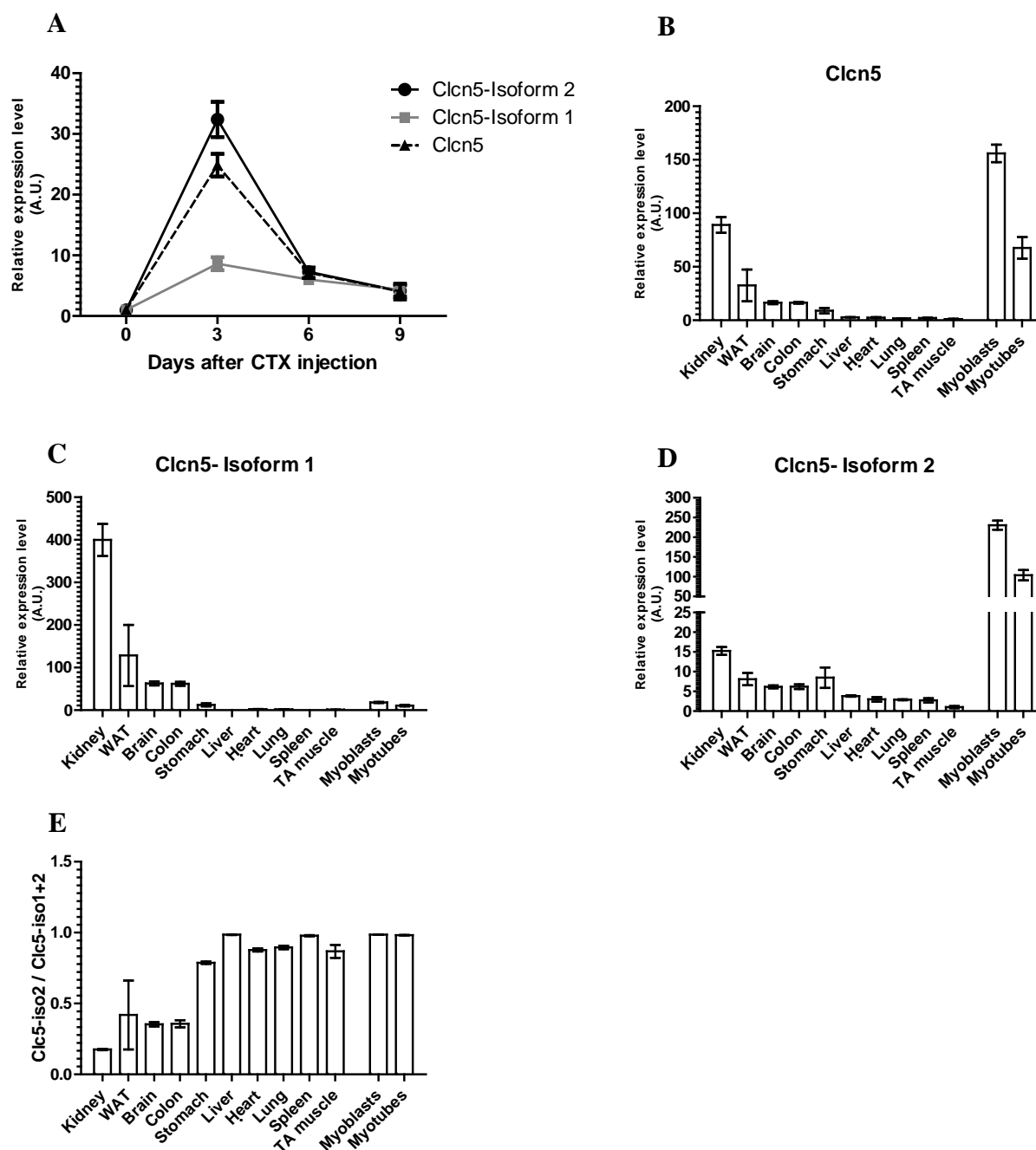
Figure 2.4. Clcn5 is upregulated in regenerating skeletal muscle and highly expressed in primary myoblasts.
A) Expression of Clcn5 isoforms in regenerating TA muscle as measured by qRT-PCR using isoform-specific primers, as depicted in Fig. 3A. F_1 and F_2 forward primers were used to specifically measure isoforms 1 and 2, respectively, and $R_{1,2}$ was used as reverse primer for both. Dashed line corresponds to the whole Clcn5 transcripts, measured by using F_C and R_C primers. N=3. **B-D)** Expression of Clcn5 and its isoforms in different mouse tissues was measured by qRT-PCR. N=3. **E)** Clcn5 isoforms are expressed in different proportions in different tissues. Plotted is the fraction of Clcn5 transcripts encoding isoform 2. All gene expression data are normalized to 18S rRNA and presented as the mean ± SEM.
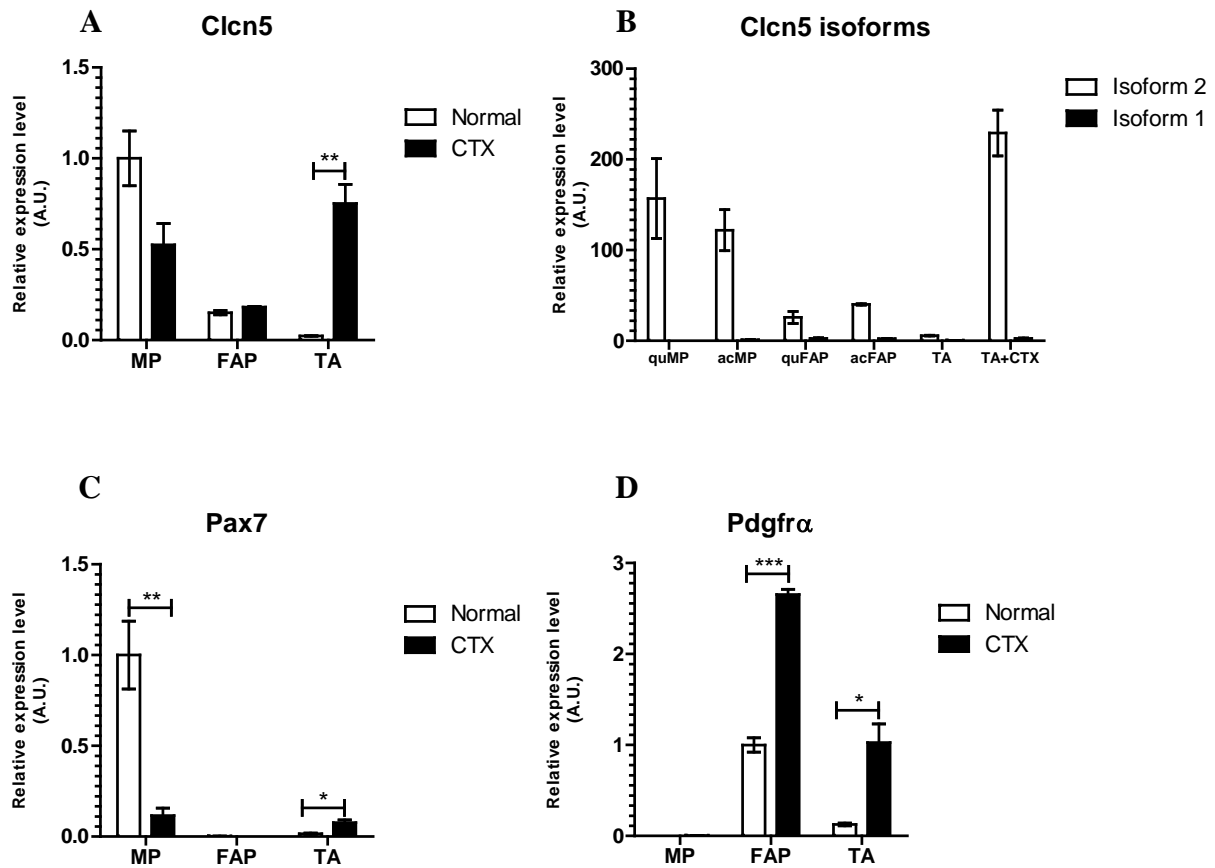
Figure 2.5. Expression of Clcn5 in two populations of progenitors in skeletal muscle.
Cell were sorted by FACS from normal or CTX-injected TA muscle (day 3), and the expression of Clcn5 **(A)** and its isoforms **(B)** was measured by qRT-PCR using isoform-specific primers. Relative expression of isoforms was calculated as in Fig. 4E. Expression of Pax7 **(C)** and Pdgfrα **(D)** as specific markers in the same cDNA panel. N=3-4, each sample was comprised of cells sorted from 3-4 mice. qPCR data in all panels are normalized to 18S rRNA. Data are presented as the mean ± SEM. *, $p < 0.05$, **, $p < 0.01$, ***, $p < 0.001$, student's t-test.

A

miR-501 sensor

B

**Primary myoblasts
Proliferation**

C

**Primary myoblasts
Apoptosis**

D

eMHC
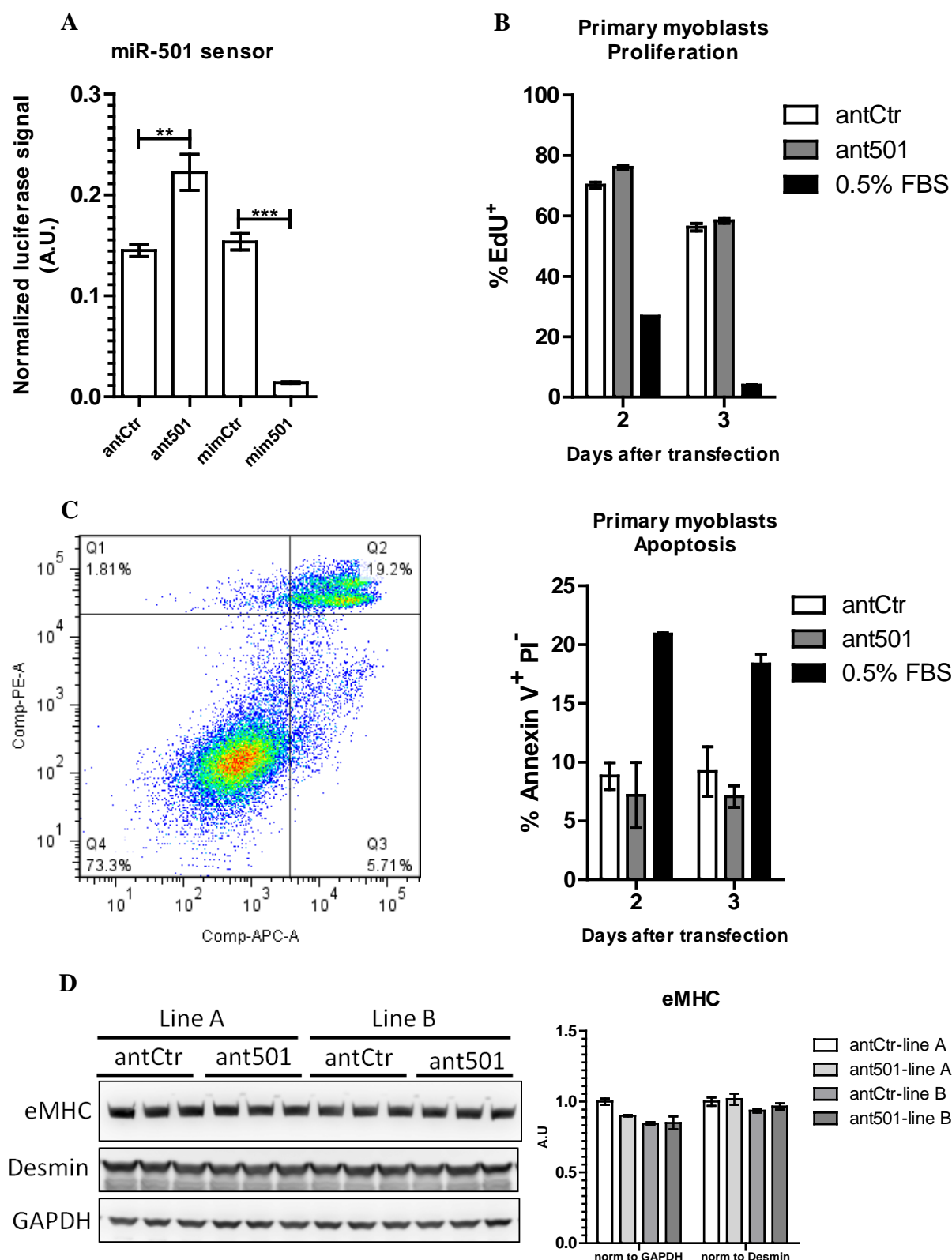
Figure 2.6. Analysis of proliferation, apoptosis, and differentiation of primary myoblasts after inhibition of miR-501.
A) Successful transfection of primary myoblasts as confirmed by co-transfecting a miR-501 sensor. Luciferase activity was measured 2 days after transfection. N=6 cultures. **B)** Primary myoblasts were transfected with antagomir-501 (ant501) or control antagomir (antCtr), and proliferation rate was measured by flow cytometry 2 and 3 days later. Cells grown in reduced FBS concentration were used as control. 1ug/ml EdU was added to the growth media 16 hours before harvesting. N=3 cultures.

C) Primary myoblasts were transfected as in B. Cells were trypsinized and stained with Annexin V-Alexa 647 and PI 2 and 3 days after transfection, and analyzed by flow cytometry. Cells grown in reduced FBS concentration were used as control. Left panel shows the gating strategy. Cells in gate Q3 are considered apoptotic. N=2 cell lines. **D)** Western blot analysis on myotubes after transfection with antagomirs. Primary myoblasts were transfected as in B, and transferred to differentiation media 24 hours later. Cells were harvested after 2 days of differentiation. Desmin and GAPDH served as loading control. The bar graph indicates quantification of eMHC protein expression by densitometry normalized to GAPDH or Desmin. In all bar graphs data are presented as the mean ± SEM. **, p<0.01, ***, p<0.001, student's t-test.
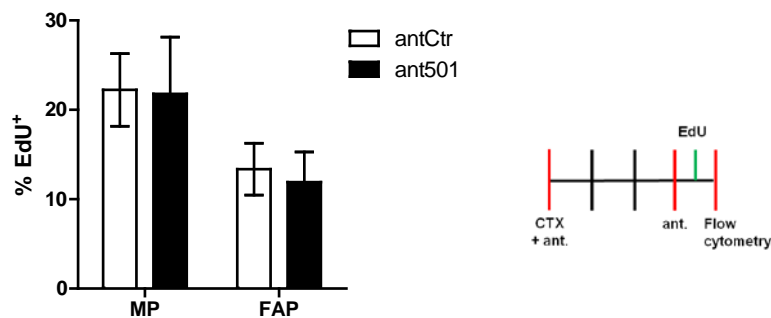
Figure 2.7. Analysis of proliferation of MPs and FAPs in regenerating skeletal muscle after inhibition of miR-501. Mouse TA muscles were injected with CTX and control antagomir (antCtr) or antagomir-501 (ant501). Antagomir injection was repeated on day 3, and muscles were harvested on day 4. Mice were injected i.p. with 10ug EdU per gram body weight 12 hours before analysis. Proliferation rate in MPs and FAPs was measured by flow cytometry based on EdU incorporation. Data are presented as the mean ± SEM, n=7 mice per group.
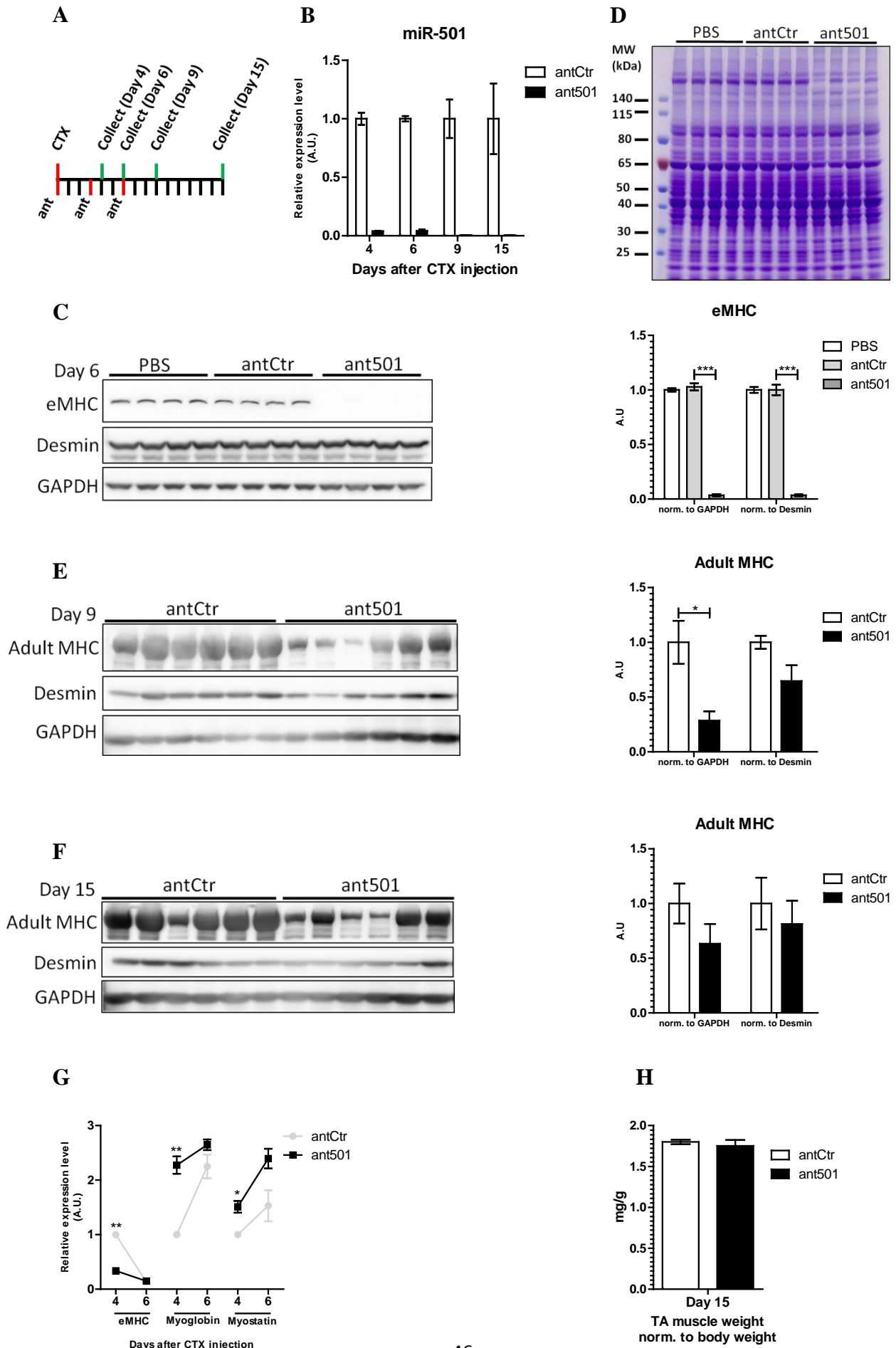
Figure 2.8. Inhibition of miR-501 in regenerating skeletal muscle downregulates myosin heavy chain isoforms.

A) As indicated, mouse TA muscles were injected with CTX and control antagomir (antCtr) or antagomir-501 (ant501). Antagomir injection was repeated after 3 and 6 days, and muscles were harvested on day 4, 6, 9, and 15. PBS group received PBS instead of antagomir. **B)** Efficient downregulation of miR-501 in the muscle as measured by qRT-PCR. Data are normalized to sno234 and shown relative to antCtr group. **C)** Western blot analysis for eMHC shows a dramatic decrease in eMHC protein level on day 6 of regeneration. N=4 mice per group, one TA from each mouse. **D)** Coomassie Blue staining after resolving muscle lysates on a 4-12% Bis-Tris gel. Samples are as in panel C. **E, F)** Western blot analysis for adult MHC on day 9 and 15 after CTX injection. N=3 mice (6 TA muscles in total) for each time point. Bar graphs in C, E, and F show densitometry quantification of western blots normalized to GAPDH or Desmin. **G)** Expression of eMHC and adult muscle markers myoglobin and myostatin transcripts in TA muscles on day 4 and 6 after CTX injection as measured by qRT-PCR. Data are normalized to 18S rRNA and shown relative to day 4 in antCtr group, N=2-3 mice (4-6 TA muscles) per group and time point. Average weight of the two TA muscles from each mouse was used for plotting. **H)** TA muscle weight measured 15 days after CTX injection, as described in A. N=2-3 mice per group. Data are presented as the mean ± SEM. *, p <0.05, **, p <0.01, ***, p <0.001.
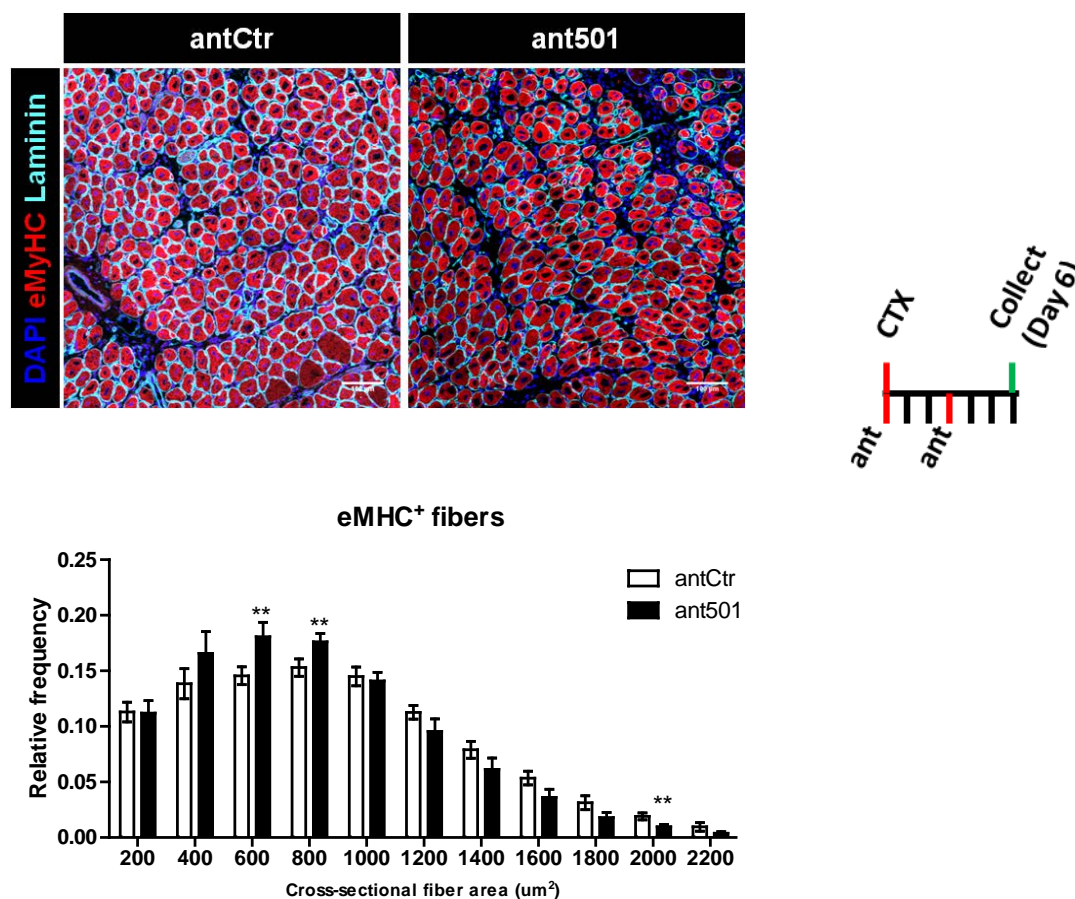
Figure 2.9. Impaired development of regenerated myofibers by miR-501 inhibition.

A) As indicated in Fig. 2.8A, mouse TA muscles were injected with CTX and control antagomir (antCtr) or antagomir-501 (ant501). Antagomir injection was repeated after 3 days, and muscles were harvested on day 6. Frozen sections of the muscles were probed with anti-eMHC, anti-Laminin, and DAPI. Fiber diameter was analyzed based on Laminin immunofluorescence and shown relative to the total number of fibers. N=7-8 mice per group. Data are presented as the mean ± SEM. **, p <0.01. Immunofluorescence and fiber diameter measurements were performed by Dr. Edlira Luca.
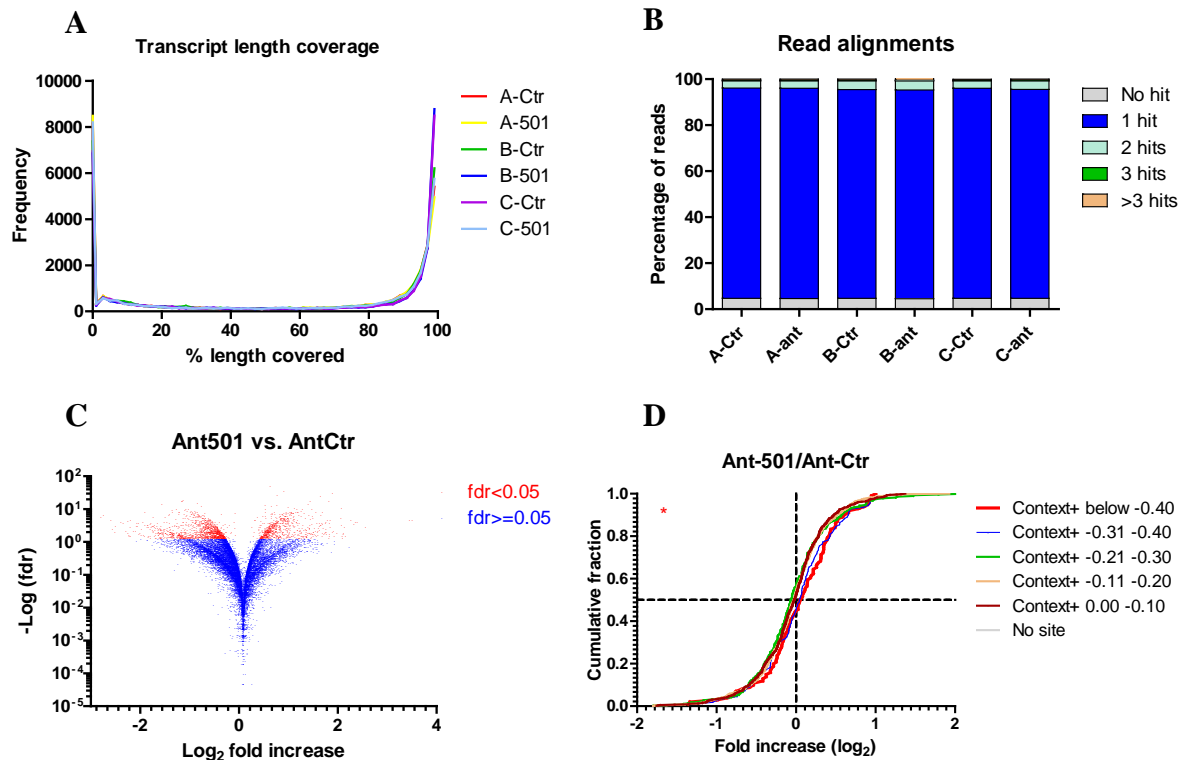
Figure 2.10. Quality contro l of RNA-seq data, evidence for regulation of target genes.
RNA from three primary myoblast cultures, harvested 48 hours after transfection with control antagomir or antagomir-501, was used for mRNA sequencing. **A)** Frequency of transcripts with indicated percentage of the length detected in RNA-seq. Only for 30% of transcripts the coverage was below 70%. **B)** Alignment of sequencing reads to mouse reference genome. Indicated are the fraction of reads mapping to different number of loci in the genome. **C)** Volcano plot for the differential gene expression results. There is no systematic bias towards down- or up-regulation. **D)** Cumulative distribution of fold changes for mRNAs predicted as miR-501 targets, with different efficacies, or non-target genes. *, $p < 0.05$, Kolmogorov-Smirnov test.

Gene	Average FPKM antCtr	Average FPKM ant501	p-value	q-value
Esrrg-V1	78	218	5.57E-6	2.88E-4
Kctd9-V1	551	1043	4.78E-8	5.64E-6
Dclk1-V4	5076	9009	2.50E-10	6.24E-8
Dclk1-V5	1511	2540	4.31E-6	2.34E-4
Ptprf	271	549	9.60E-6	4.48E-4
Cpeb2-V1	214	386	3.15E-4	6.97E-3
Gan	213	326	1.17E-2	8.67E-2
Sertad2-V1	67	136	3.14E-3	3.58E-2
Col19a1	1367	1718	2.00E-2	1.25E-1
Hmgcs	1431	2069	5.77E-4	1.07E-2
Amotl1	2198	3188	6.11E-3	5.64E-2
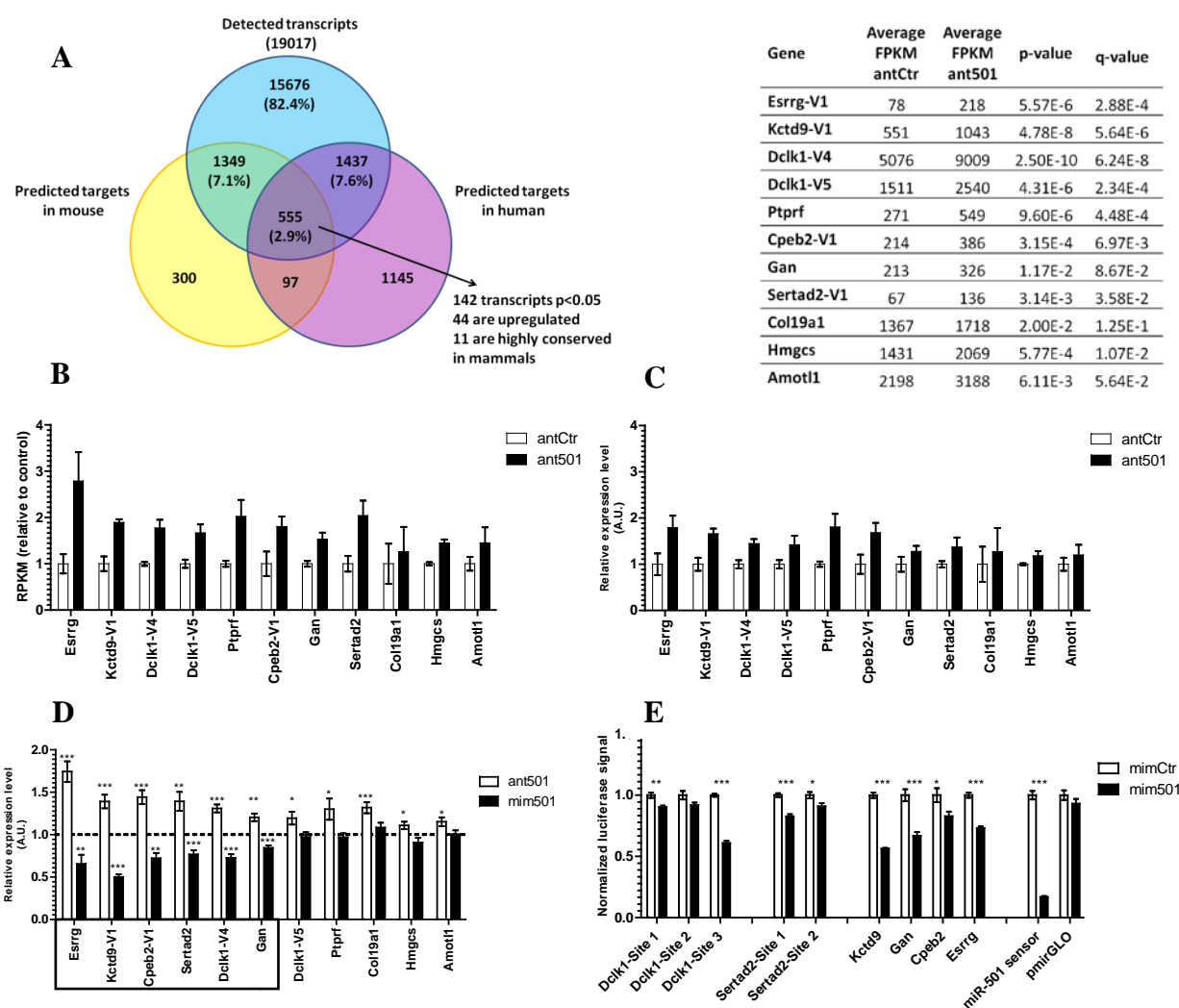
Figure 2.11. Identification and validation of miR-501 target genes in myoblasts.
A) Primary myoblasts were transfected with control antagomir or antagomir-501 in growth media, and harvested after 48 hours. RNA was extracted and used for cDNA synthesis and RNA-seq after DNase-treatment (n=3). Venn diagram shows the overlap between predicted target genes for miR-501 in mouse and human, based on TargetScan v6.2. The 11 transcripts which were significantly upregulated, predicted as miR-501 target in mouse and human, and conserved among mammals were considered for further analysis. Corresponding FPKM values and statistics are shown on the right side. **B)** RNA-seq expression values, reported as FPKM, for the selected genes. Numbers following - V specify the splice variant as in RefSeq. FPKM values are presented as normalized to antCtr group. **C)** Expression of the selected genes as measured by qRT-PCR. cDNA was made from the same RNA samples used for RNA-seq (n=3 per group). Data are presented as the mean ± SEM. **D)** Regulation of gene expression in the selected subset of genes after inhibition or overexpression of miR-501 in primary myoblasts. Cells were transfected with antagomirs or miRNA mimics (control or miR-501) for 48 hours. Gene expression values for miR-501 mimic (mim501) and antagomir (ant501) were normalized to values from cells transfected with control mimic or antagomir, respectively, as indicated by the dashed line. Based on the results, a set of 6 genes was selected for further analysis. N=11-12 cultures. **E)** The 3′ UTR of the indicated genes in human were cloned downstream of Firefly luciferase ORF in pmirGLO vector. A miR-501 sensor construct, explained in section 2-3, was used as positive control. pmirGLO was used as negative control. Constructs were transfected along with control mimic (mimCtr) or miR-501 mimic (mim501) to HEK293 cells and luciferase activity was measured after 48 hours. Firefly luciferase activity was normalized to Renilla luciferase activity. Data are presented relative to mimCtr as the mean ± SEM, n=6. The experiment was repeated with very similar results. *, p <0.05, **, p <0.01, ***, p<0.001. All qRT-PCR data are normalized to 18S rRNA.
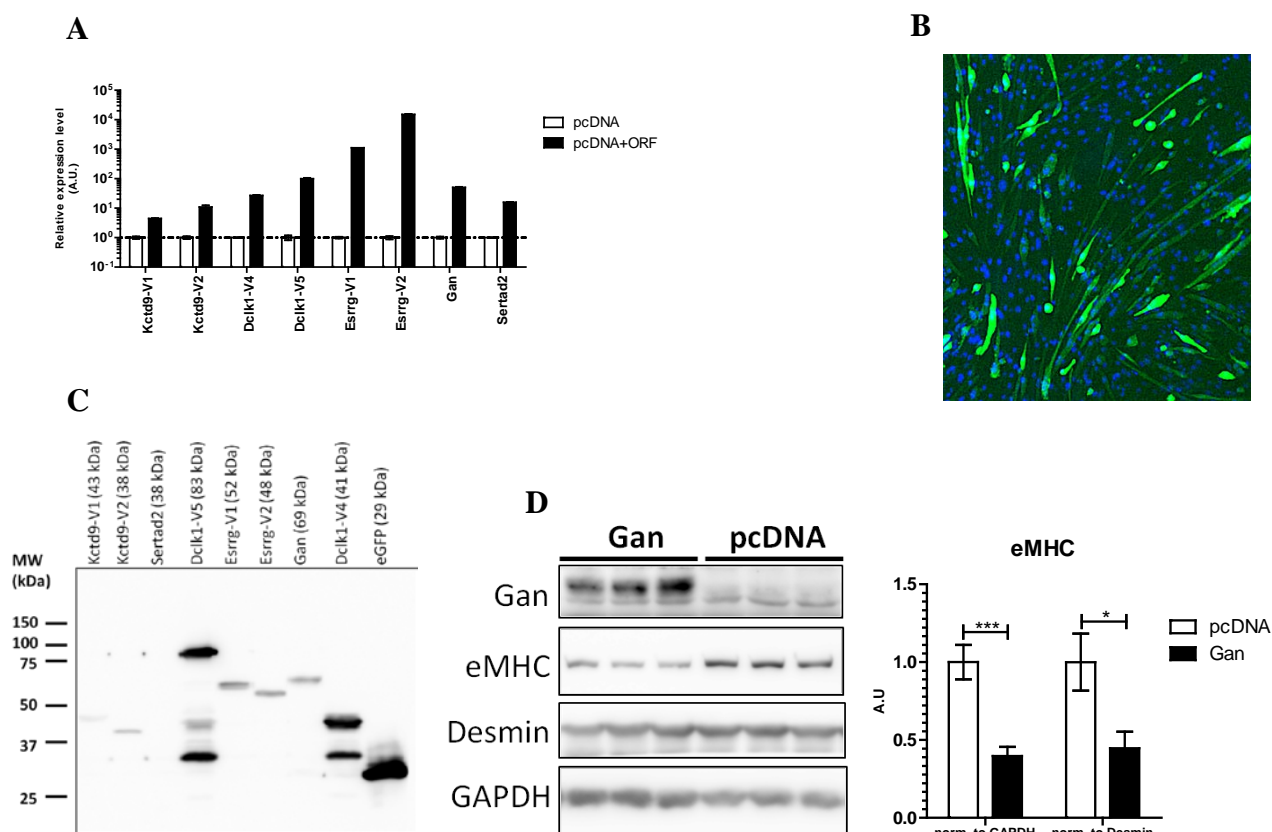
Figure 2.12. Overexpression in primary myoblasts identifies gigaxonin as mediator of miR-501 action in vivo.

A) Confirmation of overexpression by qRT-PCR in primary myoblasts. Cells were transfected with pcDNA3.1 expression vectors encoding for the indicated genes, and transferred to differentiation media for 2 days 24 hours after transfection. Extracted RNA was treated with DNase and absence of DNA contamination from the transfected plasmids was confirmed. Gene expression levels were measured relative to the cells transfected with the empty vector. Data are presented as the mean ± SEM, n=2.

B) Expression of eGFP in primary myoblasts transfected with pcDNA-eGFP detected by fluorescence microscopy. Nuclei are stained by DAPI (blue). **C)** Confirmation of overexpression by western blot analysis. HEK293 cells were transfected with pcDNA3.1 vectors encoding N-terminally FLAG-tagged proteins. Cells were harvested after 2 days and proteins were detected using anti-FLAG antibody. All constructs were confirmed by restriction mapping and DNA sequencing.

D) Overexpression of gigaxonin lowers eMHC protein levels in primary myoblasts. Cells were transfected with pcDNA3.1 expression vector encoding for gigaxonin. Empty vector was used as negative control. Cells were transfection as in A. Overexpression of gigaxonin was confirmed using a specific antibody. The bar graph shows densitometry quantification of eMHC protein normalized to GAPDH or Desmin. Data are presented as the mean ± SEM. *, $p < 0.05$, ***, $p < 0.001$, student's t-test. N=6 in densitometry, a representative blot with n=3 cultures is shown.
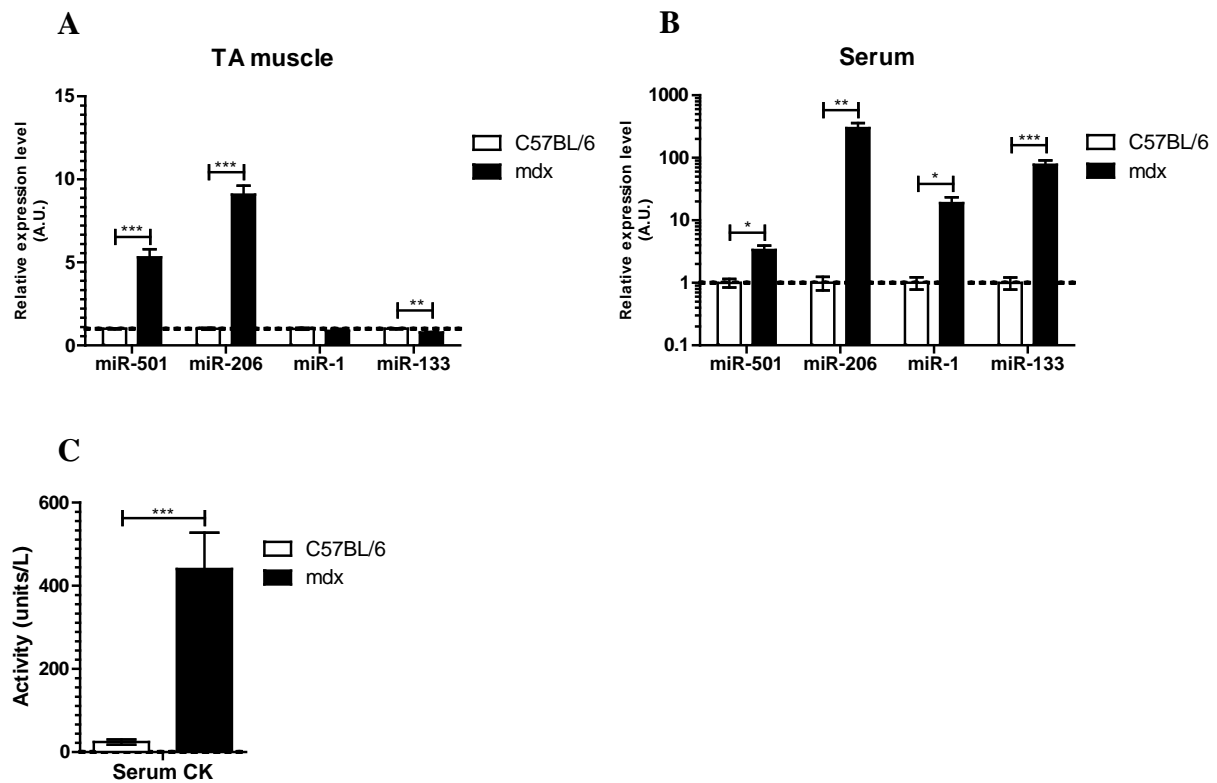
Figure 2.13. Increased levels of miR-501 in skeletal muscle and sera from *mdx* mice.
Expression of miR-501 and myomiRs in TA muscles **(A)** and sera **(B)** from 12-week-old C57BL/6 and *mdx* mice as measured by qRT-PCR. Data are normalized to sno234 (A) or to the spiked cel-miR-39 (B), respectively. N=3 (A) or 5-9 (B) mice. Data are presented as the mean ± SEM. **C)** Serum creatine kinase activity in 12-week-old *mdx* and C57BL/6 mice. Data are presented as the mean ± SEM, n=9. *, p <0.05, **, p <0.01, ***, p <0.001, student's t-test.
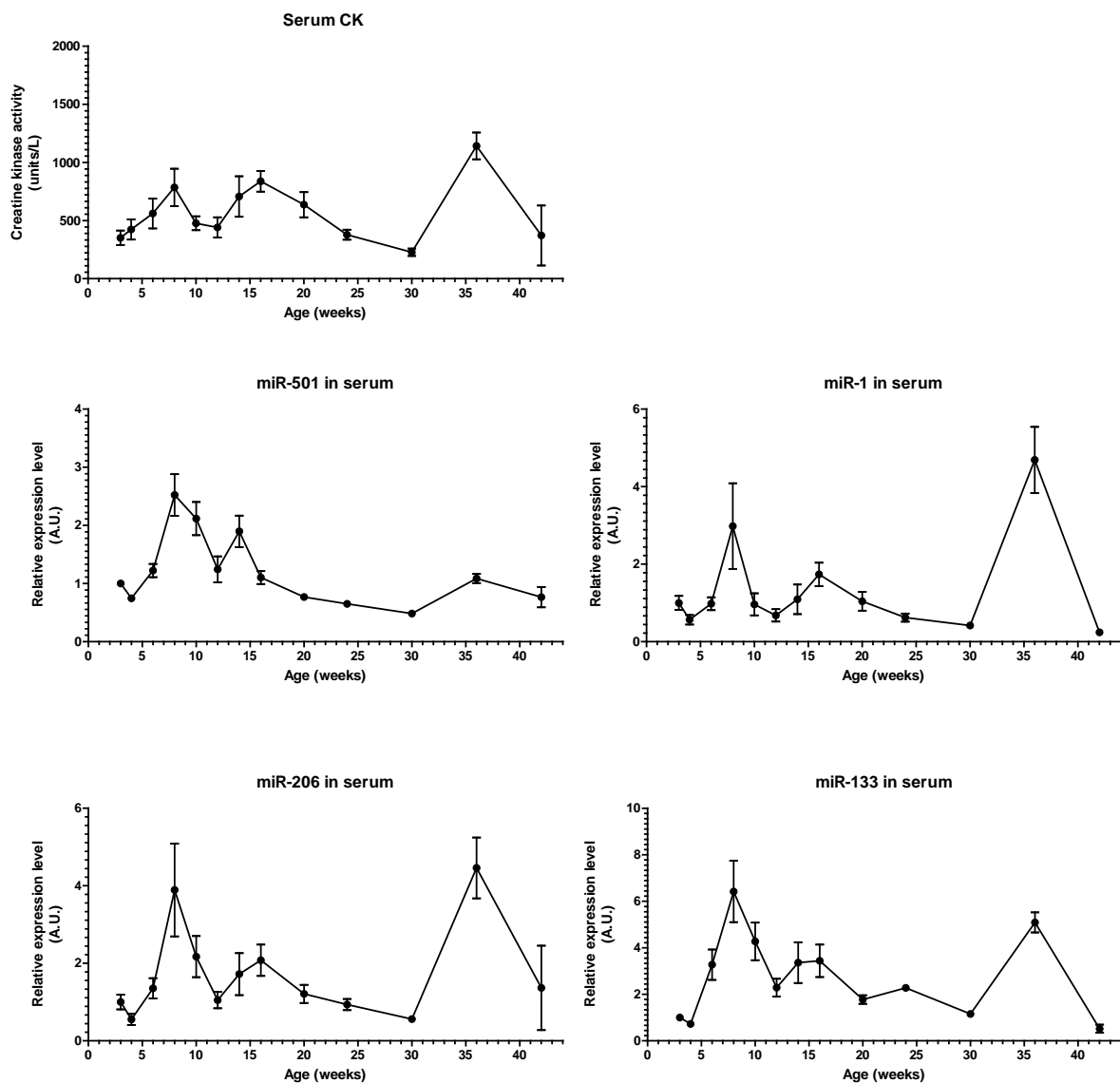
Figure 2.14. Serum miR-501 levels correlate with disease severity in aging *mdx* mice.
Creatine kinase activity and expressions of miR-501 and myomirs in sera from *mdx* mice with different ages, ranging from 3 weeks to 42 weeks. miRNA expression levels were measured by qRT-PCR and the values were normalized to the spiked cel-miR-39. Data are presented as the mean ± SEM, n=3-10 mice per time point.

Chapter 3- Material and methods

3.1 Animals

3.1.1 Animal husbandry

C57BL6/6J and C57BL/10ScSn-Dmd^{mdx} mice were purchased from Harlan and Jackson Laboratories, respectively. Animals were housed in a pathogen-free animal facility in University Hospital Zurich on an inverted 12-hour light cycle (dark phase began at 6 AM), fed *ad libitum* with chow diet. All animal studies were approved by the ethics committee of the Canton of Zurich Veterinary Office. Guidelines set by the Swiss Federal Veterinary Office were followed in all procedures.

3.1.2 Cardiotoxin and antagomir injection

Cardiotoxin from *Naja mossambica mossambica* (Sigma-Aldrich) was dissolved in PBS to a final concentration of 10μM and injected into C57BL6/6J mouse Tibialis anterior (TA) muscles using 1ml insulin syringes (50μl per muscle). Antagomirs (Sigma) were dissolved in ddH$_2$O in room temperature to a concentration of 1μg/μl based on the amount stated by the company. 7.5μg antagomir was injected mixed with CTX (day 0) or injected alone, diluted in PBS. In either case the total injection volume was adjusted 50μl per muscle. One hour before injection, 5mg/kg Carprofen (Rimadyl®) was injected subcutaneously. Mice were anesthetized with 3-5% isoflurane vaporized in oxygen (inhaled) before CTX injection. For tissue harvesting, mice were sacrificed by cervical dislocation, TA muscles were dissected, snap-frozen in liquid nitrogen and stored in -80°C.

3.1.3 Measurement of creatine kinase activity in mouse serum

Mice were euthanized by CO$_2$ inhalation, and 600-900μl blood was collected using 25G syringes from heart ventricles and transferred to 1.5ml eppendorf tubes. Blood samples were incubated at 37°C for 30 min to coagulate. Tubes were centrifuged in 2000g for 8 min. and the supernatant was again centrifuged at 12000g for 15 min to precipitate the residual cell debris. The supernatants were transferred to new tubes and stored at -80°C.

Serum creatine kinase activity was measured using Creatine Kinase Activity Assay Kit (Sigma) according to the manufacturer's instructions. Due to high levels of creatine kinase in sera of *mdx* mice, 1:10 dilution of sera samples was used to avoid exceeding the assay linear range.

3.2 Isolation of primary myogenic and fibro/adipogenic progenitors by FACS

Mouse TA muscles were minced in cold PBS on ice. Samples were incubated three times each with 5ml 0.2% solution of collagenase type II (Life technologies) in HBSS buffer supplemented with 1.5% BSA at 37°C in a shaking waterbath. After each round the suspension was vortexed shortly and centrifuged for 30 seconds at 700g and the supernatant, containing the cells detached from the tissue, was added to 15ml low-glucose DMEM supplemented with 10% FBS on ice. The final suspension was passed through a 100-μm Cell strainer (BD Biosciences) and centrifuged at 1400g for 5 min. The pellet was dissolved in 2ml erythrocyte lysis buffer (154 mMNH_4Cl, 10mM $KHCO_3$, 0.1mM EDTA) on ice, followed by adding 25ml cold PBS. The suspension was passed through a 40-μm Cell strainer (BD Biosciences) and centrifuged at 1400g for 5 min. Cells were suspended in 500μl FACS buffer (0.5% BSA in PBS) and incubated with antibodies on a rotating chamber in 4°C. Cells were washed three times and resuspended in 300-700μl FACS buffer. Counterstaining with 600 pg/μl 7-AAD was done to exclude dead cells. We used the following monoclonal antibodies: Alexa Fluor 488 anti-mouse CD45 (clone 30-F11, Biolegend, 1:1000), Alexa Fluor 488 anti-mouse CD31 (clone 390, Biolegend, 1:1000), APC anti-mouse Sca1 (clone D7, Biolegend, 1:1000), and PE anti-mouse α7-integrin (R&D Systems, 1:100). Compensation matrix was calculated using antibody-capturing beads (BD CompBead) for all the channels, and gates were refined based on fluorescent minus one (FMO) control samples. Cells from hematopoietic or endothelial lineages were gated out using CD45 and CD31 surface markers, respectively. Among double negative cells, $ScaI^+$ $\alpha7$-integrin$^-$ cells and $ScaI^-$ $\alpha7$-integrin$^+$ cells were sorted to enrich for fibro/ adipogenic and myogenic progenitors, respectively. Sorting was performed on FACSAria III (BD Biosciences) equipped with 5 lasers using 85-μm nozzle. Cells were sorted into culture media or Trizol reagent (Invitrogen).

3.3 Analysis of proliferation of muscle-resident progenitors by flow cytometry

Mice were injected in TA muscle with CTX and antagomir on day 0 and received antagomir intramuscularly again on day 3. Twelve hours later, 10μg EdU per gram body weight was injected i.p. to the animals. Muscles were harvested on day 4, and preparation of muscle cell suspension was performed as described in the previous section. However, after passing the cells through the 40-μm Cell strainer, cells were centrifuged, dissolved in 2ml 1% BSA in PBS and subjected to staining for detection of the incorporated EdU using the Click-iT EdU Alexa Fluor 647 Flow Cytometry Assay Kit (Life technologies). Briefly, cells were washed once in 1% BSA in PBS and the pellet was dissolved in 100μl 1X Click-iT saponin-based permeabilization and wash buffer. The Click-iT reaction cocktail was prepared according to the manufacturer's instructions and added to the cell suspension. Cells were washed once with the permeabilization and wash buffer. The pellet was taken up in 500μl FACS buffer, and antibody incubation and flow cytometry analysis proceeded as described previously. A FMO sample for EdU, made by omitting Alexa Fluor 647 dye from the reaction cocktail, was always included in the analysis. Flow cytometry was performed on a FACSAria III (BD Biosciences) equipped with 5 lasers. FlowJo software (Treestar) was used for making the compensation matrix and data analysis.

3.4 Culture and transfection of primary myoblasts

Collagen-coated plates were prepared by overnight incubation with 0.1mg/ml Collagen I (Life technologies), dried under UV light and used for cell culture. Cells were cultured in growth media, consisted of 40% (v/v) low-glucose DMEM, 40% (v/v) HAM's F-10 medium, 20% fetal bovine serum, 5ng/ml basic FGF, and 100U/ml Penicillin/Streptomycin (all from Life technologies). To prevent spontaneous differentiation, at 70% confluency cells were detached by short (max. 1 min) incubation with Trypsin-EDTA 0.05% (Life technologies), washed with DMEM and seeded in new cell culture plates. To induce differentiation, myoblasts were transferred to differentiation media after reaching 80% confluency. Differentiation media consisted of low-glucose DMEM supplemented with 2% horse serum and 100U/ml Penicillin-Streptomycin. Lipofectamine RNAiMax was used for transfecting miRNA mimics or antagomirs to the cells. miRNA mimics and antagomirs were transfected to a final concentration of 38 nM and 12 nM, respectively. Lipofectamine LTX and Plus Reagent was used for DNA transfection,

and co-transfection of DNA with miRNA mimics or antagomirs was performed using Lipofectamine 2000. All reagents were purchased from Invitrogen, and transfection was done according to manufacturer's instructions.

3.5 Culture and transfection of HEK 293 cells

HEK 293 cells were cultured in high-glucose DMEM supplemented with 10% fetal bovine serum and 100U/ml Penicillin/Streptomycin (all from Life technologies). Cells were grown in TPP T75 flasks, and seeded in 24-well or 6-well plates for transfection. Lipofectamine 2000 (Invitrogen) was used for co-transfection of DNA with miRNA mimics or antagomirs, according to manufacturer's instructions. Transfection of DNA was performed using PEI (Polyethylenimine, Sigma). Briefly, PEI was dissolved in warm ddH$_2$O to a concentration of 1mg/ml and filtered through a 0.22μm filter. Aliquots were stored at 4°C. For one well of a 6-well plate, 2μg of plasmid DNA was added to 2ml of serum-free culture medium and mixed. 4μl PEI solution was added to the mixture, briefly vortexed, and incubated in room temperature for 15 min. The mixture was added to the cells, and was replaced by normal growth media 6-8 hours later. Cells were harvested after 2 days and protein expression was checked by western blotting. A well transfected with pEGP-N3 was included to check for transfection efficiency. EGFP fluorescence was visible 12-16 hours after transfection under a fluorescence microscope.

3.6 Analysis of proliferation and apoptosis in primary myoblasts by flow cytometry

Proliferation rate of the cultured myoblasts was measured based on incorporation of EdU in newly synthesized genomic DNA followed by a chemical reaction to detect the EdU by a fluorescent dye. Briefly, EdU was added to the cells in growth media to a final concentration of 1.25 μg/ml. Cells were harvested 14-18 hours later and staining was performed using Click-iT EdU Alexa Fluor 647 Flow Cytometry Assay Kit (Life technologies) according to the manufacturer's instructions. Flow cytometry was performed on a FACSCanto II (BD Biosciences) equipped with three lasers. Flow cytometry data was analyzed using FlowJo software (Treestar).

Apoptosis rate of primary myoblasts was measured by staining with APC-conjugated Annexin V in conjunction with propidium iodide (PI) as a viability marker. Cells were trypsinized and

washed once in PBS without calcium and magnesium salts. The pellet was washed once in 1ml Annexin V binding buffer (BD Biosciences), and cells were resuspended in 100μl Annexin V binding buffer. 5μl APC-Annexin V (Biolegend) was added and cells were incubated for 15 min in room temperature in dark. Afterwards, 100μl Annexin V binding buffer was added followed by 4μl of a 0.1mg/ml solution of PI in Annexin V binding buffer. Cells were incubated for another 15 min at room temperature in dark, washed in 500μl Annexin V binding buffer, and resuspended in 1ml of a 1:1 mixture of Annexin V binding buffer and 2% formaldehyde. Cells were kept on ice and analyzed by flow cytometry on a FACSCanto II equipped with three lasers. Compensation was done using single-stained samples, and FlowJo (Treestar) was used for data analysis.

3.7 Gene and miRNA expression analysis

3.7.1 RNA isolation

Total RNA was isolated from primary tissue cultures using Trizol reagent (Invitrogen) according to the manufacturer's instructions. Tissues were first homogenized in 1.2 ml Trizol on ice by an electric tissue homogenizer and 1ml supernatant was taken for RNA isolation after centrifuging at 12000g for 15 min. RNA Clean-Up and Concentration kit (Norgen Biotek) was used for RNA extraction from sorted myogenic progenitors. Isolation of RNA from sera samples was done using miRNeasy Mini kit (Qiagen) from 50μl serum added to 700μl Qiazol (Qiagen) and spiked with cel-miR-39 as an internal control, according to the manufacturer's instructions for isolating RNA from serum.

3.7.2 Reverse transcription and real time PCR

Potential DNA contamination was removed from RNA samples prior to setting cDNA synthesis reaction by using RNase-free DNase I kit (Ambion). RNA was precipitated in 70% ethanol containing 0.1M ammonium acetate in -80°C overnight. RNA purity and concentration was measured using Nanodrop (Thermo scientific). Integrity of the RNA was confirmed by electrophoresis on denaturing agarose gel or using Agilent RNA 6000 Pico kits on an Agilent 2100 Bioanalyzer. First-strand cDNA was synthesized with 0.4-2μg total RNA using SuperScript III Reverse Transcriptase kit (Thermo Fisher Scientific) with random hexamers according to the

manufacturer's instructions. Finally, RNA strand was degraded by adding 1 unit RNase H and incubating at 37°C for 20 min. The cDNA was diluted 1:5 with nuclease-free water and 1μl was used per PCR reaction. FastStart Universal SYBR Green Master (Roche) was used to run the real time PCR reactions on a 7500 Fast Real-Time PCR system (Applied Biosystems). All measurements were performed using absolute quantifications method. Serial dilutions of a PCR reaction (starting from 1:10,000) by the same primers were used to draw the standard curve. Specific amplification of the target genes were confirmed by melt-curve analysis. Gene expression levels were normalized to 18S rRNA. Primers used for real time PCR are listed in Table 1.

For quantification of miRNA expression levels, first-strand cDNA was synthesized using TaqMan MicroRNA Reverse Transcription Kit (Applied Biosystems). The reaction was done on 5ng total RNA with one or more miRNA-specific RT primers in total volume of 10μl. Due to specificity of the stem-loop RT primers for mature miRNA molecules, DNase-treatment of RNA was not required. The qPCR reaction was done using TaqMan Universal PCR Master Mix (Thermo Fisher Scientific). Serial dilutions of a mixture of all RNA samples were included in the RT and qPCR reaction to draw the standard curve for absolute quantification method. Relative miRNA expression levels were normalized to sno234.

3.7.3 Quantification of relative expression of Clcn5 isoforms

Three primer sets were designed for measuring Clcn5 gene expression: a general primer set (F_C and R_C), which amplifies both Clcn5 splice variants, a primer set specific for isoform 1 (F_1 and $R_{1,2}$), and a primer set specific for isoform 2 (F_2 and $R_{1,2}$). First, two PCR reactions were performed on a mouse cDNA sample with either F_1 and R_C, or F_2 and R_C primers. PCR products were purified and named Iso1-std and Iso2-std, respectively. Since the binding site for R_C primer is downstream of that of $R_{1,2}$, each of the resulting PCR products had the part which could be amplified by the general primers (F_C and R_C) preceded by their corresponding isoform-specific sequence. Serial dilutions of Iso1-std and Iso2-std were used as standard samples to measure isoform 1 or isoform 2 transcripts in unknown samples, respectively, using isoform-specific primers. In a separate reaction, using F_C and R_C primers, the Iso1-std serial dilutions were measured against serial dilutions of Iso2-std as standards. This enabled adjusting the absolute copy numbers ascribed to the Iso1-std serial dilutions, and consequently scaling the values obtained for isoform 1 to those for isoform 2.

3.7.4 RNA sequencing

For small RNA deep sequencing, RNA was isolated using RNA Clean-Up and Concentration kit (Norgen Biotek). Further processing steps, RNA sequencing, and analysis of raw data were done as a service by LC Sciences (Houston, TX, USA). Expression of miRNAs were measured by the relative frequency of reads assigned to each miRNA, stated as RPM (reads per million).

For mRNA sequencing, miRNeasy Mini kit (Qiagen) was used, accompanied by on-column DNase-treatment according to the manufacturer's instructions. RNA integrity was checked using Bioanalyzer RNA pico chips. Poly (A) enrichment, library preparation, and single-end sequencing of 100-nucleotide sequences on Illumina HiSeq-2000 was performed as a service by the Functional Genomics Center Zurich (FGCZ). Mapping of raw sequence reads to the genome was performed using bowtie program with mouse genome build mm10 as reference. Transcript quantification and differential expression analysis were done using RSEM and edgeR software, respectively, on Bioconductor package in R. FastQC program in Java was used for quality control of the high-throughput data.

3.7.5 Northern blotting

Polyacrylamide gels were made by mixing 24ml concentrate, 21ml diluents, and 5ml buffer (all from SequaGel), 400μl APS 10%, and 20μl TEMED. 15μg of total RNA was mixed with equal volume of 2X RNA loading buffer (8M Urea, 50mM EDTA, and 0.4 mg/ml Bromphenol blue). RNA was kept on ice after denaturing by incubating the samples in 95°C for 1 min followed by 5 min in 65°C. Wells of the PAGE gel were rinsed 3 times with the running buffer (0.5X TBE) and the gel was pre-run for 10 min. at 45 mA. Denatured RNA samples were loaded and the gel was run at 45 mA until the dye was a few centimeters away from the end of the gel. RNA bands were visualized by incubating the gel in 0.5μg/ml Ethidium Bromide in 0.5X TBE for 15 min to check for RNA integrity and equal loading of RNA. The ethidium bromide was removed by further incubation in 0.5X TBE, and RNA was transferred onto Hybond+ membranes (Amersham) in running buffer for 2 hours at 50V. Blotting was performed in 4°C and the chamber was put on ice to prevent heating up and diffusing the RNA. The membrane was dried and cross-linked under UV radiation (1200 J/m^2) for 30 seconds, followed by 1 hour incubation at 80°C. Prehybridization was done by incubating the membrane in hybridization buffer for 1 hour at 50°C. Radioactive labeling of the probe was done by incubating 20 picomole of the probe (a

DNA oligonucleotide complementary to the intended mature miRNA) with 3µl γ-^{32}P-ATP (10mCi/ml), 2µl T4 PNK buffer, 0.5µl T4 PNK enzyme (both from NEB) in 37°C for 15 min. The reaction was stopped by adding 30ul EDTA (30mM, pH8.0), and the probe was purified by loading on Sephadex G25 spin columns (Amersham) and centrifuging in 735g for 1 min. The radioactivity of the probe was checked by a beta counter, and then the probe was denatured for 1 min at 95°C and putting on ice afterwards. The membrane was hybridized in 15ml fresh hybridization buffer containing half of the prepared radiolabeled probe. Hybridization was done at 50°C overnight. Unbound probe molecules were removed by washing the membrane twice each time for 10 min in wash buffer 1, followed by washing once with wash buffer 2, all performed at 50°C. The membrane was exposed to a phosphorimager for three days to detect the radioactivity signal. Signal density of the bands was measured using ImageJ (NIH).

Buffers used for Northern blotting are as below

SSC (20X)

NaCl	175.3 g
Tri-Sodium Citrate.2H$_2$0	88.2 g

Dissolved in 1L ddH$_2$O. pH was adjusted to 7.0 using HCl

Denhardt's solution (50X)

Albumin fraction V	1g
Polyvinylpyrrolidone K30	1g
Ficoll 400	1g

Dissolved in 100ml ddH$_2$O.

Hybridization Buffer

SDS 10%	35ml
SSC 20X	12.5ml
Na$_2$HPO$_4$ (1M, pH 7.2)	1ml
50X Denhardt`s solution	1ml
Herring Sperm DNA (10mg/ml)	500µl

The DNA was incubated at 100°C for 5 min. before adding to the hybridization buffer.

Washing buffer 1

SDS 10%   250ml

SSC 20X   125ml

ddH$_2$O   125ml

Washing buffer 2

SDS 10%   50ml

SSC 20X   25ml

ddH$_2$O   425ml

3.8 Protein isolation, SDS-PAGE and Western blotting

For protein isolation from cultured cells, growth media was removed, wells were rinsed twice with PBS, and cells were lysed in cold RIPA buffer (25 mM Tris HCl pH 7.6, 150 mM NaCl, 1% NP- 40, 1% sodium deoxycholate, 0.1% SDS) supplemented with cOmplete EDTA-free protease inhibitor cocktail and PhosSTOP phosphatase inhibitor cocktail (Roche) while being detached using a cell scraper. Tissues were ground in liquid nitrogen using a mortar and pestle and the resulting powder was added to the complemented RIPA buffer as above. Samples were briefly sonicated and then centrifuged in 14000g for 15 min. Supernatant containing soluble proteins was collected and protein concentration was measured using Pierce BCA protein assay kit (Thermo Fisher), using serial dilutions of a 1mg/ml BSA stock to draw the standard curve.

SDS-PAGE was done on NuPAGE Novex 4-12% Bis-Tris protein gels, according to the manufacturere's instructins. Briefly, equal amount of proteins were mixed with 4X LDS sample buffer and 10X reducing agent and heated for 10 min at 70°C. Samples were loaded in the wells and the gel was run in the provided MPS SDS running buffer in 120V. The gel was then used for Coomassie Blue staining or western blotting.

Blotting of the proteins from gel to PDVF membrane was done using Mini Trans-Blot Cell chambers (Biorad) in cold NuPage transfer buffer supplemented with 20% methanol and 0.1% NuPage antioxidant in 100V for 2 hours. Proper transfer of the proteins was confirmed by reversible staining of the membrane with Ponceau S solution (Thermo Fisher). Membranes were blocked in NET-G for one hour and incubated in 4°C with the intended primary antibodies diluted in NET-G for at least 16 hours. Incubation with appropriate HRP-conjugated secondary antibodies diluted in NET buffer was done for 1 hour, and Lumi-Light western blotting substrate

(Roche) was used to detect the signal in a LAS-3000 imager (Fujifilm). Densitometry analysis of the images was done using Aida image analyzer software v.2.3.

3.9 Luciferase activity assay

The 3′UTR fragments of the selected genes were amplified by PCR from human muscle cDNA using High fidelity PCR enzyme mix (Thermo scientific) and the primers listed in the Table 2. PCR products were run on agarose gel and the specific band was cut and DNA was purified using GenElute gel extraction kit (Sigma). Addition of 3′ A overhang was done by adding the DNA to a Taq DNA polymerase (Invitrogen) reaction mixture containing 0.2mM dATP and incubating at 72°C for 20 min. The product was cloned in pCR2.1 vector using TOPO TA cloning kit (Life technologies). Orientation and integrity of the inserts were determined by restriction mapping and DNA sequencing. The resulting constructs were digested with SacI + XhoI restriction enzymes and the fragments containing the inserts were cloned into pmirGLO Dual-Luciferase miRNA Target Expression Vector (Promega), downstream of firefly luciferase ORF. To make the miR-501 sensor construct, two pairs of oligonucleotides (501-full1a,b and 501-full2a,b- Table 3), each pair having a full complementary biding site for miR-501, were annealed and cloned into XbaI site after firefly luciferase ORF in pmirGLO vector. DNA constructs were transfected to HEK 293 cells or primary myoblasts along with miRNA mimics or antagomirs using Lipofectamine 2000 (Invitrogen) according to the manufacturer's instructions. Final concentrations of DNA, miRNA mimic and antagomirs were 200 ng/ml, 38 nM, and 12 nM, respectively. Growth media was changed after 24 hours and cells were harvested one day later in passive lysis buffer (Promega). Plates were frozen and thawed once to enhance cell lysis. Activity of Firefly and Renilla luciferase enzymes was measured using Dual-Luciferase Reporter Assay System (Promega) with a Tecan plate reader.

3.10 Generation of overexpression DNA constructs

A double-stranded DNA molecule containing the Kozak consensus sequence including start codon (ATG) followed by a sequence encoding the FLAG-tag (Asp-Tyr-Lys-Asp-Asp-Asp-Asp-Lys) was made by annealing two oligonucleotides (Kozak-Flag-F, R- Table 3). The DNA was designed to have sticky ends compatible with NheI and HindIII restriction enzymes in its 5′ and 3′ ends, respectively. pcDNA3.1 (+) mammalian expression vector (Invitrogen) was digested in

its multiple cloning site with NheI and HindIII enzymes, and the Kozak-Flag DNA was ligated there to recircularize the vector. The resulting construct (pcDNA-Kozak-Flag) was used to make overexpression constructs encoding for FLAG-tagged proteins.

Open reading frames of the genes were amplified by PCR from mouse multi-tissue cDNA using High fidelity PCR enzyme mix (Thermo scientific) and specific primers as described in Table 4. A HindIII restriction site was included at the end of both forward and reverse primers. PCR products were digested with HindIII enzyme and cloned in the HindIII site of the pcDNA-Kozak-Flag vector. All constructs were confirmed by restriction mapping and DNA sequencing.

3.11 Skeletal muscle immunofluorescence

Skeletal muscle was dissected and flash frozen in isopentane/liquid nitrogen. Frozen sections of 10 μm were prepared from 3 different areas of the tibialis anterior muscle, 500 μm apart. Sections were then processed for immunofluorescence using the Vector M.O.M. Immunodetection kit and protocol (Vector Laboratories). Slides were mounted with Fluoroshield with DAPI (Sigma). Antibodies against eMHC (BF-G6, 1:20) were obtained from the Developmental Studies Hybridoma Bank, University of Iowa and against laminin (L9393, 1:500) were obtained from Sigma. Images for each section were obtained using Leica confocal laser scanning microscope SP5 Mid UV-VIS and evaluated for fiber and cell counts using Ilastic and ImageJ software.

3.12 Statistical analysis

Unless specified otherwise, two-sided unpaired student's t-test was used to compare sample groups, and the null hypothesis (no difference between the groups) was rejected if $p < 0.05$. When applicable, one-sample t-test with a hypothetical mean value of 1 was used to analyze the significance based on fold-change values. Differential expression analysis of RNA-seq data was performed by edgeR software, and two-sample Kolmogorov-Smirnov test was used on fold-change distribution of different groups of transcripts. Data in bar graphs are shown as mean ± SEM.

Table 1. Primers for real time PCR using SYBR Green.

Target gene	Forward primer	Reverse primer
18S	GACACGGACAGGATTGACAGATTG	AAATCGCTCCACCAACTAAGAACG
Esrrg-V1	TGATTTATAGGTGGGGTGCACAA	CTGTAACTCCCACTGGCGTC
Ptprf	CCTGGCGGTCATTCTCATCA	GTCCTTCAGCCCGATTGACT
Cpeb2-V1	GCAGCCGGAACATCCAGAATA	GTCGGTTCCTGGATGTGGAT
Amotl1	AGCCTGCGAGAACAGAAGTG	GACGGAGTGCAGAGTACCAC
Gan	TCGGTGGATAGCACACGATG	CCCTCCGATGGTCACTATGC
Col19a1	AATACACGGGGAGAAAGGCG	GGAACATTCACCCCTCCCTG
Sertad2-V1	TTTAGCCTGTCTCGCCCATC	ACCCAACATATATCTTCCGCGA
Hmgcs1	CTATGATTGCATTGGGCGGC	CCAGAGCATATCGTCCATCCC
Kctd9-V1	CTTTCTGGATCAGTGCTCGAC	CGTTTGAGCAGAGCATCTTG
Dclk1-V4	TAGATGAAAGTGAATGTCGAGTGGT	CATCGCTCCATTGTGTCTTTT
Dclk1-V5	GAGTTTCTGTAATAGCAACCACCGC	GTTTTACAGAAGTTTGGGGAGGG
Clcn5	GCACTGTTGCTGGAATTCTG	AAGAGCCCAGAGGACGTACA
Clcn5-V1	CTGCCAAGGTTGTTTCTTCC	TCCATGACTCTATTTGAAGAGCCTA
Clcn5-V2	TTCATCAGGGGAGTTTTAGTAGCTT	TCCATGACTCTATTTGAAGAGCCTA
Myh3	AGAGGGTTTCTCATGCGTGT	TGTTGTACTGGATGCAGAAGATG
Mb	ATCACACGCCACCAAGCAC	GTCCCCGGAATGTCTCTTCTTCA
Mstn	AGATGGGCTGAATCCCTTTTTA	AATCGACCGTGAGGGGGTA

Table 2. Primers used for cloning of 3′ UTR fragments.

Target gene	Forward primer	Reverse primer
Esrrg	TAAATATCTAGAGCAATTTTGTGCTGGCTTTG	TATAAATCTAGAAGGTGTAATCTCATCCTTTGTG
Gan	GGAGGAAGCAGAGCAGAGTG	TGAGAAGGCAGAATGGCACTG
Sertad2-Site 1	CAGGGACCCAGCGACTATG	CCTGGCCCTTTCTTAAAGCAC
Sertad2-Site 2	GCCCTGAGGTCAATCAAGGA	TACAAAAGTAAGACTGCTCATTTCC
Kctd9	GAATTTTAGGGGCTGGAGGAAGA	CTAAGCTGGCCCTATGTAAACTAT
Dclk1- Site 1	CAGCTCCTCCCGAACTCAAC	TGGGGCGTCATCAGTACATC
Dclk1- Site 2	GGTTCATCTCTGTGGTCTGTGT	AGCACTGGCTAAAAGCAAAGC
Dclk1- Site 3	TCACCACCGGTGTTTCCATATT	GCCTGGGGCACATTTTTATG
Cpeb2	GAATAGCAAACTGGCCTCTGTT	ACATTTGCAATACCTCACCTCGTTA

Table 3. Oligodeoxynucleotides.

Name	Sequence
501-full-1a	CTAGTCCAAATCCTTGCCCGGGTGCATTC
501-full-1b	TCGAGAATGCACCCGGGCAAGGATTTGGA
501-full-2a	TCGAGCCAAATCCTTGCCCGGGTGCATTGC
501-full-2b	GGCCGCAATGCACCCGGGCAAGGATTTGGC
Kozak-Flag-F	CTAGCCGCCACCATGGATTACAAGGATGACGATGACA
Kozak-Flag-R	AGCTTGTCATCGTCATCCTTGTAATCCATGGTGGCGG

Table 4. Primers used for cloning of ORFs.

Target gene	Forward primer	Reverse primer
Esrrg-V1	ATGGTTAAGCTTGATTCGGTAGAACTTTGC	AATATAAAGCTTTCAGACCTTGGCCTCCAG
Esrrg-V2	ACGCATAAGCTTTCAAACAAAGATCGACAC	AATATAAAGCTTTCAGACCTTGGCCTCCAG
Gan	TAAATTAAGCTTGCCGAGGGCAGCGC	ATAATAAAGCTTTCAAGGGGAATGGACCCG
Sertad2	AGGTTAAGCTTTTGGGTAAAGGAGGAAAAC	AATATAAAGCTTTCAGGAGCCAACAAGCAC
Kctd9- V1 and V2	ATATATAAGCTTCGGCGGGTCACGCT	GTCCTCAAGCTTTCATCTGACACTCT
Dclk1- V4	ATGTTTAAGCTTTCGTTCGGCAGAGATATG	CGCATGAAGCTTTTACACTGAGTCTCCTAC
Dclk1- V5	ATGTTTAAGCTTTCGTTCGGCAGAGATATG	ATGACTAAGCTTTTAAAAGGGCGAATTGGG

Discussion

Skeletal muscle regeneration is an elaborately regulated process requiring coordination of various cellular responses. It is well established that satellite cells are the only source of the new myofiber nuclei, either during development or regeneration. On the other hand, there is increasing body of evidence that miRNAs are major regulators of proper satellite cell function, either in quiescent, proliferating, or differentiating states (364). Several miRNAs have been identified and functionally characterized in myogenic progenitors; however, most of screenings have been performed on the primary cells cultured ex vivo or immortalized myoblast cell lines. Despite facilitating the experimental procedures and enabling application of a wider range of methods, the inevitable differences between in vitro and in vivo conditions is always a major concern. The aim of this study was to identify novel miRNAs involved in the activation of the satellite cells, induced by muscle injury.

By high-throughput screening of miRNAs in activated satellite cells, we identified miR-501-3p as a new myoblast-specific miRNA. Tissue distribution profile of miR-501 and its remarkable upregulation during skeletal muscle regeneration is suggestive of a specific role of this miRNA in adult muscle stem cells. miR-501 is upregulated immediately after muscle injury, when the satellite cells are activated, and is gradually declined afterwards. This pattern of transient upregulation is previously suggested to be associated with miRNAs involved in regulation of transition from proliferation to differentiation of myogenic progenitors (365). Within this category, while miR-351 is shown to play a role in protecting differentiating myoblasts against apoptosis and promote their proliferation to some extent (365), miR-501 seems not to regulate proliferation or apoptosis of the myoblasts. On the other hand, miR-206, and skeletal-muscle-specific miRNA, is upregulated later on, and is indicated to promote myoblast differentiation by regulating several target genes important in this process (352).

Analysis of the miR-501 genomic locus in mouse and human shows that miR-501 is located in a cluster of miRNAs in one of the introns of Clcn5 gene. Clustering of miRNAs is generally associated with their co-expression; however, we observed that within the five different pri-miRNAs in the intron 2 of Clcn5 in mouse, only miR-501-3p is processed and expressed in functional levels in activated mouse myogenic progenitors. This indicates a high degree of regulation during the miRNA maturation, and that miR-501 is preferentially processed out of a long primary transcript, implying a functional basis for this selectivity.

Alternative splicing leads to generation of two different mRNA transcripts encoding two Clcn5 isoforms. The intron harboring miR-501 is located between the exons present only in isoform 2 of Clcn5. Interestingly, we observed a massive upregulation of isoform 2 during skeletal muscle regeneration, while miR-501 level is increasing as well. This confirms miR-501 as an intronic miRNA, sharing promoter and transcription regulatory elements with its host gene. Measurement of relative expression levels of Clcn5 isoforms in different tissues indicated that while isoform 1 is expressed in relatively very high levels in kidney, as already reported (366), myoblasts express isoform 2 in much higher levels than any examined tissue. In fact, there is a remarkable difference in the proportion of isoforms in different tissues; while the majority of transcripts belong to isoform 1 in kidney, isoform 2 comprises nearly all of Clcn5 transcripts in skeletal muscle, quiescent or activated satellite cells, and myoblasts. However, on our tissue panel and comparing quiescent versus activated MPs we observed that miR-501 levels do not show a perfect correlation with Clcn5 or its isoforms' expression levels. This indicates that although induction of miR-501 during skeletal muscle regeneration is at least in part due to upregulation of Clcn5, maturation of miR-501 is regulated by other factors as well, and this miRNA is not just simply a by-product of Clcn5 transcription and splicing events. To our surprise, there is no report on isoform 2 of Clcn5 to date. Based on its specific upregulation during muscle regeneration, we believe that this isoform deserves functional characterization during this process.

The expression pattern of miR-501 during skeletal muscle regeneration suggests a role for this miRNA in regulating proliferation of myoblasts or their early differentiation. Pharmacological inhibition of miR-501 in regenerating muscle using intramuscular injection of antagomirs, followed by analysis of proliferation rate in MPs and FAPs, indicated that miR-501 is not involved in regulating proliferation of the muscle-resident progenitors. This was corroborated by inhibition of miR-501 in cultured primary myoblasts as well. Furthermore, miR-501 regulates neither apoptosis nor differentiation in primary myoblasts. This might explain why this miRNA has not been previously identified as a regulator of myoblast proliferation or differentiation.

Differentiation of myoblasts is concomitant with expression of contractile proteins, including myosin heavy chains. There are several myosin heavy chain isoforms in all vertebrates, and their expression pattern is determined by the muscle fiber type and the developmental stage. The first isoform expressed in all myofibers, during both development and regeneration, is the embryonic myosin heavy chain, encoded by Myh3 gene. To determine the role of miR-501 in regulating the differentiation of myoblasts in vivo, we measured eMHC protein levels in the regenerating

skeletal muscle injected with antagomir-501. We observed a dramatic decrease in eMHC in the muscle when miR-501 was inhibited. Surprisingly, this was not due to the myoblasts being in a less differentiated state, since we did not observe reduced levels of myoglobin and myostatin. Therefore, eMHC must be downregulated by a factor controlled by miR-501, independent of the general differentiation status of the myoblasts.

Transcriptome analysis of cultured myoblasts transfected with antagomir-501 indicated upregulation of miR-501 predicted target genes. Application of several criteria and confirming the direct binding of miR-501 to the 3′UTRs by luciferase assay led us to a list of six target genes. Cloning and overexpression of these genes in primary myoblasts indicated that only gigaxonin was able to downregulate eMHC levels in differentiating myoblasts, mimicking the effect of miR-501 inhibition in regenerating skeletal muscle. We cannot exclude that there are other targets such as gigaxonin. In fact, further studies that employ sequencing studies in vivo could reveal further targets that are preventing efficient and normal muscle regeneration. Since miRNAs frequently target multiple targets of a similar molecular pathway, miR-501 might be a critical checkpoint during muscle regeneration to prevent the expression of gene products disadvantageous for the newly built fibers, such as gigaxonin.

Protein product of Gan gene is named gigaxonin, since mutation of Gan in human causes an autosomal recessive sensorimotor disease, called Giant axonal neuropathy (367). The disease is characterized by distended axons, deteriorating with age, which impairs the transmission of impulses through the axons. This has been indicated to be due to accumulation of neurofilaments, which are a group of cytoskeleton intermediate filaments in the neurons (368). Gigaxonin structure consists of a BTB and a Kelch repeat domain. The BTB domain mediates binding of Gigaxonin to Cullin3 complexed with E3 ubiquitin ligases, and Kelch domain in gigaxonin is indicated to bind the intermediate filaments (369-372). Therefore, gigaxonin acts as a ubiquitin ligase adaptor, mediating ubiquitation and degradation of intermediate filaments by proteasome (373). It is indicated that gigaxonin binds Vimentin via its central rod domain (373); interestingly, this domain (pfam00038) is also present in eMHC protein. Hence, we suggest a model in which upregulation of miR-501 during skeletal muscle regeneration leads to downregulation of gigaxonin, preventing degradation of eMHC contractile proteins. Consistent with this model, downregulation of miR-501 after day 6 of regeneration is paralleled to the degradation of eMHC, allowing the adult myosin heavy chains to replace the embryonic isoform.

There is a paucity of information in literature about the exact molecular mechanisms how eMHC is regulated and how it contributes to the skeletal muscle development and regeneration. However, its significance is highlighted by recent studies indicating that mutations in eMHC gene, Myh3, cause a range of congenital distal arthrogryposis (DA), being the only known genetic cause of the most severe form of DA, Freeman-Sheldon syndrome. However, no animal model for these disorders is developed yet. Our work underscores the importance of eMHC during skeletal muscle regeneration, and introduces miR-501 as the first miRNA known to regulate the turnover of eMHC. Further studies to better understand the pathways regulated by miR-501, and also gigaxonin in skeletal muscle, possibly by inducible Myh3 knockout or gigaxonin overexpression in regenerating muscle can further enhance our knowledge of eMHC and muscle regeneration and could lead to novel therapeutic strategies to improve muscle regeneration and treat a range of myopathies, such as sarcopenia and DMD.

Serum miRNAs have recently emerged as biomarkers for several diseases, such as cancer (374), liver injury (375), and myocardial infarction (376). Analysis of serum miRNA profile in DMD and BMD patients has revealed their promising applicability as disease biomarkers, with high specificity and sensitivity (362). Serum CK levels have been used for a long time as one of the first diagnostic markers for DMD; however, it is known that CK levels do not necessarily correlate with disease severity, since they vary considerably with physical activity and also age of the patient. In a study on DMD and BMD patients it was observed that serum levels of myomiRs (miR-1, miR-133, and miR-206) not only allow efficient diagnosis, but also very well reflect the disease severity as quantified by North Star Ambulatory Assessment index (NSAA), which is one of the gold standards for scoring motor ability in DMD patients (362, 377). Among the tested myomiRs, miR-206 turned out to be the most specific, allowing discriminating DMD from healthy individuals with almost absolute specificity (362, 378). Interestingly, higher serum myomiR levels were observed also in the mouse model of DMD, *mdx* mice, and the levels approached that of wild type mice after treatment of dystrophic muscle by an AAV-mediated exon-skipping strategy (362).

We observed that similar to miR-206, miR-501 levels are significantly higher in skeletal muscle of *mdx* mice compared to wild type animals. Considering the fact that skeletal muscle in *mdx* mice is continuously undergoing degeneration and regeneration, this is consistent with our previous observation that miR-501 is upregulated in activated satellite cells and regenerating skeletal muscle in an acute model of muscle injury. We also observed significantly elevated miR-

501 levels is *mdx* sera, and monitoring the miR-501 levels over a wide range of ages in these mice revealed a remarkable correlation with the disease severity trend. Interestingly, the change in miR-501 levels was similar to that of well-known myomiRs, with miR-501 showing less variation among the age-matched mice. However, being derived primarily from myoblasts rather than myofibers makes miR-501 unique among the existing miRNA biomarkers. It is known that DMD leads to exhaustion of satellite cells in human much earlier than in *mdx* mice considering their lifetime, and this has a significant influence on pathology of DMD. Therefore, miR-501 can have more advantages as a biomarker in humans, indicating the satellite cell content and activity. Such a biomarker could also be advantageous in assessing the efficacy of different therapeutic approaches as well as diagnosis of DMD.

Overall, our studies identify miR-501 as a novel muscle-specific miRNA required specifically during activation of myogenic progenitor cells. miR-501 is upregulated early during skeletal muscle regeneration, when satellite cells are activated and start to proliferate. We observed that this was accompanied by upregulation of miR-501 host gene, Clcn5, and more specifically the isoform of this gene which encompasses the intron containing miR-501. However, based on the observed expression profile of miR-501 and other miRNAs located in the same cluster and the host gene, we conclude that posttranscriptional regulation plays a major role in regulating the expression of miR-501. A loss of function approach in regenerating skeletal muscle indicated an essential role for miR-501 in maintaining eMHC protein levels in newly regenerated myofibers. By specific inhibition of miR-501 in primary myoblasts followed by transcriptome analysis we identified gigaxonin, encoded by Gan gene, as a potential mediator of miR-501 function in vivo. Based on the known function of gigaxonin in mediating ubiquitination of intermediate filaments, we hypothesize that repression of this gene by miR-501 in nascent myofibers helps maintain the eMHC proteins and to prevent their degradation before being replaced by adult MHC isoforms. Finally, we observed significantly increased miR-501 levels in both skeletal muscle and sera of *mdx* mice. Serum miR-501 levels were observed to change over a wide range of ages in *mdx* mice, correlating with disease severity and also the levels of three well known myomiRs. This highlights the potential application of serum miR-501 as a biomarker for DMD and other muscular disorders associated with chronic muscle damage and satellite cell activation.

References

1.   Huard J, Li Y, Fu FH. Muscle injuries and repair: current trends in research. The Journal of bone and joint surgery American volume. 2002;84-A(5):822-32.

2.   Boldrin L, Morgan JE. Activating muscle stem cells: therapeutic potential in muscle diseases. Current opinion in neurology. 2007;20(5):577-82.

3.   Pratesi A, Tarantini F, Di Bari M. Skeletal muscle: an endocrine organ. Clinical cases in mineral and bone metabolism : the official journal of the Italian Society of Osteoporosis, Mineral Metabolism, and Skeletal Diseases. 2013;10(1):11-4.

4.   Dumont NA, Bentzinger CF, Sincennes MC, Rudnicki MA. Satellite Cells and Skeletal Muscle Regeneration. Comprehensive Physiology. 2015;5(3):1027-59.

5.   MacIntosh BR, Gardiner PF, McComas AJ. Skeletal muscle: Human Kinetics; 2006.

6.   Laurie GW, Leblond CP, Martin GR. Localization of type IV collagen, laminin, heparan sulfate proteoglycan, and fibronectin to the basal lamina of basement membranes. The Journal of cell biology. 1982;95(1):340-4.

7.   Sambasivan R, Tajbakhsh S. Adult skeletal muscle stem cells. Results and problems in cell differentiation. 2015;56:191-213.

8.   Ten Broek RW, Grefte S, Von den Hoff JW. Regulatory factors and cell populations involved in skeletal muscle regeneration. Journal of cellular physiology. 2010;224(1):7-16.

9.   Takahashi M, Kubo T, Mizoguchi A, Carlson CG, Endo K, Ohnishi K. Spontaneous muscle action potentials fail to develop without fetal-type acetylcholine receptors. EMBO reports. 2002;3(7):674-81.

10.   Mescher A. Junqueira's Basic Histology: Text and Atlas, 12th Edition : Text and Atlas: Text and Atlas: Mcgraw-hill; 2009.

11.   Scharner J, Zammit PS. The muscle satellite cell at 50: the formative years. Skeletal muscle. 2011;1(1):28.

12.   Clark WE, Blomfield LB. The efficiency of intramuscular anastomoses, with observations on the regeneration of devascularized muscle. Journal of anatomy. 1945;79(Pt 1):15-32 4.

13.   Lewis WH, Lewis MR. Behavior of cross striated muscle in tissue cultures. American Journal of Anatomy. 1917;22(2):169-94.

14.   Mauro A. Satellite cell of skeletal muscle fibers. J Biophys Biochem Cytol. 1961;9:493-5.

15.   Katz B. The Terminations of the Afferent Nerve Fibre in the Muscle Spindle of the Frog. Philosophical Transactions of the Royal Society B: Biological Sciences. 1961;243(703):221-40.

16.   Rocheteau P, Vinet M, Chretien F. Dormancy and Quiescence of Skeletal Muscle Stem Cells. In: Brand-Saberi B, editor. Vertebrate Myogenesis. Results and Problems in Cell Differentiation. 56: Springer Berlin Heidelberg; 2015. p. 215-35.

17.   Allbrook D. Skeletal muscle regeneration. Muscle & nerve. 1981;4(3):234-45.

18.   Stocum DL. Chapter 6 - Regeneration of Musculoskeletal Tissues. In: Stocum DL, editor. Regenerative Biology and Medicine (Second Edition). San Diego: Academic Press; 2012. p. 127-60.

19.   Schmalbruch H, Lewis DM. Dynamics of nuclei of muscle fibers and connective tissue cells in normal and denervated rat muscles. Muscle & nerve. 2000;23(4):617-26.

20.   Bischoff R. Interaction between satellite cells and skeletal muscle fibers. Development. 1990;109(4):943-52.

21.   Palacios D, Puri PL. The epigenetic network regulating muscle development and regeneration. Journal of cellular physiology. 2006;207(1):1-11.

22.   Sambasivan R. Pax7-expressing satellite cells are indispensable for adult skeletal muscle regeneration. Development. 2011;138:3647-56.

23.   Zammit P, Beauchamp J. The skeletal muscle satellite cell: stem cell or son of stem cell? Differentiation. 2001;68(4-5):193-204.

24.   Anderson DJ, Gage FH, Weissman IL. Can stem cells cross lineage boundaries? Nature medicine. 2001;7(4):393-5.

25.   Collins CA, Olsen I, Zammit PS, Heslop L, Petrie A, Partridge TA, et al. Stem cell function, self-renewal, and behavioral heterogeneity of cells from the adult muscle satellite cell niche. Cell. 2005;122(2):289-301.

26.   Sacco A, Doyonnas R, Kraft P, Vitorovic S, Blau HM. Self-renewal and expansion of single transplanted muscle stem cells. Nature. 2008;456(7221):502-6.

27.   Rocheteau P, Gayraud-Morel B, Siegl-Cachedenier I, Blasco MA, Tajbakhsh S. A subpopulation of adult skeletal muscle stem cells retains all template DNA strands after cell division. Cell. 2012;148(1-2):112-25.

28.   Guttridge DC. Chapter 65 - Skeletal Muscle Regeneration. In: Olson JAHN, editor. Muscle. Boston/Waltham: Academic Press; 2012. p. 921-33.

29.   Buckingham M, Relaix F. The role of Pax genes in the development of tissues and organs: Pax3 and Pax7 regulate muscle progenitor cell functions. Annual review of cell and developmental biology. 2007;23:645-73.

30.   Olguin HC, Olwin BB. Pax-7 up-regulation inhibits myogenesis and cell cycle progression in satellite cells: a potential mechanism for self-renewal. Developmental biology. 2004;275(2):375-88.

31.   Seale P, Sabourin LA, Girgis-Gabardo A, Mansouri A, Gruss P, Rudnicki MA. Pax7 is required for the specification of myogenic satellite cells. Cell. 2000;102(6):777-86.

32.   Fukada S, Uezumi A, Ikemoto M, Masuda S, Segawa M, Tanimura N, et al. Molecular signature of quiescent satellite cells in adult skeletal muscle. Stem cells. 2007;25(10):2448-59.

33.   Kuang S, Kuroda K, Le Grand F, Rudnicki MA. Asymmetric self-renewal and commitment of satellite stem cells in muscle. Cell. 2007;129(5):999-1010.

34.   Becker KL, Nylen ES, White JC, Muller B, Snider RH, Jr. Clinical review 167: Procalcitonin and the calcitonin gene family of peptides in inflammation, infection, and sepsis: a journey from calcitonin back to its precursors. The Journal of clinical endocrinology and metabolism. 2004;89(4):1512-25.

35.   Sassoli C, Formigli L, Bini F, Tani A, Squecco R, Battistini C, et al. Effects of S1P on skeletal muscle repair/regeneration during eccentric contraction. Journal of cellular and molecular medicine. 2011;15(11):2498-511.

36.   Nagata Y, Partridge TA, Matsuda R, Zammit PS. Entry of muscle satellite cells into the cell cycle requires sphingolipid signaling. The Journal of cell biology. 2006;174(2):245-53.

37.   Yin H, Price F, Rudnicki MA. Satellite cells and the muscle stem cell niche. Physiol Rev. 2013;93:23-67.

38.   Calise S, Blescia S, Cencetti F, Bernacchioni C, Donati C, Bruni P. Sphingosine 1-phosphate stimulates proliferation and migration of satellite cells: role of S1P receptors. Biochimica et biophysica acta. 2012;1823(2):439-50.

39.   Danieli-Betto D, Peron S, Germinario E, Zanin M, Sorci G, Franzoso S, et al. Sphingosine 1-phosphate signaling is involved in skeletal muscle regeneration. American journal of physiology Cell physiology. 2010;298(3):C550-8.

40.   Belcastro AN, Shewchuk LD, Raj DA. Exercise-induced muscle injury: a calpain hypothesis. Molecular and cellular biochemistry. 1998;179(1-2):135-45.

41.   Moraczewski J, Piekarska E, Bonavaud S, Wosinska K, Chazaud B, Barlovatz-Meimon G. Differential intracellular distribution and activities of mu- and m-calpains during the differentiation of human myogenic cells in culture. Comptes rendus de l'Academie des sciences Serie III, Sciences de la vie. 1996;319(8):681-6.

42.   Murachi T. Calcium-dependent proteinases and specific inhibitors: calpain and calpastatin. Biochemical Society symposium. 1984;49:149-67.

43.   Sultan KR, Dittrich BT, Pette D. Calpain activity in fast, slow, transforming, and regenerating skeletal muscles of rat. American journal of physiology Cell physiology. 2000;279(3):C639-47.

44.   Brzoska E, Ciemerych MA, Przewozniak M, Zimowska M. Chapter Twelve - Regulation of Muscle Stem Cells Activation: The Role of Growth Factors and Extracellular Matrix. In: Gerald L, editor. Vitamins & Hormones. Volume 87: Academic Press; 2011. p. 239-76.

45.   Forsten-Williams K, Chu CL, Fannon M, Buczek-Thomas JA, Nugent MA. Control of growth factor networks by heparan sulfate proteoglycans. Annals of biomedical engineering. 2008;36(12):2134-48.

46.   Kurisaki T, Masuda A, Sudo K, Sakagami J, Higashiyama S, Matsuda Y, et al. Phenotypic analysis of Meltrin alpha (ADAM12)-deficient mice: involvement of Meltrin alpha in adipogenesis and myogenesis. Mol Cell Biol. 2003;23(1):55-61.

47.   Levi E, Fridman R, Miao HQ, Ma YS, Yayon A, Vlodavsky I. Matrix metalloproteinase 2 releases active soluble ectodomain of fibroblast growth factor receptor 1. Proceedings of the National Academy of Sciences of the United States of America. 1996;93(14):7069-74.

48.   Arsic N, Zacchigna S, Zentilin L, Ramirez-Correa G, Pattarini L, Salvi A, et al. Vascular endothelial growth factor stimulates skeletal muscle regeneration in vivo. Molecular therapy : the journal of the American Society of Gene Therapy. 2004;10(5):844-54.

49.   Deasy BM, Feduska JM, Payne TR, Li Y, Ambrosio F, Huard J. Effect of VEGF on the regenerative capacity of muscle stem cells in dystrophic skeletal muscle. Molecular therapy : the journal of the American Society of Gene Therapy. 2009;17(10):1788-98.

50.	Fielding RA, Manfredi TJ, Ding W, Fiatarone MA, Evans WJ, Cannon JG. Acute phase response in exercise. III. Neutrophil and IL-1 beta accumulation in skeletal muscle. The American journal of physiology. 1993;265(1 Pt 2):R166-72.

51.	Lu H, Huang D, Saederup N, Charo IF, Ransohoff RM, Zhou L. Macrophages recruited via CCR2 produce insulin-like growth factor-1 to repair acute skeletal muscle injury. FASEB journal : official publication of the Federation of American Societies for Experimental Biology. 2011;25(1):358-69.

52.	Shimokado K, Raines EW, Madtes DK, Barrett TB, Benditt EP, Ross R. A significant part of macrophage-derived growth factor consists of at least two forms of PDGF. Cell. 1985;43(1):277-86.

53.	Tidball JG. Inflammatory processes in muscle injury and repair. American journal of physiology Regulatory, integrative and comparative physiology. 2005;288(2):R345-53.

54.	Ciemerych MA, Archacka K, Grabowska I, Przewozniak M. Cell cycle regulation during proliferation and differentiation of mammalian muscle precursor cells. Results and problems in cell differentiation. 2011;53:473-527.

55.	Bischoff R. A satellite cell mitogen from crushed adult muscle. Developmental biology. 1986;115(1):140-7.

56.	Tatsumi R, Anderson JE, Nevoret CJ, Halevy O, Allen RE. HGF/SF is present in normal adult skeletal muscle and is capable of activating satellite cells. Developmental biology. 1998;194(1):114-28.

57.	Mezzogiorno A, Coletta M, Zani BM, Cossu G, Molinaro M. Paracrine stimulation of senescent satellite cell proliferation by factors released by muscle or myotubes from young mice. Mechanisms of ageing and development. 1993;70(1-2):35-44.

58.	Sheehan SM, Tatsumi R, Temm-Grove CJ, Allen RE. HGF is an autocrine growth factor for skeletal muscle satellite cells in vitro. Muscle & nerve. 2000;23(2):239-45.

59.	Cornelison DD, Wold BJ. Single-cell analysis of regulatory gene expression in quiescent and activated mouse skeletal muscle satellite cells. Developmental biology. 1997;191(2):270-83.

60.	Tatsumi R, Hattori A, Ikeuchi Y, Anderson JE, Allen RE. Release of hepatocyte growth factor from mechanically stretched skeletal muscle satellite cells and role of pH and nitric oxide. Molecular biology of the cell. 2002;13(8):2909-18.

61.	Tatsumi R, Liu X, Pulido A, Morales M, Sakata T, Dial S, et al. Satellite cell activation in stretched skeletal muscle and the role of nitric oxide and hepatocyte growth factor. American journal of physiology Cell physiology. 2006;290(6):C1487-94.

62.	Yamada M, Tatsumi R, Kikuiri T, Okamoto S, Nonoshita S, Mizunoya W, et al. Matrix metalloproteinases are involved in mechanical stretch-induced activation of skeletal muscle satellite cells. Muscle & nerve. 2006;34(3):313-9.

63.	Allen RE, Sheehan SM, Taylor RG, Kendall TL, Rice GM. Hepatocyte growth factor activates quiescent skeletal muscle satellite cells in vitro. Journal of cellular physiology. 1995;165(2):307-12.

64.	Basilico C, Arnesano A, Galluzzo M, Comoglio PM, Michieli P. A high affinity hepatocyte growth factor-binding site in the immunoglobulin-like region of Met. The Journal of biological chemistry. 2008;283(30):21267-77.

65.   Coolican SA, Samuel DS, Ewton DZ, McWade FJ, Florini JR. The mitogenic and myogenic actions of insulin-like growth factors utilize distinct signaling pathways. The Journal of biological chemistry. 1997;272(10):6653-62.

66.   Yin H, Price F, Rudnicki MA. Satellite cells and the muscle stem cell niche. Physiological reviews. 2013;93(1):23-67.

67.   Zhong W, Chia W. Neurogenesis and asymmetric cell division. Curr Opin Neurobiol. 2008;18(1):4-11.

68.   Wu Z, Luby-Phelps K, Bugde A, Molyneux LA, Denard B, Li WH, et al. Capacity for stochastic self-renewal and differentiation in mammalian spermatogonial stem cells. The Journal of cell biology. 2009;187(4):513-24.

69.   Morrison SJ, Kimble J. Asymmetric and symmetric stem-cell divisions in development and cancer. Nature. 2006;441(7097):1068-74.

70.   Conboy IM, Rando TA. The regulation of Notch signaling controls satellite cell activation and cell fate determination in postnatal myogenesis. Developmental cell. 2002;3(3):397-409.

71.   Le Grand F, Jones AE, Seale V, Scime A, Rudnicki MA. Wnt7a activates the planar cell polarity pathway to drive the symmetric expansion of satellite stem cells. Cell stem cell. 2009;4(6):535-47.

72.   Komiya Y, Habas R. Wnt signal transduction pathways. Organogenesis. 2008;4(2):68-75.

73.   Schultz E. Satellite cell proliferative compartments in growing skeletal muscles. Developmental biology. 1996;175(1):84-94.

74.   Koning M, Werker PM, van Luyn MJ, Krenning G, Harmsen MC. A global downregulation of microRNAs occurs in human quiescent satellite cells during myogenesis. Differentiation. 2012;84(4):314-21.

75.   Abou-Khalil R, Le Grand F, Pallafacchina G, Valable S, Authier FJ, Rudnicki MA, et al. Autocrine and paracrine angiopoietin 1/Tie-2 signaling promotes muscle satellite cell self-renewal. Cell stem cell. 2009;5(3):298-309.

76.   Le Grand F, Grifone R, Mourikis P, Houbron C, Gigaud C, Pujol J, et al. Six1 regulates stem cell repair potential and self-renewal during skeletal muscle regeneration. The Journal of cell biology. 2012;198(5):815-32.

77.   Joe AW, Yi L, Natarajan A, Le Grand F, So L, Wang J, et al. Muscle injury activates resident fibro/adipogenic progenitors that facilitate myogenesis. Nature cell biology. 2010;12(2):153-63.

78.   Uezumi A, Fukada S, Yamamoto N, Takeda S, Tsuchida K. Mesenchymal progenitors distinct from satellite cells contribute to ectopic fat cell formation in skeletal muscle. Nature cell biology. 2010;12(2):143-52.

79.   Uezumi A, Ito T, Morikawa D, Shimizu N, Yoneda T, Segawa M, et al. Fibrosis and adipogenesis originate from a common mesenchymal progenitor in skeletal muscle. Journal of cell science. 2011;124(Pt 21):3654-64.

80.   Judson RN, Zhang RH, Rossi FM. Tissue-resident mesenchymal stem/progenitor cells in skeletal muscle: collaborators or saboteurs? The FEBS journal. 2013;280(17):4100-8.

81.   Wosczyna MN, Biswas AA, Cogswell CA, Goldhamer DJ. Multipotent progenitors resident in the skeletal muscle interstitium exhibit robust BMP-dependent osteogenic activity and mediate heterotopic ossification. Journal of bone and mineral research : the official journal of the American Society for Bone and Mineral Research. 2012;27(5):1004-17.

82.   Heredia JE, Mukundan L, Chen FM, Mueller AA, Deo RC, Locksley RM, et al. Type 2 innate signals stimulate fibro/adipogenic progenitors to facilitate muscle regeneration. Cell. 2013;153(2):376-88.

83.   Natarajan A, Lemos DR, Rossi FM. Fibro/adipogenic progenitors: a double-edged sword in skeletal muscle regeneration. Cell Cycle. 2010;9(11):2045-6.

84.   Cordani N, Pisa V, Pozzi L, Sciorati C, Clementi E. Nitric oxide controls fat deposition in dystrophic skeletal muscle by regulating fibro-adipogenic precursor differentiation. Stem cells. 2014;32(4):874-85.

85.   Ruppel KM, Spudich JA. Structure-function analysis of the motor domain of myosin. Annual review of cell and developmental biology. 1996;12:543-73.

86.   Sellers JR. Myosins: a diverse superfamily. Biochimica et biophysica acta. 2000;1496(1):3-22.

87.   Schiaffino S, Reggiani C. Molecular diversity of myofibrillar proteins: gene regulation and functional significance. Physiological reviews. 1996;76(2):371-423.

88.   Schiaffino S, Reggiani C. Myosin isoforms in mammalian skeletal muscle. Journal of applied physiology. 1994;77(2):493-501.

89.   Weiss A, McDonough D, Wertman B, Acakpo-Satchivi L, Montgomery K, Kucherlapati R, et al. Organization of human and mouse skeletal myosin heavy chain gene clusters is highly conserved. Proceedings of the National Academy of Sciences of the United States of America. 1999;96(6):2958-63.

90.   Weiss A, Leinwand LA. The mammalian myosin heavy chain gene family. Annual review of cell and developmental biology. 1996;12:417-39.

91.   Schiaffino S. Fibre types in skeletal muscle: a personal account. Acta physiologica. 2010;199(4):451-63.

92.   Bottinelli R. Functional heterogeneity of mammalian single muscle fibres: do myosin isoforms tell the whole story? Pflugers Archiv : European journal of physiology. 2001;443(1):6-17.

93.   Whalen RG, Sell SM, Butler-Browne GS, Schwartz K, Bouveret P, Pinset-Harstom I. Three myosin heavy-chain isozymes appear sequentially in rat muscle development. Nature. 1981;292(5826):805-9.

94.   Periasamy M, Wieczorek DF, Nadal-Ginard B. Characterization of a developmentally regulated perinatal myosin heavy-chain gene expressed in skeletal muscle. The Journal of biological chemistry. 1984;259(21):13573-8.

95.   Wydro RM, Nguyen HT, Gubits RM, Nadal-Ginard B. Characterization of sarcomeric myosin heavy chain genes. The Journal of biological chemistry. 1983;258(1):670-8.

96.   Lyons GE, Ontell M, Cox R, Sassoon D, Buckingham M. The expression of myosin genes in developing skeletal muscle in the mouse embryo. The Journal of cell biology. 1990;111(4):1465-76.

97.	Konig S, Burkman J, Fitzgerald J, Mitchell M, Su L, Stedman H. Modular organization of phylogenetically conserved domains controlling developmental regulation of the human skeletal myosin heavy chain gene family. The Journal of biological chemistry. 2002;277(31):27593-605.

98.	Beylkin DH, Allen DL, Leinwand LA. MyoD, Myf5, and the calcineurin pathway activate the developmental myosin heavy chain genes. Developmental biology. 2006;294(2):541-53.

99.	Agbulut O, Noirez P, Beaumont F, Butler-Browne G. Myosin heavy chain isoforms in postnatal muscle development of mice. Biology of the cell / under the auspices of the European Cell Biology Organization. 2003;95(6):399-406.

100.	Lu BD, Allen DL, Leinwand LA, Lyons GE. Spatial and temporal changes in myosin heavy chain gene expression in skeletal muscle development. Developmental biology. 1999;216(1):312-26.

101.	Schiaffino S, Rossi AC, Smerdu V, Leinwand LA, Reggiani C. Developmental myosins: expression patterns and functional significance. Skeletal muscle. 2015;5:22.

102.	Butler-Browne GS, Herlicoviez D, Whalen RG. Effects of hypothyroidism on myosin isozyme transitions in developing rat muscle. FEBS letters. 1984;166(1):71-5.

103.	Gambke B, Lyons GE, Haselgrove J, Kelly AM, Rubinstein NA. Thyroidal and neural control of myosin transitions during development of rat fast and slow muscles. FEBS letters. 1983;156(2):335-9.

104.	Russell SD, Cambon N, Nadal-Ginard B, Whalen RG. Thyroid hormone induces a nerve-independent precocious expression of fast myosin heavy chain mRNA in rat hindlimb skeletal muscle. The Journal of biological chemistry. 1988;263(13):6370-4.

105.	Pandorf CE, Jiang W, Qin AX, Bodell PW, Baldwin KM, Haddad F. Regulation of an antisense RNA with the transition of neonatal to IIb myosin heavy chain during postnatal development and hypothyroidism in rat skeletal muscle. American journal of physiology Regulatory, integrative and comparative physiology. 2012;302(7):R854-67.

106.	Butler-Browne GS, Bugaisky LB, Cuenoud S, Schwartz K, Whalen RG. Denervation of newborn rat muscle does not block the appearance of adult fast myosin heavy chain. Nature. 1982;299(5886):830-3.

107.	Narusawa M, Fitzsimons RB, Izumo S, Nadal-Ginard B, Rubinstein NA, Kelly AM. Slow myosin in developing rat skeletal muscle. The Journal of cell biology. 1987;104(3):447-59.

108.	Sartore S, Gorza L, Schiaffino S. Fetal myosin heavy chains in regenerating muscle. Nature. 1982;298(5871):294-6.

109.	DiMario JX, Uzman A, Strohman RC. Fiber regeneration is not persistent in dystrophic (MDX) mouse skeletal muscle. Developmental biology. 1991;148(1):314-21.

110.	Schiaffino S, Gorza L, Dones I, Cornelio F, Sartore S. Fetal myosin immunoreactivity in human dystrophic muscle. Muscle & nerve. 1986;9(1):51-8.

111.	Eusebi V, Rilke F, Ceccarelli C, Fedeli F, Schiaffino S, Bussolati G. Fetal heavy chain skeletal myosin. An oncofetal antigen expressed by rhabdomyosarcoma. The American journal of surgical pathology. 1986;10(10):680-6.

112.	Schiaffino S, Gorza L, Sartore S, Saggin L, Carli M. Embryonic myosin heavy chain as a differentiation marker of developing human skeletal muscle and rhabdomyosarcoma. A monoclonal antibody study. Experimental cell research. 1986;163(1):211-20.

113.	d'Albis A, Couteaux R, Janmot C, Roulet A, Mira JC. Regeneration after cardiotoxin injury of innervated and denervated slow and fast muscles of mammals. Myosin isoform analysis. European journal of biochemistry / FEBS. 1988;174(1):103-10.

114.	Esser K, Gunning P, Hardeman E. Nerve-dependent and -independent patterns of mRNA expression in regenerating skeletal muscle. Developmental biology. 1993;159(1):173-83.

115.	Whalen RG, Harris JB, Butler-Browne GS, Sesodia S. Expression of myosin isoforms during notexin-induced regeneration of rat soleus muscles. Developmental biology. 1990;141(1):24-40.

116.	Kalhovde JM, Jerkovic R, Sefland I, Cordonnier C, Calabria E, Schiaffino S, et al. "Fast" and "slow" muscle fibres in hindlimb muscles of adult rats regenerate from intrinsically different satellite cells. The Journal of physiology. 2005;562(Pt 3):847-57.

117.	Jerkovic R, Argentini C, Serrano-Sanchez A, Cordonnier C, Schiaffino S. Early myosin switching induced by nerve activity in regenerating slow skeletal muscle. Cell structure and function. 1997;22(1):147-53.

118.	White J, Barro MV, Makarenkova HP, Sanger JW, Sanger JM. Localization of sarcomeric proteins during myofibril assembly in cultured mouse primary skeletal myotubes. Anatomical record. 2014;297(9):1571-84.

119.	Lyons GE, Schiaffino S, Sassoon D, Barton P, Buckingham M. Developmental regulation of myosin gene expression in mouse cardiac muscle. The Journal of cell biology. 1990;111(6 Pt 1):2427-36.

120.	Sieck GC, Prakash YS, Han YS, Fang YH, Geiger PC, Zhan WZ. Changes in actomyosin ATP consumption rate in rat diaphragm muscle fibers during postnatal development. Journal of applied physiology. 2003;94(5):1896-902.

121.	Sartore S, Mascarello F, Rowlerson A, Gorza L, Ausoni S, Vianello M, et al. Fibre types in extraocular muscles: a new myosin isoform in the fast fibres. Journal of muscle research and cell motility. 1987;8(2):161-72.

122.	Alvarado DM, Buchan JG, Gurnett CA, Dobbs MB. Exome sequencing identifies an MYH3 mutation in a family with distal arthrogryposis type 1. The Journal of bone and joint surgery American volume. 2011;93(11):1045-50.

123.	Tajsharghi H, Kimber E, Kroksmark AK, Jerre R, Tulinius M, Oldfors A. Embryonic myosin heavy-chain mutations cause distal arthrogryposis and developmental myosin myopathy that persists postnatally. Archives of neurology. 2008;65(8):1083-90.

124.	Toydemir RM, Rutherford A, Whitby FG, Jorde LB, Carey JC, Bamshad MJ. Mutations in embryonic myosin heavy chain (MYH3) cause Freeman-Sheldon syndrome and Sheldon-Hall syndrome. Nature genetics. 2006;38(5):561-5.

125.	Bamshad M, Van Heest AE, Pleasure D. Arthrogryposis: a review and update. The Journal of bone and joint surgery American volume. 2009;91 Suppl 4:40-6.

126.	Bamshad M, Jorde LB, Carey JC. A revised and extended classification of the distal arthrogryposes. American journal of medical genetics. 1996;65(4):277-81.

127.   Freeman EA, Sheldon JH. Cranio-carpo-tarsal dystrophy. Archives of Disease in Childhood. 1938;13(75):277-83.

128.   Burian F. The "whistling face" characteristic in a compound cranio-facio-corporal syndrome. British journal of plastic surgery. 1963;16:140-3.

129.   Moser H. Duchenne muscular dystrophy: pathogenetic aspects and genetic prevention. Human genetics. 1984;66(1):17-40.

130.   Emery AE. Duchenne muscular dystrophy--Meryon's disease. Neuromuscular disorders : NMD. 1993;3(4):263-6.

131.   Brown SC, Lucy JA. Dystrophin: Cambridge University Press; 1997.

132.   Manzur AY, Kuntzer T, Pike M, Swan A. Glucocorticoid corticosteroids for Duchenne muscular dystrophy. The Cochrane database of systematic reviews. 2008(1):Cd003725.

133.   Wagner KR. Approaching a new age in Duchenne muscular dystrophy treatment. Neurotherapeutics : the journal of the American Society for Experimental NeuroTherapeutics. 2008;5(4):583-91.

134.   Ward PA, Hejtmancik JF, Witkowski JA, Baumbach LL, Gunnell S, Speer J, et al. Prenatal diagnosis of Duchenne muscular dystrophy: prospective linkage analysis and retrospective dystrophin cDNA analysis. American journal of human genetics. 1989;44(2):270-81.

135.   Muller B, Dechant C, Meng G, Liechti-Gallati S, Doherty RA, Hejtmancik JF, et al. Estimation of the male and female mutation rates in Duchenne muscular dystrophy (DMD). Human genetics. 1992;89(2):204-6.

136.   Haldane JB. The rate of spontaneous mutation of a human gene. Journal of genetics. 1935;31:317-26.

137.   Scherer S. Guide to the human genome: Cold Spring Harbor Laboratory Press; 2010.

138.   Blake DJ, Weir A, Newey SE, Davies KE. Function and genetics of dystrophin and dystrophin-related proteins in muscle. Physiological reviews. 2002;82(2):291-329.

139.   Aartsma-Rus A, Van Deutekom JC, Fokkema IF, Van Ommen GJ, Den Dunnen JT. Entries in the Leiden Duchenne muscular dystrophy mutation database: an overview of mutation types and paradoxical cases that confirm the reading-frame rule. Muscle & nerve. 2006;34(2):135-44.

140.   Zhang Z, Habara Y, Nishiyama A, Oyazato Y, Yagi M, Takeshima Y, et al. Identification of seven novel cryptic exons embedded in the dystrophin gene and characterization of 14 cryptic dystrophin exons. Journal of human genetics. 2007;52(7):607-17.

141.   Beroud C, Carrie A, Beldjord C, Deburgrave N, Llense S, Carelle N, et al. Dystrophinopathy caused by mid-intronic substitutions activating cryptic exons in the DMD gene. Neuromuscular disorders : NMD. 2004;14(1):10-8.

142.   Madden HR, Fletcher S, Davis MR, Wilton SD. Characterization of a complex Duchenne muscular dystrophy-causing dystrophin gene inversion and restoration of the reading frame by induced exon skipping. Human mutation. 2009;30(1):22-8.

143.   Oshima J, Magner DB, Lee JA, Breman AM, Schmitt ES, White LD, et al. Regional genomic instability predisposes to complex dystrophin gene rearrangements. Human genetics. 2009;126(3):411-23.

144.   Koenig M, Monaco AP, Kunkel LM. The complete sequence of dystrophin predicts a rod-shaped cytoskeletal protein. Cell. 1988;53(2):219-28.

145.   Koenig M, Kunkel LM. Detailed analysis of the repeat domain of dystrophin reveals four potential hinge segments that may confer flexibility. The Journal of biological chemistry. 1990;265(8):4560-6.

146.   Ervasti JM, Campbell KP. A role for the dystrophin-glycoprotein complex as a transmembrane linker between laminin and actin. The Journal of cell biology. 1993;122(4):809-23.

147.   Manning J, O'Malley D. What has the mdx mouse model of Duchenne muscular dystrophy contributed to our understanding of this disease? Journal of muscle research and cell motility. 2015;36(2):155-67.

148.   Lapidos KA, Kakkar R, McNally EM. The dystrophin glycoprotein complex: signaling strength and integrity for the sarcolemma. Circulation research. 2004;94(8):1023-31.

149.   Durbeej M, Campbell KP. Muscular dystrophies involving the dystrophin-glycoprotein complex: an overview of current mouse models. Curr Opin Genet Dev. 2002;12(3):349-61.

150.   Ervasti JM, Campbell KP. Membrane organization of the dystrophin-glycoprotein complex. Cell. 1991;66(6):1121-31.

151.   Sunada Y, Bernier SM, Kozak CA, Yamada Y, Campbell KP. Deficiency of merosin in dystrophic dy mice and genetic linkage of laminin M chain gene to dy locus. The Journal of biological chemistry. 1994;269(19):13729-32.

152.   Campanelli JT, Roberds SL, Campbell KP, Scheller RH. A role for dystrophin-associated glycoproteins and utrophin in agrin-induced AChR clustering. Cell. 1994;77(5):663-74.

153.   Gee SH, Montanaro F, Lindenbaum MH, Carbonetto S. Dystroglycan-alpha, a dystrophin-associated glycoprotein, is a functional agrin receptor. Cell. 1994;77(5):675-86.

154.   Talts JF, Andac Z, Gohring W, Brancaccio A, Timpl R. Binding of the G domains of laminin alpha1 and alpha2 chains and perlecan to heparin, sulfatides, alpha-dystroglycan and several extracellular matrix proteins. The EMBO journal. 1999;18(4):863-70.

155.   Bowe MA, Mendis DB, Fallon JR. The small leucine-rich repeat proteoglycan biglycan binds to alpha-dystroglycan and is upregulated in dystrophic muscle. The Journal of cell biology. 2000;148(4):801-10.

156.   Weller B, Karpati G, Carpenter S. Dystrophin-deficient mdx muscle fibers are preferentially vulnerable to necrosis induced by experimental lengthening contractions. Journal of the neurological sciences. 1990;100(1-2):9-13.

157.   Petrof BJ, Shrager JB, Stedman HH, Kelly AM, Sweeney HL. Dystrophin protects the sarcolemma from stresses developed during muscle contraction. Proceedings of the National Academy of Sciences of the United States of America. 1993;90(8):3710-4.

158.   Kobayashi YM, Campbell KP. Chapter 66 - Skeletal Muscle Dystrophin-Glycoprotein Complex and Muscular Dystrophy. In: Olson JAHN, editor. Muscle. Boston/Waltham: Academic Press; 2012. p. 935-42.

159.   Koenig M, Hoffman EP, Bertelson CJ, Monaco AP, Feener C, Kunkel LM. Complete cloning of the Duchenne muscular dystrophy (DMD) cDNA and preliminary genomic organization of the DMD gene in normal and affected individuals. Cell. 1987;50(3):509-17.

160.   Hoffman EP, Brown RH, Jr., Kunkel LM. Dystrophin: the protein product of the Duchenne muscular dystrophy locus. Cell. 1987;51(6):919-28.

161.   Deconinck N, Dan B. Pathophysiology of duchenne muscular dystrophy: current hypotheses. Pediatric neurology. 2007;36(1):1-7.

162.   Schmalbruch H. Regenerated muscle fibers in Duchenne muscular dystrophy: a serial section study. Neurology. 1984;34(1):60-5.

163.   McDouall RM, Dunn MJ, Dubowitz V. Nature of the mononuclear infiltrate and the mechanism of muscle damage in juvenile dermatomyositis and Duchenne muscular dystrophy. Journal of the neurological sciences. 1990;99(2-3):199-217.

164.   Bockhold KJ, Rosenblatt JD, Partridge TA. Aging normal and dystrophic mouse muscle: analysis of myogenicity in cultures of living single fibers. Muscle & nerve. 1998;21(2):173-83.

165.   Deconinck N, Ragot T, Marechal G, Perricaudet M, Gillis JM. Functional protection of dystrophic mouse (mdx) muscles after adenovirus-mediated transfer of a dystrophin minigene. Proceedings of the National Academy of Sciences of the United States of America. 1996;93(8):3570-4.

166.   Tinsley J, Deconinck N, Fisher R, Kahn D, Phelps S, Gillis JM, et al. Expression of full-length utrophin prevents muscular dystrophy in mdx mice. Nature medicine. 1998;4(12):1441-4.

167.   Rybakova IN, Patel JR, Ervasti JM. The dystrophin complex forms a mechanically strong link between the sarcolemma and costameric actin. The Journal of cell biology. 2000;150(5):1209-14.

168.   Williams MW, Bloch RJ. Differential distribution of dystrophin and beta-spectrin at the sarcolemma of fast twitch skeletal muscle fibers. Journal of muscle research and cell motility. 1999;20(4):383-93.

169.   Bradley WG, Fulthorpe JJ. Studies of sarcolemmal integrity in myopathic muscle. Neurology. 1978;28(7):670-7.

170.   Clarke MS, Khakee R, McNeil PL. Loss of cytoplasmic basic fibroblast growth factor from physiologically wounded myofibers of normal and dystrophic muscle. Journal of cell science. 1993;106 (Pt 1):121-33.

171.   Straub V, Rafael JA, Chamberlain JS, Campbell KP. Animal models for muscular dystrophy show different patterns of sarcolemmal disruption. The Journal of cell biology. 1997;139(2):375-85.

172.   Straub V, Donahue KM, Allamand V, Davisson RL, Kim YR, Campbell KP. Contrast agent-enhanced magnetic resonance imaging of skeletal muscle damage in animal models of muscular dystrophy. Magnetic resonance in medicine. 2000;44(4):655-9.

173.   Berchtold MW, Brinkmeier H, Muntener M. Calcium ion in skeletal muscle: its crucial role for muscle function, plasticity, and disease. Physiological reviews. 2000;80(3):1215-65.

174.   Cullen MJ, Fulthorpe JJ. Stages in fibre breakdown in Duchenne muscular dystrophy. An electron-microscopic study. Journal of the neurological sciences. 1975;24(2):179-200.

175.   Bodensteiner JB, Engel AG. Intracellular calcium accumulation in Duchenne dystrophy and other myopathies: a study of 567,000 muscle fibers in 114 biopsies. Neurology. 1978;28(5):439-46.

176.   Duncan CJ. Role of intracellular calcium in promoting muscle damage: a strategy for controlling the dystrophic condition. Experientia. 1978;34(12):1531-5.

177.   Franco A, Jr., Lansman JB. Calcium entry through stretch-inactivated ion channels in mdx myotubes. Nature. 1990;344(6267):670-3.

178.   Hopf FW, Turner PR, Denetclaw WF, Jr., Reddy P, Steinhardt RA. A critical evaluation of resting intracellular free calcium regulation in dystrophic mdx muscle. The American journal of physiology. 1996;271(4 Pt 1):C1325-39.

179.   Tutdibi O, Brinkmeier H, Rudel R, Fohr KJ. Increased calcium entry into dystrophin-deficient muscle fibres of MDX and ADR-MDX mice is reduced by ion channel blockers. The Journal of physiology. 1999;515 (Pt 3):859-68.

180.   De Backer F, Vandebrouck C, Gailly P, Gillis JM. Long-term study of Ca(2+) homeostasis and of survival in collagenase-isolated muscle fibres from normal and mdx mice. The Journal of physiology. 2002;542(Pt 3):855-65.

181.   Vandebrouck C, Martin D, Colson-Van Schoor M, Debaix H, Gailly P. Involvement of TRPC in the abnormal calcium influx observed in dystrophic (mdx) mouse skeletal muscle fibers. The Journal of cell biology. 2002;158(6):1089-96.

182.   Carafoli E, Molinari M. Calpain: a protease in search of a function? Biochemical and biophysical research communications. 1998;247(2):193-203.

183.   Raymackers JM, Debaix H, Colson-Van Schoor M, De Backer F, Tajeddine N, Schwaller B, et al. Consequence of parvalbumin deficiency in the mdx mouse: histological, biochemical and mechanical phenotype of a new double mutant. Neuromuscular disorders : NMD. 2003;13(5):376-87.

184.   Salimena MC, Lagrota-Candido J, Quirico-Santos T. Gender dimorphism influences extracellular matrix expression and regeneration of muscular tissue in mdx dystrophic mice. Histochemistry and cell biology. 2004;122(5):435-44.

185.   Spencer MJ, Croall DE, Tidball JG. Calpains are activated in necrotic fibers from mdx dystrophic mice. The Journal of biological chemistry. 1995;270(18):10909-14.

186.   Spencer MJ, Mellgren RL. Overexpression of a calpastatin transgene in mdx muscle reduces dystrophic pathology. Human molecular genetics. 2002;11(21):2645-55.

187.   Fong PY, Turner PR, Denetclaw WF, Steinhardt RA. Increased activity of calcium leak channels in myotubes of Duchenne human and mdx mouse origin. Science. 1990;250(4981):673-6.

188.   Turner PR, Schultz R, Ganguly B, Steinhardt RA. Proteolysis results in altered leak channel kinetics and elevated free calcium in mdx muscle. The Journal of membrane biology. 1993;133(3):243-51.

189.   Bulfield G, Siller WG, Wight PA, Moore KJ. X chromosome-linked muscular dystrophy (mdx) in the mouse. Proceedings of the National Academy of Sciences of the United States of America. 1984;81(4):1189-92.

190.   Hoffman EP, Monaco AP, Feener CC, Kunkel LM. Conservation of the Duchenne muscular dystrophy gene in mice and humans. Science. 1987;238(4825):347-50.

191.   Sugita H, Arahata K, Ishiguro T, Suhara Y, Tsukahara T, Ishiura S, et al. Negative Immunostaining of Duchenne Muscular Dystrophy (DMD) and mdx Muscle Surface Membrane with Antibody against Synthetic Peptide Fragment predicted from DMD cDNA. Proceedings of the Japan Academy, Series B. 1988;64(2):37-9.

192.   Sicinski P, Geng Y, Ryder-Cook AS, Barnard EA, Darlison MG, Barnard PJ. The molecular basis of muscular dystrophy in the mdx mouse: a point mutation. Science. 1989;244(4912):1578-80.

193.   Turk R, Sterrenburg E, de Meijer EJ, van Ommen GJ, den Dunnen JT, t Hoen PA. Muscle regeneration in dystrophin-deficient mdx mice studied by gene expression profiling. BMC genomics. 2005;6:98.

194.   Dangain J, Vrbova G. Muscle development in mdx mutant mice. Muscle & nerve. 1984;7(9):700-4.

195.   Anderson JE, Ovalle WK, Bressler BH. Electron microscopic and autoradiographic characterization of hindlimb muscle regeneration in the mdx mouse. The Anatomical record. 1987;219(3):243-57.

196.   Tanabe Y, Esaki K, Nomura T. Skeletal muscle pathology in X chromosome-linked muscular dystrophy (mdx) mouse. Acta neuropathologica. 1986;69(1-2):91-5.

197.   Anderson JE, Bressler BH, Ovalle WK. Functional regeneration in the hindlimb skeletal muscle of the mdx mouse. Journal of muscle research and cell motility. 1988;9(6):499-515.

198.   Pastoret C, Sebille A. mdx mice show progressive weakness and muscle deterioration with age. Journal of the neurological sciences. 1995;129(2):97-105.

199.   Luz MA, Marques MJ, Santo Neto H. Impaired regeneration of dystrophin-deficient muscle fibers is caused by exhaustion of myogenic cells. Brazilian journal of medical and biological research = Revista brasileira de pesquisas medicas e biologicas / Sociedade Brasileira de Biofisica [et al]. 2002;35(6):691-5.

200.   Marshall PA, Williams PE, Goldspink G. Accumulation of collagen and altered fiber-type ratios as indicators of abnormal muscle gene expression in the mdx dystrophic mouse. Muscle & nerve. 1989;12(7):528-37.

201.   Lefaucheur JP, Pastoret C, Sebille A. Phenotype of dystrophinopathy in old mdx mice. The Anatomical record. 1995;242(1):70-6.

202.   Love DR, Hill DF, Dickson G, Spurr NK, Byth BC, Marsden RF, et al. An autosomal transcript in skeletal muscle with homology to dystrophin. Nature. 1989;339(6219):55-8.

203.   Tinsley JM, Blake DJ, Roche A, Fairbrother U, Riss J, Byth BC, et al. Primary structure of dystrophin-related protein. Nature. 1992;360(6404):591-3.

204.   Davies KE, Nowak KJ. Molecular mechanisms of muscular dystrophies: old and new players. Nature reviews Molecular cell biology. 2006;7(10):762-73.

205.   Ohlendieck K, Campbell KP. Dystrophin-associated proteins are greatly reduced in skeletal muscle from mdx mice. The Journal of cell biology. 1991;115(6):1685-94.

206.   Nguyen TM, Ellis JM, Love DR, Davies KE, Gatter KC, Dickson G, et al. Localization of the DMDL gene-encoded dystrophin-related protein using a panel of nineteen monoclonal antibodies: presence at neuromuscular junctions, in the sarcolemma of dystrophic skeletal muscle, in vascular and

other smooth muscles, and in proliferating brain cell lines. The Journal of cell biology. 1991;115(6):1695-700.

207.　Bewick GS, Nicholson LV, Young C, O'Donnell E, Slater CR. Different distributions of dystrophin and related proteins at nerve-muscle junctions. Neuroreport. 1992;3(10):857-60.

208.　Karpati G, Carpenter S, Morris GE, Davies KE, Guerin C, Holland P. Localization and quantitation of the chromosome 6-encoded dystrophin-related protein in normal and pathological human muscle. Journal of neuropathology and experimental neurology. 1993;52(2):119-28.

209.　Kleopa KA, Drousiotou A, Mavrikiou E, Ormiston A, Kyriakides T. Naturally occurring utrophin correlates with disease severity in Duchenne muscular dystrophy. Human molecular genetics. 2006;15(10):1623-8.

210.　Deconinck AE, Rafael JA, Skinner JA, Brown SC, Potter AC, Metzinger L, et al. Utrophin-dystrophin-deficient mice as a model for Duchenne muscular dystrophy. Cell. 1997;90(4):717-27.

211.　Jejurikar SS, Kuzon WM, Jr. Satellite cell depletion in degenerative skeletal muscle. Apoptosis : an international journal on programmed cell death. 2003;8(6):573-8.

212.　Sacco A, Mourkioti F, Tran R, Choi J, Llewellyn M, Kraft P, et al. Short telomeres and stem cell exhaustion model Duchenne muscular dystrophy in mdx/mTR mice. Cell. 2010;143(7):1059-71.

213.　Ambros V. The functions of animal microRNAs. Nature. 2004;431(7006):350-5.

214.　Griffiths-Jones S, Saini HK, van Dongen S, Enright AJ. miRBase: tools for microRNA genomics. Nucleic acids research. 2008;36(Database issue):D154-8.

215.　Bartel DP. MicroRNAs: target recognition and regulatory functions. Cell. 2009;136(2):215-33.

216.　Friedman JM, Jones PA. MicroRNAs: critical mediators of differentiation, development and disease. Swiss medical weekly. 2009;139(33-34):466-72.

217.　Gomase VS, Parundekar AN. microRNA: human disease and development. International journal of bioinformatics research and applications. 2009;5(5):479-500.

218.　Bushati N, Cohen SM. microRNA functions. Annual review of cell and developmental biology. 2007;23:175-205.

219.　Starega-Roslan J, Koscianska E, Kozlowski P, Krzyzosiak WJ. The role of the precursor structure in the biogenesis of microRNA. Cellular and molecular life sciences : CMLS. 2011;68(17):2859-71.

220.　Croce CM. Causes and consequences of microRNA dysregulation in cancer. Nature reviews Genetics. 2009;10(10):704-14.

221.　Ventura A, Jacks T. MicroRNAs and cancer: short RNAs go a long way. Cell. 2009;136(4):586-91.

222.　Melo SA, Esteller M. Dysregulation of microRNAs in cancer: playing with fire. FEBS letters. 2011;585(13):2087-99.

223.　Hebert SS, De Strooper B. Alterations of the microRNA network cause neurodegenerative disease. Trends in neurosciences. 2009;32(4):199-206.

224.	Lau P, de Strooper B. Dysregulated microRNAs in neurodegenerative disorders. Seminars in cell & developmental biology. 2010;21(7):768-73.

225.	Friedman RC, Farh KK, Burge CB, Bartel DP. Most mammalian mRNAs are conserved targets of microRNAs. Genome research. 2009;19(1):92-105.

226.	Lee RC, Feinbaum RL, Ambros V. The C. elegans heterochronic gene lin-4 encodes small RNAs with antisense complementarity to lin-14. Cell. 1993;75(5):843-54.

227.	Wightman B, Ha I, Ruvkun G. Posttranscriptional regulation of the heterochronic gene lin-14 by lin-4 mediates temporal pattern formation in C. elegans. Cell. 1993;75(5):855-62.

228.	Reinhart BJ, Slack FJ, Basson M, Pasquinelli AE, Bettinger JC, Rougvie AE, et al. The 21-nucleotide let-7 RNA regulates developmental timing in Caenorhabditis elegans. Nature. 2000;403(6772):901-6.

229.	Slack FJ, Basson M, Liu Z, Ambros V, Horvitz HR, Ruvkun G. The lin-41 RBCC gene acts in the C. elegans heterochronic pathway between the let-7 regulatory RNA and the LIN-29 transcription factor. Molecular cell. 2000;5(4):659-69.

230.	Pasquinelli AE, Reinhart BJ, Slack F, Martindale MQ, Kuroda MI, Maller B, et al. Conservation of the sequence and temporal expression of let-7 heterochronic regulatory RNA. Nature. 2000;408(6808):86-9.

231.	Lagos-Quintana M, Rauhut R, Lendeckel W, Tuschl T. Identification of novel genes coding for small expressed RNAs. Science. 2001;294(5543):853-8.

232.	Lau NC, Lim LP, Weinstein EG, Bartel DP. An abundant class of tiny RNAs with probable regulatory roles in Caenorhabditis elegans. Science. 2001;294(5543):858-62.

233.	Lee RC, Ambros V. An extensive class of small RNAs in Caenorhabditis elegans. Science. 2001;294(5543):862-4.

234.	Bartel DP. MicroRNAs: genomics, biogenesis, mechanism, and function. Cell. 2004;116(2):281-97.

235.	Griffiths-Jones S. The microRNA registry. Nucleic Acids Res. 2004;32:D109-D11.

236.	Rodriguez A, Griffiths-Jones S, Ashurst JL, Bradley A. Identification of mammalian microRNA host genes and transcription units. Genome research. 2004;14(10A):1902-10.

237.	Ghatak S, Sen CK. Chapter 1 - MicroRNA Biogenesis in Regenerative Medicine. In: Sen CK, editor. MicroRNA in Regenerative Medicine. Oxford: Academic Press; 2015. p. 3-46.

238.	Hammond SM. An overview of microRNAs. Advanced drug delivery reviews. 2015;87:3-14.

239.	Kim VN, Han J, Siomi MC. Biogenesis of small RNAs in animals. Nature reviews Molecular cell biology. 2009;10(2):126-39.

240.	Calin GA, Dumitru CD, Shimizu M, Bichi R, Zupo S, Noch E, et al. Frequent deletions and down-regulation of micro- RNA genes miR15 and miR16 at 13q14 in chronic lymphocytic leukemia. Proceedings of the National Academy of Sciences of the United States of America. 2002;99(24):15524-9.

241.	Ying SY, Lin SL. Intronic microRNAs. Biochemical and biophysical research communications. 2005;326(3):515-20.

242. Ying SY, Chang DC, Lin SL. The microRNA (miRNA): overview of the RNA genes that modulate gene function. Molecular biotechnology. 2008;38(3):257-68.

243. Lin SL, Miller JD, Ying SY. Intronic microRNA (miRNA). Journal of biomedicine & biotechnology. 2006;2006(4):26818.

244. Ruby JG, Jan CH, Bartel DP. Intronic microRNA precursors that bypass Drosha processing. Nature. 2007;448(7149):83-6.

245. Okamura K, Hagen JW, Duan H, Tyler DM, Lai EC. The mirtron pathway generates microRNA-class regulatory RNAs in Drosophila. Cell. 2007;130(1):89-100.

246. Berezikov E, Chung WJ, Willis J, Cuppen E, Lai EC. Mammalian mirtron genes. Molecular cell. 2007;28(2):328-36.

247. Tam W. Identification and characterization of human BIC, a gene on chromosome 21 that encodes a noncoding RNA. Gene. 2001;274(1-2):157-67.

248. Higuchi T, Sakamoto S, Kakinuma Y, Kai S, Yagyu K, Todaka H, et al. High expression of nuclear factor 90 (NF90) leads to mitochondrial degradation in skeletal and cardiac muscles. PloS one. 2012;7(8):e43340.

249. Lee Y, Kim M, Han J, Yeom KH, Lee S, Baek SH, et al. MicroRNA genes are transcribed by RNA polymerase II. The EMBO journal. 2004;23(20):4051-60.

250. Cai X, Hagedorn CH, Cullen BR. Human microRNAs are processed from capped, polyadenylated transcripts that can also function as mRNAs. Rna. 2004;10(12):1957-66.

251. Johnson SM, Lin SY, Slack FJ. The time of appearance of the C. elegans let-7 microRNA is transcriptionally controlled utilizing a temporal regulatory element in its promoter. Developmental biology. 2003;259(2):364-79.

252. Johnston RJ, Hobert O. A microRNA controlling left/right neuronal asymmetry in Caenorhabditis elegans. Nature. 2003;426(6968):845-9.

253. Borchert GM, Lanier W, Davidson BL. RNA polymerase III transcribes human microRNAs. Nature structural & molecular biology. 2006;13(12):1097-101.

254. Lee Y, Jeon K, Lee JT, Kim S, Kim VN. MicroRNA maturation: stepwise processing and subcellular localization. The EMBO journal. 2002;21(17):4663-70.

255. Lee Y, Ahn C, Han J, Choi H, Kim J, Yim J, et al. The nuclear RNase III Drosha initiates microRNA processing. Nature. 2003;425(6956):415-9.

256. Han J, Lee Y, Yeom KH, Kim YK, Jin H, Kim VN. The Drosha-DGCR8 complex in primary microRNA processing. Genes Dev. 2004;18(24):3016-27.

257. Denli AM, Tops BB, Plasterk RH, Ketting RF, Hannon GJ. Processing of primary microRNAs by the Microprocessor complex. Nature. 2004;432(7014):231-5.

258. Gregory RI, Yan KP, Amuthan G, Chendrimada T, Doratotaj B, Cooch N, et al. The Microprocessor complex mediates the genesis of microRNAs. Nature. 2004;432(7014):235-40.

259. Landthaler M, Yalcin A, Tuschl T. The human DiGeorge syndrome critical region gene 8 and Its D. melanogaster homolog are required for miRNA biogenesis. Current biology : CB. 2004;14(23):2162-7.

260.   Blaszczyk J, Tropea JE, Bubunenko M, Routzahn KM, Waugh DS, Court DL, et al. Crystallographic and modeling studies of RNase III suggest a mechanism for double-stranded RNA cleavage. Structure (London, England : 1993). 2001;9(12):1225-36.

261.   Zhang H, Kolb FA, Jaskiewicz L, Westhof E, Filipowicz W. Single processing center models for human Dicer and bacterial RNase III. Cell. 2004;118(1):57-68.

262.   Wang Y, Medvid R, Melton C, Jaenisch R, Blelloch R. DGCR8 is essential for microRNA biogenesis and silencing of embryonic stem cell self-renewal. Nature genetics. 2007;39(3):380-5.

263.   Kim YK, Kim VN. Processing of intronic microRNAs. The EMBO journal. 2007;26(3):775-83.

264.   Morlando M, Ballarino M, Gromak N, Pagano F, Bozzoni I, Proudfoot NJ. Primary microRNA transcripts are processed co-transcriptionally. Nature structural & molecular biology. 2008;15(9):902-9.

265.   Pawlicki JM, Steitz JA. Primary microRNA transcript retention at sites of transcription leads to enhanced microRNA production. The Journal of cell biology. 2008;182(1):61-76.

266.   Han J, Pedersen JS, Kwon SC, Belair CD, Kim YK, Yeom KH, et al. Posttranscriptional crossregulation between Drosha and DGCR8. Cell. 2009;136(1):75-84.

267.   Babiarz JE, Ruby JG, Wang Y, Bartel DP, Blelloch R. Mouse ES cells express endogenous shRNAs, siRNAs, and other Microprocessor-independent, Dicer-dependent small RNAs. Genes Dev. 2008;22(20):2773-85.

268.   Glazov EA, Cottee PA, Barris WC, Moore RJ, Dalrymple BP, Tizard ML. A microRNA catalog of the developing chicken embryo identified by a deep sequencing approach. Genome research. 2008;18(6):957-64.

269.   Flynt AS, Greimann JC, Chung WJ, Lima CD, Lai EC. MicroRNA biogenesis via splicing and exosome-mediated trimming in Drosophila. Molecular cell. 2010;38(6):900-7.

270.   Kim VN. MicroRNA precursors in motion: exportin-5 mediates their nuclear export. Trends in cell biology. 2004;14(4):156-9.

271.   Lund E, Guttinger S, Calado A, Dahlberg JE, Kutay U. Nuclear export of microRNA precursors. Science. 2004;303(5654):95-8.

272.   Yi R, Doehle BP, Qin Y, Macara IG, Cullen BR. Overexpression of exportin 5 enhances RNA interference mediated by short hairpin RNAs and microRNAs. Rna. 2005;11(2):220-6.

273.   Bohnsack MT, Czaplinski K, Gorlich D. Exportin 5 is a RanGTP-dependent dsRNA-binding protein that mediates nuclear export of pre-miRNAs. Rna. 2004;10(2):185-91.

274.   Gwizdek C, Ossareh-Nazari B, Brownawell AM, Doglio A, Bertrand E, Macara IG, et al. Exportin-5 mediates nuclear export of minihelix-containing RNAs. The Journal of biological chemistry. 2003;278(8):5505-8.

275.   Basyuk E, Suavet F, Doglio A, Bordonne R, Bertrand E. Human let-7 stem-loop precursors harbor features of RNase III cleavage products. Nucleic acids research. 2003;31(22):6593-7.

276.   Zeng Y, Cullen BR. Structural requirements for pre-microRNA binding and nuclear export by Exportin 5. Nucleic acids research. 2004;32(16):4776-85.

277.   Hutvagner G, McLachlan J, Pasquinelli AE, Balint E, Tuschl T, Zamore PD. A cellular function for the RNA-interference enzyme Dicer in the maturation of the let-7 small temporal RNA. Science. 2001;293(5531):834-8.

278.   Grishok A, Pasquinelli AE, Conte D, Li N, Parrish S, Ha I, et al. Genes and mechanisms related to RNA interference regulate expression of the small temporal RNAs that control C. elegans developmental timing. Cell. 2001;106(1):23-34.

279.   Ketting RF, Fischer SE, Bernstein E, Sijen T, Hannon GJ, Plasterk RH. Dicer functions in RNA interference and in synthesis of small RNA involved in developmental timing in C. elegans. Genes Dev. 2001;15(20):2654-9.

280.   Bernstein E, Caudy AA, Hammond SM, Hannon GJ. Role for a bidentate ribonuclease in the initiation step of RNA interference. Nature. 2001;409(6818):363-6.

281.   Haase AD, Jaskiewicz L, Zhang H, Laine S, Sack R, Gatignol A, et al. TRBP, a regulator of cellular PKR and HIV-1 virus expression, interacts with Dicer and functions in RNA silencing. EMBO reports. 2005;6(10):961-7.

282.   Chendrimada TP, Gregory RI, Kumaraswamy E, Norman J, Cooch N, Nishikura K, et al. TRBP recruits the Dicer complex to Ago2 for microRNA processing and gene silencing. Nature. 2005;436(7051):740-4.

283.   Azuma-Mukai A, Oguri H, Mituyama T, Qian ZR, Asai K, Siomi H, et al. Characterization of endogenous human Argonautes and their miRNA partners in RNA silencing. Proceedings of the National Academy of Sciences of the United States of America. 2008;105(23):7964-9.

284.   Marti E, Pantano L, Banez-Coronel M, Llorens F, Minones-Moyano E, Porta S, et al. A myriad of miRNA variants in control and Huntington's disease brain regions detected by massively parallel sequencing. Nucleic acids research. 2010;38(20):7219-35.

285.   Ohanian M, Humphreys DT, Anderson E, Preiss T, Fatkin D. A heterozygous variant in the human cardiac miR-133 gene, MIR133A2, alters miRNA duplex processing and strand abundance. BMC genetics. 2013;14:18.

286.   Baran-Gale J, Fannin EE, Kurtz CL, Sethupathy P. Beta cell 5'-shifted isomiRs are candidate regulatory hubs in type 2 diabetes. PloS one. 2013;8(9):e73240.

287.   Vickers KC, Sethupathy P, Baran-Gale J, Remaley AT. Complexity of microRNA function and the role of isomiRs in lipid homeostasis. Journal of lipid research. 2013;54(5):1182-91.

288.   Hammond SM, Boettcher S, Caudy AA, Kobayashi R, Hannon GJ. Argonaute2, a link between genetic and biochemical analyses of RNAi. Science. 2001;293(5532):1146-50.

289.   Tabara H, Sarkissian M, Kelly WG, Fleenor J, Grishok A, Timmons L, et al. The rde-1 gene, RNA interference, and transposon silencing in C. elegans. Cell. 1999;99(2):123-32.

290.   Tomari Y, Du T, Haley B, Schwarz DS, Bennett R, Cook HA, et al. RISC assembly defects in the Drosophila RNAi mutant armitage. Cell. 2004;116(6):831-41.

291.   Meister G, Landthaler M, Peters L, Chen PY, Urlaub H, Luhrmann R, et al. Identification of novel argonaute-associated proteins. Current biology : CB. 2005;15(23):2149-55.

292.   Nykanen A, Haley B, Zamore PD. ATP requirements and small interfering RNA structure in the RNA interference pathway. Cell. 2001;107(3):309-21.

293.   Robb GB, Rana TM. RNA helicase A interacts with RISC in human cells and functions in RISC loading. Molecular cell. 2007;26(4):523-37.

294.   Liu X, Jin DY, McManus MT, Mourelatos Z. Precursor microRNA-programmed silencing complex assembly pathways in mammals. Molecular cell. 2012;46(4):507-17.

295.   Han J, Lee Y, Yeom KH, Nam JW, Heo I, Rhee JK, et al. Molecular basis for the recognition of primary microRNAs by the Drosha-DGCR8 complex. Cell. 2006;125(5):887-901.

296.   Khvorova A, Reynolds A, Jayasena SD. Functional siRNAs and miRNAs exhibit strand bias. Cell. 2003;115(2):209-16.

297.   Yang JS, Phillips MD, Betel D, Mu P, Ventura A, Siepel AC, et al. Widespread regulatory activity of vertebrate microRNA* species. Rna. 2011;17(2):312-26.

298.   Lai EC, Tam B, Rubin GM. Pervasive regulation of Drosophila Notch target genes by GY-box-, Brd-box-, and K-box-class microRNAs. Genes Dev. 2005;19(9):1067-80.

299.   Lewis BP, Shih IH, Jones-Rhoades MW, Bartel DP, Burge CB. Prediction of mammalian microRNA targets. Cell. 2003;115(7):787-98.

300.   Doench JG, Sharp PA. Specificity of microRNA target selection in translational repression. Genes Dev. 2004;18(5):504-11.

301.   Brennecke J, Stark A, Russell RB, Cohen SM. Principles of microRNA-target recognition. PLoS biology. 2005;3(3):e85.

302.   Lewis BP, Burge CB, Bartel DP. Conserved seed pairing, often flanked by adenosines, indicates that thousands of human genes are microRNA targets. Cell. 2005;120(1):15-20.

303.   Grimson A, Farh KK, Johnston WK, Garrett-Engele P, Lim LP, Bartel DP. MicroRNA targeting specificity in mammals: determinants beyond seed pairing. Molecular cell. 2007;27(1):91-105.

304.   Nilsen TW. Mechanisms of microRNA-mediated gene regulation in animal cells. Trends in genetics : TIG. 2007;23(5):243-9.

305.   Liu J, Carmell MA, Rivas FV, Marsden CG, Thomson JM, Song JJ, et al. Argonaute2 is the catalytic engine of mammalian RNAi. Science. 2004;305(5689):1437-41.

306.   Doench JG, Petersen CP, Sharp PA. siRNAs can function as miRNAs. Genes Dev. 2003;17(4):438-42.

307.   Pfaff J, Meister G. Argonaute and GW182 proteins: an effective alliance in gene silencing. Biochemical Society transactions. 2013;41(4):855-60.

308.   Braun JE, Huntzinger E, Izaurralde E. The role of GW182 proteins in miRNA-mediated gene silencing. Advances in experimental medicine and biology. 2013;768:147-63.

309.   Fabian MR, Sonenberg N. The mechanics of miRNA-mediated gene silencing: a look under the hood of miRISC. Nature structural & molecular biology. 2012;19(6):586-93.

310.   Chekulaeva M, Hentze MW, Ephrussi A. Bruno acts as a dual repressor of oskar translation, promoting mRNA oligomerization and formation of silencing particles. Cell. 2006;124(3):521-33.

311. Richter JD, Sonenberg N. Regulation of cap-dependent translation by eIF4E inhibitory proteins. Nature. 2005;433(7025):477-80.

312. Cho PF, Poulin F, Cho-Park YA, Cho-Park IB, Chicoine JD, Lasko P, et al. A new paradigm for translational control: inhibition via 5'-3' mRNA tethering by Bicoid and the eIF4E cognate 4EHP. Cell. 2005;121(3):411-23.

313. Kiriakidou M, Tan GS, Lamprinaki S, De Planell-Saguer M, Nelson PT, Mourelatos Z. An mRNA m7G cap binding-like motif within human Ago2 represses translation. Cell. 2007;129(6):1141-51.

314. Chendrimada TP, Finn KJ, Ji X, Baillat D, Gregory RI, Liebhaber SA, et al. MicroRNA silencing through RISC recruitment of eIF6. Nature. 2007;447(7146):823-8.

315. Petersen CP, Bordeleau ME, Pelletier J, Sharp PA. Short RNAs repress translation after initiation in mammalian cells. Molecular cell. 2006;21(4):533-42.

316. Mootz D, Ho DM, Hunter CP. The STAR/Maxi-KH domain protein GLD-1 mediates a developmental switch in the translational control of C. elegans PAL-1. Development. 2004;131(14):3263-72.

317. Olsen PH, Ambros V. The lin-4 regulatory RNA controls developmental timing in Caenorhabditis elegans by blocking LIN-14 protein synthesis after the initiation of translation. Developmental biology. 1999;216(2):671-80.

318. Guo H, Ingolia NT, Weissman JS, Bartel DP. Mammalian microRNAs predominantly act to decrease target mRNA levels. Nature. 2010;466(7308):835-40.

319. Bernstein E, Kim SY, Carmell MA, Murchison EP, Alcorn H, Li MZ, et al. Dicer is essential for mouse development. Nature genetics. 2003;35(3):215-7.

320. Harris KS, Zhang Z, McManus MT, Harfe BD, Sun X. Dicer function is essential for lung epithelium morphogenesis. Proceedings of the National Academy of Sciences of the United States of America. 2006;103(7):2208-13.

321. Andl T, Murchison EP, Liu F, Zhang Y, Yunta-Gonzalez M, Tobias JW, et al. The miRNA-processing enzyme dicer is essential for the morphogenesis and maintenance of hair follicles. Current biology : CB. 2006;16(10):1041-9.

322. Yi R, O'Carroll D, Pasolli HA, Zhang Z, Dietrich FS, Tarakhovsky A, et al. Morphogenesis in skin is governed by discrete sets of differentially expressed microRNAs. Nature genetics. 2006;38(3):356-62.

323. Harfe BD, McManus MT, Mansfield JH, Hornstein E, Tabin CJ. The RNaseIII enzyme Dicer is required for morphogenesis but not patterning of the vertebrate limb. Proceedings of the National Academy of Sciences of the United States of America. 2005;102(31):10898-903.

324. Chen JF, Murchison EP, Tang R, Callis TE, Tatsuguchi M, Deng Z, et al. Targeted deletion of Dicer in the heart leads to dilated cardiomyopathy and heart failure. Proceedings of the National Academy of Sciences of the United States of America. 2008;105(6):2111-6.

325. O'Rourke JR, Georges SA, Seay HR, Tapscott SJ, McManus MT, Goldhamer DJ, et al. Essential role for Dicer during skeletal muscle development. Developmental biology. 2007;311(2):359-68.

326.   Wang H, Sun H, Guttridge DC. microRNAs: novel components in a muscle gene regulatory network. Cell Cycle. 2009;8(12):1833-7.

327.   Lagos-Quintana M, Rauhut R, Yalcin A, Meyer J, Lendeckel W, Tuschl T. Identification of tissue-specific microRNAs from mouse. Current biology : CB. 2002;12(9):735-9.

328.   Sempere LF, Freemantle S, Pitha-Rowe I, Moss E, Dmitrovsky E, Ambros V. Expression profiling of mammalian microRNAs uncovers a subset of brain-expressed microRNAs with possible roles in murine and human neuronal differentiation. Genome biology. 2004;5(3):R13.

329.   McCarthy JJ. MicroRNA-206: the skeletal muscle-specific myomiR. Biochimica et biophysica acta. 2008;1779(11):682-91.

330.   Small EM, O'Rourke JR, Moresi V, Sutherland LB, McAnally J, Gerard RD, et al. Regulation of PI3-kinase/Akt signaling by muscle-enriched microRNA-486. Proceedings of the National Academy of Sciences of the United States of America. 2010;107(9):4218-23.

331.   van Rooij E, Quiat D, Johnson BA, Sutherland LB, Qi X, Richardson JA, et al. A family of microRNAs encoded by myosin genes governs myosin expression and muscle performance. Developmental cell. 2009;17(5):662-73.

332.   van Rooij E, Sutherland LB, Qi X, Richardson JA, Hill J, Olson EN. Control of stress-dependent cardiac growth and gene expression by a microRNA. Science. 2007;316(5824):575-9.

333.   McCarthy JJ. The MyomiR network in skeletal muscle plasticity. Exercise and sport sciences reviews. 2011;39(3):150-4.

334.   Williams AH, Valdez G, Moresi V, Qi X, McAnally J, Elliott JL, et al. MicroRNA-206 delays ALS progression and promotes regeneration of neuromuscular synapses in mice. Science. 2009;326(5959):1549-54.

335.   Goljanek-Whysall K, Sweetman D, Munsterberg AE. microRNAs in skeletal muscle differentiation and disease. Clinical science. 2012;123(11):611-25.

336.   Williams AH, Liu N, van Rooij E, Olson EN. MicroRNA control of muscle development and disease. Current opinion in cell biology. 2009;21(3):461-9.

337.   Zhao Y, Samal E, Srivastava D. Serum response factor regulates a muscle-specific microRNA that targets Hand2 during cardiogenesis. Nature. 2005;436(7048):214-20.

338.   Rosenberg MI, Georges SA, Asawachaicharn A, Analau E, Tapscott SJ. MyoD inhibits Fstl1 and Utrn expression by inducing transcription of miR-206. The Journal of cell biology. 2006;175(1):77-85.

339.   Rao PK, Kumar RM, Farkhondeh M, Baskerville S, Lodish HF. Myogenic factors that regulate expression of muscle-specific microRNAs. Proceedings of the National Academy of Sciences of the United States of America. 2006;103(23):8721-6.

340.   Liu N, Williams AH, Kim Y, McAnally J, Bezprozvannaya S, Sutherland LB, et al. An intragenic MEF2-dependent enhancer directs muscle-specific expression of microRNAs 1 and 133. Proceedings of the National Academy of Sciences of the United States of America. 2007;104(52):20844-9.

341.   Gherzi R, Lee KY, Briata P, Wegmuller D, Moroni C, Karin M, et al. A KH domain RNA binding protein, KSRP, promotes ARE-directed mRNA turnover by recruiting the degradation machinery. Molecular cell. 2004;14(5):571-83.

342.   Trabucchi M, Briata P, Garcia-Mayoral M, Haase AD, Filipowicz W, Ramos A, et al. The RNA-binding protein KSRP promotes the biogenesis of a subset of microRNAs. Nature. 2009;459(7249):1010-4.

343.   McCarthy JJ, Esser KA. MicroRNA-1 and microRNA-133a expression are decreased during skeletal muscle hypertrophy. Journal of applied physiology. 2007;102(1):306-13.

344.   Jeng SF, Rau CS, Liliang PC, Wu CJ, Lu TH, Chen YC, et al. Profiling muscle-specific microRNA expression after peripheral denervation and reinnervation in a rat model. Journal of neurotrauma. 2009;26(12):2345-53.

345.   Greco S, De Simone M, Colussi C, Zaccagnini G, Fasanaro P, Pescatori M, et al. Common micro-RNA signature in skeletal muscle damage and regeneration induced by Duchenne muscular dystrophy and acute ischemia. FASEB journal : official publication of the Federation of American Societies for Experimental Biology. 2009;23(10):3335-46.

346.   Yuasa K, Hagiwara Y, Ando M, Nakamura A, Takeda S, Hijikata T. MicroRNA-206 is highly expressed in newly formed muscle fibers: implications regarding potential for muscle regeneration and maturation in muscular dystrophy. Cell structure and function. 2008;33(2):163-9.

347.   Chen JF, Tao Y, Li J, Deng Z, Yan Z, Xiao X, et al. microRNA-1 and microRNA-206 regulate skeletal muscle satellite cell proliferation and differentiation by repressing Pax7. The Journal of cell biology. 2010;190(5):867-79.

348.   Chen JF, Callis TE, Wang DZ. microRNAs and muscle disorders. Journal of cell science. 2009;122(Pt 1):13-20.

349.   Chen JF, Mandel EM, Thomson JM, Wu Q, Callis TE, Hammond SM, et al. The role of microRNA-1 and microRNA-133 in skeletal muscle proliferation and differentiation. Nature genetics. 2006;38(2):228-33.

350.   Lu L, Zhou L, Chen EZ, Sun K, Jiang P, Wang L, et al. A Novel YY1-miR-1 regulatory circuit in skeletal myogenesis revealed by genome-wide prediction of YY1-miRNA network. PloS one. 2012;7(2):e27596.

351.   Anderson C, Catoe H, Werner R. MIR-206 regulates connexin43 expression during skeletal muscle development. Nucleic acids research. 2006;34(20):5863-71.

352.   Kim HK, Lee YS, Sivaprasad U, Malhotra A, Dutta A. Muscle-specific microRNA miR-206 promotes muscle differentiation. The Journal of cell biology. 2006;174(5):677-87.

353.   Liu N, Williams AH, Maxeiner JM, Bezprozvannaya S, Shelton JM, Richardson JA, et al. microRNA-206 promotes skeletal muscle regeneration and delays progression of Duchenne muscular dystrophy in mice. The Journal of clinical investigation. 2012;122(6):2054-65.

354.   Niu Z, Li A, Zhang SX, Schwartz RJ. Serum response factor micromanaging cardiogenesis. Current opinion in cell biology. 2007;19(6):618-27.

355.   Boutz PL, Chawla G, Stoilov P, Black DL. MicroRNAs regulate the expression of the alternative splicing factor nPTB during muscle development. Genes Dev. 2007;21(1):71-84.

356.   van Rooij E, Quiat D, Johnson BA, Sutherland LB, Qi X, Richardson JA, et al. A Family of microRNAs Encoded by Myosin Genes Governs Myosin Expression and Muscle Performance. Developmental cell. 2009;17(5):662-73.

357.   Sun H, Cao Y, Zhao Y, Lu L, Zhou L, Wang L, et al. Chapter 17 - MicroRNAs in Skeletal Muscle Differentiation. In: Sen CK, editor. MicroRNA in Regenerative Medicine. Oxford: Academic Press; 2015. p. 419-46.

358.   Hawke TJ, Garry DJ. Myogenic satellite cells: physiology to molecular biology. Journal of applied physiology. 2001;91(2):534-51.

359.   Lourdel S, Grand T, Burgos J, Gonzalez W, Sepulveda FV, Teulon J. ClC-5 mutations associated with Dent's disease: a major role of the dimer interface. Pflugers Archiv : European journal of physiology. 2012;463(2):247-56.

360.   Garcia DM, Baek D, Shin C, Bell GW, Grimson A, Bartel DP. Weak seed-pairing stability and high target-site abundance decrease the proficiency of lsy-6 and other microRNAs. Nature structural & molecular biology. 2011;18(10):1139-46.

361.   Roberts TC, Blomberg KE, McClorey G, El Andaloussi S, Godfrey C, Betts C, et al. Expression analysis in multiple muscle groups and serum reveals complexity in the microRNA transcriptome of the mdx mouse with implications for therapy. Molecular therapy Nucleic acids. 2012;1:e39.

362.   Cacchiarelli D, Legnini I, Martone J, Cazzella V, D'Amico A, Bertini E, et al. miRNAs as serum biomarkers for Duchenne muscular dystrophy. EMBO molecular medicine. 2011;3(5):258-65.

363.   McArdle A, Edwards RH, Jackson MJ. How does dystrophin deficiency lead to muscle degeneration?--evidence from the mdx mouse. Neuromuscular disorders : NMD. 1995;5(6):445-56.

364.   Brown DM, Goljanek-Whysall K. microRNAs: Modulators of the underlying pathophysiology of sarcopenia? Ageing research reviews. 2015;24(Pt B):263-73.

365.   Chen Y, Melton DW, Gelfond JA, McManus LM, Shireman PK. MiR-351 transiently increases during muscle regeneration and promotes progenitor cell proliferation and survival upon differentiation. Physiological genomics. 2012;44(21):1042-51.

366.   Tanaka K, Fisher SE, Craig IW. Characterization of novel promoter and enhancer elements of the mouse homologue of the Dent disease gene, CLCN5, implicated in X-linked hereditary nephrolithiasis. Genomics. 1999;58(3):281-92.

367.   Bomont P, Cavalier L, Blondeau F, Ben Hamida C, Belal S, Tazir M, et al. The gene encoding gigaxonin, a new member of the cytoskeletal BTB/kelch repeat family, is mutated in giant axonal neuropathy. Nature genetics. 2000;26(3):370-4.

368.   Yang Y, Allen E, Ding J, Wang W. Giant axonal neuropathy. Cellular and molecular life sciences : CMLS. 2007;64(5):601-9.

369.   Perez-Torrado R, Yamada D, Defossez PA. Born to bind: the BTB protein-protein interaction domain. BioEssays : news and reviews in molecular, cellular and developmental biology. 2006;28(12):1194-202.

370.   Xu L, Wei Y, Reboul J, Vaglio P, Shin TH, Vidal M, et al. BTB proteins are substrate-specific adaptors in an SCF-like modular ubiquitin ligase containing CUL-3. Nature. 2003;425(6955):316-21.

371. Furukawa M, He YJ, Borchers C, Xiong Y. Targeting of protein ubiquitination by BTB-Cullin 3-Roc1 ubiquitin ligases. Nature cell biology. 2003;5(11):1001-7.

372. Pintard L, Willems A, Peter M. Cullin-based ubiquitin ligases: Cul3-BTB complexes join the family. The EMBO journal. 2004;23(8):1681-7.

373. Mahammad S, Murthy SN, Didonna A, Grin B, Israeli E, Perrot R, et al. Giant axonal neuropathy-associated gigaxonin mutations impair intermediate filament protein degradation. The Journal of clinical investigation. 2013;123(5):1964-75.

374. Mitchell PS, Parkin RK, Kroh EM, Fritz BR, Wyman SK, Pogosova-Agadjanyan EL, et al. Circulating microRNAs as stable blood-based markers for cancer detection. Proceedings of the National Academy of Sciences of the United States of America. 2008;105(30):10513-8.

375. Starkey Lewis PJ, Dear J, Platt V, Simpson KJ, Craig DG, Antoine DJ, et al. Circulating microRNAs as potential markers of human drug-induced liver injury. Hepatology. 2011;54(5):1767-76.

376. Gidlof O, Smith JG, Miyazu K, Gilje P, Spencer A, Blomquist S, et al. Circulating cardio-enriched microRNAs are associated with long-term prognosis following myocardial infarction. BMC cardiovascular disorders. 2013;13:12.

377. Mazzone E, Martinelli D, Berardinelli A, Messina S, D'Amico A, Vasco G, et al. North Star Ambulatory Assessment, 6-minute walk test and timed items in ambulant boys with Duchenne muscular dystrophy. Neuromuscular disorders : NMD. 2010;20(11):712-6.

378. Hu J, Kong M, Ye Y, Hong S, Cheng L, Jiang L. Serum miR-206 and other muscle-specific microRNAs as non-invasive biomarkers for Duchenne muscular dystrophy. Journal of neurochemistry. 2014;129(5):877-83.